A THESIS TO BE SUBMITTED TO

THE UNIVERSITY OF TRANS-DISCIPLINARY HEALTH SCIENCES AND TECHNOLOGY

DISCOVERY OF NOVEL HYPERTROPHIC CARDIOMYOPATHY GENES AND THEIR FUNCTIONAL IMPLICATIONS USING MULTI-MODEL APPROACH

FOR THE AWARD OF THE DEGREE OF
DOCTOR OF PHILOSOPHY

BY

PRATUL KUMAR JAIN

UNDER THE GUIDANCE OF

DR. DHANDAPANY S PERUNDURAI

INSTITUTE FOR STEM CELL SCIENCE AND REGENERATIVE MEDICINE, BENGALURU

MAY 2024

THE UNIVERSITY OF TRANS-DISCIPLINARY HEALTH SCIENCES AND TECHNOLOGY

Private University Established in Karnataka by ACT 35 of 2013

BENGALURU - 560064

DECLARATION BY THE CANDIDATE

I declare that this thesis entitled "***Discovery of novel hypertrophic cardiomyopathy genes and their functional implications using multi-model approach***" submitted for the award of Doctor of Philosophy to THE UNIVERSITY OF TRANS-DISCIPLINARY HEALTH SCIENCES AND TECHNOLOGY, Bengaluru, is my original work, conducted under the supervision of my guide Dr. Dhandapany S Perundurai, at Institute for Stem Cell Sciences and Regenerative medicine, Bengaluru. I also wish to inform you that no part of the research has been submitted for a degree or examination at any university. References, help, and material obtained from other sources have been duly acknowledged.

I hereby confirm the originality of the work and that there is no plagiarism in any part of the dissertation.

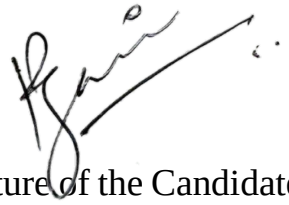

Place: Bengaluru Signature of the Candidate

Date: 09-August-2024

PRATUL KUMAR JAIN

Reg. No.: 20219021504

Month Year of Admission: February 2019

THE UNIVERSITY OF TRANS-DISCIPLINARY HEALTH SCIENCES AND TECHNOLOGY

Private University Established in Karnataka by ACT 35 of 2013

BENGALURU - 560064

CERTIFICATE

This is to certify that the work in this thesis, "***Discovery of novel hypertrophic cardiomyopathy genes and their functional implications using multi-model approach***" submitted by Mr. Pratul Kumar Jain was carried out under my supervision. No part of this thesis has been submitted for a degree or examination at any university. References, help, and material obtained from other sources have been duly acknowledged. I hereby confirm the originality of the work and that there is no plagiarism in any part of the dissertation.

Research Supervisor **Date:** 09-August-2024

Dr. Dhandapany S Perundurai,
Associate Professor and Scientist F
Institute for Stem Cell Science and Regenerative Medicine (inStem),
Dept. of Biotechnology, Government of India
Bangalore 560065
GKVK Campus, Bellary Road, Bangalore, Karnataka 560065, India

ACKNOWLEDGEMENT

With profound gratitude and deep reverence, I extend my heartfelt appreciation to those who have been the unwavering cornerstone of my academic journey, offering their boundless support and encouragement, leading to the fruition of this thesis.

First and foremost, I express my deepest appreciation to my beloved parents without whom this journey was unthinkable, my father late Shri Narendra Kumar Jain, and my mother Smt. Chanda Jain, whose unwavering support and encouragement have been my guiding light throughout. Your love, sacrifices, and belief in me have been the foundation of my achievements. Your constant encouragement and understanding have been invaluable to my dear family, especially my sister Niruti Singhai and brother-in-law Rohan Singhai. Your belief in my abilities has spurred me during challenging times.

I am extremely thankful to my wife, Prachi Jain, for her endless patience, love, and unwavering support. Your encouragement and understanding have been the driving force behind my academic pursuits, providing me with the strength and determination to succeed. To my respected in-laws, thank you for your continuous support and encouragement throughout this journey. Your belief in my abilities has been a source of inspiration. I am truly grateful to my two gorgeous nieces, Navika (Kuhu) and Riyanshi (Charu), for their adorable smiles that have illuminated even the darkest of days. Your existence has been a continuous source of happiness and inspiration. I am truly fortunate to have such a nurturing and loving family. Your presence in my life has made a significant difference, and I will always be appreciative of your unswerving support and love.

I am extremely grateful to Dr. Dhandapany Perundurai (Dhan), my esteemed mentor and supervisor, whose direction and backing have been crucial in molding this thesis and my academic journey. I thank you for believing in me when I doubted myself, for presenting endless openings for progress, and for nurturing my potential even during the most testing times. Your steadfast support and encouragement have been a driving force, propelling me forward in my research endeavors.

I am likewise appreciative of your comprehension and compassion during the difficult circumstances I encountered throughout my tenure. Your tolerance and guidance during those times have been priceless, assisting me in overcoming obstacles with resilience and determination.

I am truly fortunate to have had the opportunity to work under your mentorship, and I am indebted to you for your wisdom, support and unwavering belief in my abilities. Thank you, Dhan, for your exceptional guidance and for being not only a supervisor but also a mentor and a source of inspiration.

I extend my heartfelt gratitude to Dr. Minhaj Sirajuddin and Dr. Dimple Notani, esteemed members of my thesis committee, for their invaluable contributions to the progress of my research. Their insightful feedback, expert guidance has been pivotal in shaping the direction

of my thesis and enhancing its quality. I would like to extend my gratitude to Dr. Minhaj and Sushobhan Mahanty for their expertise and experimental assistance in protein purification, tyrosination assay, and MD simulation studies significantly enriched the research outcomes. Their dedication and collaboration were invaluable in advancing this work. Thank you both for your outstanding support.

To my much-loved friends, Vinay Dubey, Shariq, Dipannita, Akshara, Sukanya, Ankita and Ajay, your presence in my time at inStem has been a true blessing. Your companionship, amusement, and steadfast support have made my academic journey more enjoyable and unforgettable. Through the good times and the bad, you have stood by me with enthusiasm and solidarity, creating treasured memories. From countless discussions and tea sessions, your friendship has been a perpetual source of strength and motivation. Thank you for your comprehension and for making every moment on campus remarkable.

To my cherished friends from outside campus, Sauhard, Kaustubh, Sameer, Sajjan, Ravi, Rajat and Dushyant, your friendship has been a pillar of support and joy in my life beyond the confines of academia. Lending a listening ear during moments of uncertainty, your presence has enriched my life in countless ways. Your unwavering loyalty, friendship, and genuine care have made every experience memorable and meaningful. Throughout my times be it good or bad you've been there, offering encouragement, understanding, and a sense of belonging that transcends distance and time. I am immensely grateful for your friendship and the countless moments of happiness and brotherhood we've shared together.

I express my heartfelt gratitude to all the present and past lab members for their invaluable contributions. I would like to extend special appreciation to Dr. Anupam Mittal and Dr. Ankit Sharma for their guidance. I am grateful to Vinay Rao for always being there, and I acknowledge the support and help of Prasanth, Saswata, Saptashwa, Harshil, Radhika, Guna, Vismaya, Steffi, and Saravanan throughout my time in the lab. Your collective efforts, knowledge, enlightening academic discussions and spirit of cooperation have greatly influenced the working atmosphere in our laboratory and have contributed to our lab's success. I am grateful for your contributions to our shared journey. I am thankful to all (present and past) Minhaj and Tina lab members for always making a laboratory a happening and happy workplace.

I extend sincere thanks to the facilities at inStem and NCBS for their outstanding support, ensuring a conducive environment for research. Thanks to all the teams IT, stores, lab support, canteen, sports complex, housekeeping, AC, electrical, civil, architectural, dispatch, hospitality, and security. Special appreciation to the lab kitchen, instrumentation team and confocal microscopy for their essential services and making my life easier at campus. Additionally, heartfelt gratitude to the academic office team and accounts for their assistance and administrative support. Your dedication and efforts contribute immensely to our work, and we are grateful for your invaluable contributions to our research endeavors.

I would like to express my heartfelt gratitude to my esteemed educators at the University of Hyderabad, specifically Dr. Sharmishtha Banerjee, Dr. Naresh Babu Sepuri, Dr. Niyaz Ahmed, Dr. Sunanda Bhattacharya, Dr. GB Madhu Babu, Dr. Rajagopal, Dr. Suresh, Dr. Brahmanandan, late Dr. Aparna Dutta Gupta, and Dr. Venkataramana. Their unwavering commitment, mentorship, and passion for research have inspired and nurtured my research journey. I am deeply indebted to their guidance, which was instrumental in shaping my early academic endeavors, particularly during my master's thesis. Their invaluable insights and encouragement have had a significant impact on my academic and scientific pursuits.

I express deep gratitude TDU for my PhD registration. I owe a significant debt of gratitude to the Department of Biotechnology (DBT) and the Indian Council of Medical Research (ICMR) for their generous support through the provision of Junior and Senior Research Fellowships (JRF-SRF). The financial backing provided by these organizations has been pivotal in facilitating my research endeavors, and I am immensely appreciative of the chance to pursue my academic and scientific aspirations.

Lastly, I offer my heartfelt gratitude to the revered Jain Tirthankaras and monks and the profound principles they embody. Their teachings of non-violence (ahimsa), truth (satya), non-possessiveness (aparigraha), and compassion (karuna) have been guiding beacons, shaping my ethical compass and influencing my actions. I am deeply thankful for the divine wisdom they impart and the spiritual strength they instill within me. In their divine presence, I find solace, inspiration, and the unwavering belief that righteousness and selflessness pave the path to true fulfillment and enlightenment.

In closing, I extend heartfelt thanks to all who have supported me. Your encouragement and guidance have been invaluable. Grateful for the role each of you has played in shaping my journey.

I would like to acknowledge BioRender for all the illustrations used in the thesis.

LIST OF FIGURES

LIST OF TABLES

LIST OF ABBREVATIONS

Abbreviations	Full form
4EBP1	Eukaryotic translation initiation factor 4E binding protein 1
ACTA1	Skeletal alpha actin
ACTC1	Cardiac alpha actin
ACTN2	Alpha2 actinin
AF	Atrial fibrillation
ALPK3	Alpha kinase 3
ANKRD1	Ankyrin repeat domain 1
ARVC/D	Arrhythmogenic right ventricular cardiomyopathy/dysplasia
ATAC-Seq	Assay for transposase-accessible chromatin with sequencing
ATP	Adenosine tri-phosphate
c-myc	Myelocytomatosis oncogene
CACNA1C	Calcium Voltage-Gated Channel Subunit Alpha1 C
CADD	Combined Annotation Dependent Depletion
CAMK2B	Calcium/Calmodulin Dependent Protein Kinase II Beta
CASQ2	Calsequestrin-2
CAV3	Caveolin 3
CDM	Cardiac differentiation media
Chip-Seq	Chromatin immune-precipitation sequencing
CMM	Cardiac maturation media
CMs	Cardiomyocytes
CSRP3	Cysteine and glycine rich protein 3
CTT	C terminal tail
CVDs	Cardiovascular disorders
DAP5	Death associated protein 5
dbSNP	Single Nucleotide Polymorphism database
DCM	Dilated cardiomyopathy
DD	Diastolic dysfunction
DES	Desmin
ECG	Electrocardiogram
eEF2	Eukaryotic elongation factor 2
eIF4A	Eukaryotic initiation factor 4A
eIF4E	Eukaryotic initiation factor 4E
eIF4G	Eukaryotic initiation factor 4G
ERK1/2	Extracellular regulated kinase 1/2
FHL1	Four and a half LIM domains 1
FHOD3	Formin Homology 2 Domain- Containing 3

FLNC	filamin C
GATA4	GATA binding protein 4
GCLC	Glutamate cysteine ligase catalytic subunit
GCLM	Glutamate cysteine ligase modifier subunit
gnomAD	Genome aggregation database
GO	Gene ontology
HCM	Hypertrophic cardiomyopathy
iPSC	Induced pluripotent stem cells
IVRT	Isovolumetric relaxation time
JPH2	Junctophilin-2
Klf4	Krüppel like factor 4
KOVA	Korean Variant Archive
LA	Left atrium
LAMP2	Lysosomal associated membrane protein 2
LDB3	Lim domain binding 3
LV	Left ventricle
LVNC	Left ventricular non compaction
LVOT	Left ventricular outflow tract obstruction
MHY7	β-myosin heavy chain
MRI	Magnetic resonance imaging
mTORC1	Mammalian target of rapamycin complex 1
MV	Mitral valve
MYBPC3	myosin binding protein C3
MYH6	Myosin heavy chain alpha
MYL2	Regulatory myosin light chain 2
MYL3	Essential myosin light chain 3
MYLK2	Myosin light chain kinase 2
MYOZ2	Myozenin 2 (calsarcin 1)
Nestin	Neuroepithelial stem cell protein
NEXN	Nexilin
NGS	Next-generation sequencing
NIPT	Non-invasive prenatal testing
NODAL	Nodal growth differentiation factor
NOX4	NADPH oxidases-4
NPPA	Natriuretic peptide A
NPPB	Natriuretic peptide B
NRF2	Nuclear factor erythroid 2-related factor 2
NSVT	Non-sustained ventricular tachycardia

NVT/NPT	Number of particle (N), system volume (V), system temperature (T), system pressure
NYHA	New York Heart Association
Oct3/4	Octamer binding transcription factor 3/4
PLN	Phospholamban
PolyPhen	Polymorphism phenotyping
PRKAG2	Protein Kinase AMP-activated non catalytic subunit gamma 2
RCM	Restrictive cardiomyopathy
Rg	Radius of gyration
RMSD	Root mean square deviations
RMSF	Root mean square fluctuations
ROS	Reactive oxygen species
rpS6	Ribosomal protein S6
RPS6KB1	Ribosomal protein S6 kinase beta 1
RyR2	Ryanodine receptor
SERCA2	Sarco(endo)plamsic reticulum calcium ATPase 2
SIFT	Sorting intolerant from tolerant
Sox2	Sex determining region Y-box 2
SSEA3	Stage-specific embryonic antigen 3
SSEA4	Stage-specific embryonic antigen 4
TCAP	Tcap (telethonin)
TNNC1	Cardiac troponin C1
TNNI3	Cardiac troponin I3
TNNT2	Cardiac troponin T2
Topmed	Trans-Omics for precision Medicine
TPM1	α-Tropomyosin
Tra 1-60	T cell receptor alpha locus 1-60
Tra-1-81	T cell receptor alpha locus 1-81(Podocalyxin)
TRIM63	Tripartite motif containing 63
TTL	Tubulin tyrosine ligase
TTN	titin
VCL	vinculin
WES	Whole exome sequencing
WGS	Whole genome sequencing
WHO	World health organization

SYNOPSIS

1) Introduction and background:

Cardiomyopathies are heterogenous group of muscle disorder resulting in impaired structural and functional ability of myocardium[1]. Commonly characterized by change in its size, shape, or thickness, leading to the heart's inability to pump blood effectively. There are different types of cardiomyopathies, including hypertrophic cardiomyopathy, dilated cardiomyopathy, and restrictive cardiomyopathy. These types affect the heart in various ways, such as causing the heart muscle to weaken, enlarge, thicken, or stiffen[2,3]. Some cardiomyopathies are inherited and can run in families due to genetic differences.

Focus of my study is restricted to hypertrophic cardiomyopathy (HCM) which is genetically autosomal dominant and clinically heterogenous in nature and characterized by increase in left ventricular wall and inter-septal wall thickness, in absence of any other systemic or cardiac condition that can lead to significant enlargement of heart wall like systemic hypertension or aortic valve stenosis[3]. HCM is among the most common form of cardiomyopathy with high prevalence rate of 1:250 to 1:500 and most common cause of sudden cardiac arrest in young individuals[3]. Multiple cardiac sarcomere contractile protein mutations cause HCM[4]. Currently, 11 mutated genes usually linked to HCM include β-myosin heavy chain (first discovered) and myosin-binding protein C. Other 9 genes, including as troponin T and I, regulatory and essential myosin light chains, titin, α-tropomyosin, α-actin, α-myosin heavy chain, and muscle LIM protein, are associated with less HCM instances. With almost 400 mutations, intragenic heterogeneity enhances genetic diversity[5]. However still 50 percent of cases are idiopathic in nature with no known definitive cause[5]. So far only three non sarcomeric genes have been implicated in HCM namely γ-2-regulatory subunit of the AMP-activated protein kinase (*PRKAG2*)[6], *LAMP-2*[7] and *ALKP3*[8]. Evidently there is big void in context of non sarcomeric gene variant identification and limited knowledge regarding the genetic influence of non sarcomeric proteins in HCM. In my thesis, I will outline our discovery of three novel non-sarcomeric HCM genes and their critical regulatory mechanisms in the disease pathogenesis in three distinct chapters.

The current study titled "***Discovery of Novel Hypertrophic Cardiomyopathy Genes and their functional implications using multi-model approach"*** is divided into seven chapters. The first chapter is introduction which highlights and reviews the literature on cardiomyopathy and its

different types along with the global burden of the disease as well as discusses open questions. The second chapter describes the objectives of the study highlighting the need of the study. Chapter three deals with material and methods of the thesis. Genetics (next generation sequencing), immuno-blotting, immuno-histochemistry, confocal imaging and quantitative real time PCR etc. has been predominantly utilized to achieve the objectives of the thesis. Chapter four and five discusses the findings of the thesis with respect to discovery of three novel gene loci associated with hypertrophic cardiomyopathy. Chapter four of the thesis discussing about the identification of novel gene variant (p.G47W) in ribosomal S6 kinase beta 1 (*RPS6KB1*) through whole exome sequencing and the mechanism involved in pathogenesis. This study have been published in Journal of medical genetics in 2021[9]. Chapter five highlights the discovery of a novel gene variant in tubulin tyrosine ligase gene (p.G219S) and its implication in disease pathogenesis via perturbing redox homeostasis in patient specific induced pluripotent stem cells derived cardiomyocytes (iPSCs-CMs). Sixth chapter discusses the summary and our contribution to current status of the disease understanding and the under-explored signaling gene involvement in disease causation and pathogenesis. And chapter seven consists of bibliography.

1) Objectives:

Specific objectives of my study are:

1.1) Identification of novel gene loci through next generation sequencing (NGS) for HCM

1.2) Deciphering the key mechanisms involved in disease pathogenesis corresponding to respective variants

2) Ribosomal protein S6 kinase beta-1 gene variants cause HCM by activating S6K1/rpS6/ERK signaling:

Using the above NGS methods, we discovered identical mutations (p.G47W) in the gene encoding ribosomal protein S6 kinase beta-1 (RPS6KB1 or S6K1) in two Indian families. We further identified two heterozygous variants (p.Q49K and p.Y62H) from the UK cardiomyopathy cohort in replication association studies. These variations are absent in both region-specific controls and various population genomic datasets. Further, we detected additional S6K1 mutation (p.P445S) in an Arab HCM patient. The functional effects of these mutants were assessed in cellular models by comparing representative mutant proteins of S6K1 with the wild type. The mutated proteins activated the S6K1 and hyperphosphorylated the rpS6/ERK signaling cascades, suggesting a gain-of-function effect[9].

3) ***TTL* variant causes HCM by inducing oxidative stress in patient-specific iPSC-derived cardiomyocytes:**

We used Next Generation sequencing techniques to examine two cohorts of Indian HCM patients and their respective controls. We identified an HCM patient-carrying tubulin tyrosine ligase (*TTL*) gene variant (p.G219S) that is absent in controls. TTL is involved in post-translational modification of alpha-tubulin by adding tyrosine residue to its C-terminal tail[10]. This absence leads to an abnormal de-tyrosinated and tyrosinated tubulin ratio, affecting the contractility in cardiomyocytes[11]. Our biochemical study suggests that *TTL* mutant proteins displayed delayed activity in tubulin tyrosination compared to the wild type. We modeled the patient HCM phenotypes by generating and characterizing the *TTL* mutant patient-specific iPSCs-derived cardiomyocytes (iPSC-CMs). The iPSC-CMs recapitulated hypertrophy, contractile dysfunction, and sarcomeric disarray due to increased de-tyrosinated alpha-tubulin. Furthermore, transcriptomic analysis from iPSCs-CMs revealed perturbed redox homeostasis, specifically activating NRF2 pathways leading to oxidative stress[12].

4) **Material and Methods:**

We performed whole exome sequencing (WES) of various patients and controls of different ethnicities. For functional evaluation, in accordance with different gene variants, we have used different cell lines like HEK293T, HL-1, H9C2, including human embryonic stem cells (hESCs) derived cardiomyocytes and for modeling disease in human system, we generated and characterized patient specific induced pluripotent stem cells (iPSCs) line from patient's PBMCs and differentiated to cardiomyocytes. For transcripts levels studies quantitative real time PCR was done against gene specific primers. Immunoblotting and immunohistochemistry were employed for understanding the protein levels in accordance with the need of the study against specific antibodies. Confocal imaging was used to investigate the cell size analysis and to look for levels of certain protein types.

5) **Discussion and future perspective:**

HCM is frequently characterized as a sarcomere-related disorder, mostly because of the numerous sarcomere gene mutations that have been detected in individuals and families affected by the condition[4,5]. Significant advances have been made in understanding the impact of sarcomere mutations in cardiac hypertrophy. Advancements in this field have resulted in the development of treatments that specifically address issues related to sarcomere dysfunction.

However there has been limited knowledge in comprehending the relationship between non-sarcomeric gene variants and cardiac hypertrophy. Despite several theories suggesting non-sarcomeric pathways, the knowledge remains incomplete. To add to current knowledge, this study leads to identification of three different non-sarcomeric gene variants and their associated mechanism culminating into pathological hypertrophy. Investigating non-sarcomeric gene variations in hypertrophic cardiomyopathy is critical for gaining a more complete picture of the disease's genetic landscape. This understanding has implications for diagnostics, patient care, and the development of targeted medicines (personalized/precision medicine), all of which aim to improve outcomes for HCM patients.

References:

1. Maron BJ, Towbin JA, Thiene G, et al. Contemporary definitions and classification of the cardiomyopathies: an American Heart Association Scientific Statement from the Council on Clinical Cardiology, Heart Failure and Transplantation Committee; Quality of Care and Outcomes Research and Functional Genomics and Translational Biology Interdisciplinary Working Groups; and Council on Epidemiology and Prevention. *Circulation*. 2006;113(14):1807-1816. doi:10.1161/CIRCULATIONAHA.106.174287

2. Chaffin M, Papangeli I, Simonson B, et al. Single-nucleus profiling of human dilated and hypertrophic cardiomyopathy. *Nature*. 2022;608(7921):174-180. doi:10.1038/s41586-022-04817-8

3. Maron BJ, Desai MY, Nishimura RA, et al. Diagnosis and Evaluation of Hypertrophic Cardiomyopathy. *J Am Coll Cardiol*. 2022;79(4):372-389. doi:10.1016/j.jacc.2021.12.002

4. Seidman CE, Seidman JG. Identifying sarcomere gene mutations in hypertrophic cardiomyopathy: a personal history. *Circ Res*. 2011;108(6):743-750. doi:10.1161/CIRCRESAHA.110.223834

5. Marian AJ, Braunwald E. Hypertrophic Cardiomyopathy: Genetics, Pathogenesis, Clinical Manifestations, Diagnosis, and Therapy. *Circ Res*. 2017;121(7):749-770. doi:10.1161/CIRCRESAHA.117.311059

6. Arad M, Benson DW, Perez-Atayde AR, et al. Constitutively active AMP kinase mutations cause glycogen storage disease mimicking hypertrophic cardiomyopathy. *J Clin Invest*. 2002;109(3):357-362. doi:10.1172/JCI14571

7. Maron BJ, Roberts WC, Arad M, et al. CLINICAL OUTCOME AND PHENOTYPIC EXPRESSION IN LAMP2 CARDIOMYOPATHY. *JAMA J Am Med Assoc*. 2009;301(12):1253-1259. doi:10.1001/jama.2009.371

8. Lopes LR, Garcia-Hernández S, Lorenzini M, et al. Alpha-protein kinase 3 (ALPK3) truncating variants are a cause of autosomal dominant hypertrophic cardiomyopathy. *Eur Heart J*. 2021;42(32):3063-3073. doi:10.1093/eurheartj/ehab424
9. Jain PK, Jayappa S, Sairam T, et al. Ribosomal protein S6 kinase beta-1 gene variants cause hypertrophic cardiomyopathy. *J Med Genet*. 2022;59(10):984-992. doi:10.1136/jmedgenet-2021-107866
10.McKenna ED, Sarbanes SL, Cummings SW, Roll-Mecak A. The Tubulin Code, from Molecules to Health and Disease. *Annu Rev Cell Dev Biol*. 2023;39(1):331-361. doi:10.1146/annurev-cellbio-030123-032748
11.Kerr JP, Robison P, Shi G, et al. Detyrosinated microtubules modulate mechanotransduction in heart and skeletal muscle. *Nat Commun*. 2015;6(1):8526. doi:10.1038/ncomms9526
12.Tonelli C, Chio IIC, Tuveson DA. Transcriptional Regulation by Nrf2. *Antioxid Redox Signal*. 2018;29(17):1727-1745. doi:10.1089/ars.2017.7342

PUBLICATION

Novel disease loci

BMJ Journals

Journal of Medical Genetics

Original research

Ribosomal protein S6 kinase beta-1 gene variants cause hypertrophic cardiomyopathy

Pratul Kumar Jain,[1,2] Shashank Jayappa,[1] Thiagarajan Sairam,[1] Anupam Mittal,[1,3] Sayan Paul,[1] Vinay J Rao,[1] Harshil Chittora,[1,4] Deepak K Kashyap,[1,5] Dasaradhi Palakodeti,[6] Kumarasamy Thangaraj,[5,7] Jayaprakash Shenthar,[8] Rakesh Koranchery,[9] Ranjith Rajendran,[9] Haghighi Alireza,[10,11,12] Kurukkanparampil Sreedharan Mohanan,[9] Andiappan Rathinavel,[13,14] Perundurai S Dhandapany [1,15,16]

CHAPTER: 1

INTRODUCTION

1.1 **Cardiomyopathy:**

Cardiomyopathy refers to heterogenous heart muscle disease that affects its ability to pump blood effectively. Because of high complexity in defining the disease panel members of AHA have defined the disease as "*Cardiomyopathies are a heterogeneous group of diseases of the myocardium associated with mechanical and/or electrical dysfunction that usually (but not invariably) exhibit inappropriate ventricular hypertrophy or dilatation and are due to a variety of causes that frequently are genetic. Cardiomyopathies either are confined to the heart or are part of generalized systemic disorders*."[1]

Primary cardiomyopathies are majorly classified into genetic, acquired or mixed (both genetic and acquired). And subclassified into following types: hypertrophic cardiomyopathy (HCM), left ventricular non compaction (LVNC) and Arrhythmogenic Right Ventricular Cardiomyopathy/Dysplasia (ARVC/D) falls under genetic, myocarditis (inflammatory cardiomyopathy) falls under acquired whereas dilated cardiomyopathy (DCM) and restrictive cardiomyopathy (RCM) falls under mixed.[2]

DCM is characterized by weakening and enlargement of heart muscle, leading to major systolic dysfunction[3], HCM on the other hand, is characterized by an abnormal thickening of the heart muscle, making it harder for the heart to relax and fill with blood leading to primarily diastolic dysfunction[4]. RCM involves the stiffening of the heart muscle, which restricts its ability to expand and contract properly[5], LVNC results in softening of the ventricular wall due to increased trabeculation while ARVD/D is characterized by fibrofatty replacement of myocardium.[6]

1.2 Epidemiology of Cardiomyopathies:

Cardiovascular diseases are significant global health concern contributing to morbidity and mortality. WHO reports suggests that CVDs are leading cause of death worldwide with 17.9 million death in year 2019, representing 32% of deaths globally and the numbers are suggested to increase to much higher scale in coming years.[7] This frequency underscores the urgent need to address the risk and causative factors to improve prevention and treatment strategies.

Among CVDs, cardiomyopathies contribute a to a big portion (~10%) of inherited cardiovascular diseases. Cardiomyopathies can be caused by various factors including predominantly genetic predisposition, infections and epigenetic factors etc. This often leads to complications like heart failure, arrhythmias and sudden cardiac deaths.

Among inheritable genetic primary cardiomyopathies prevalence rate of HCM is 1:250 to 1:500 in adults irrespective of different ethnicities usually occurs in adolescents and young adults. For DCM a very thorough study on epidemiology is lacking, however estimate suggests the incidence ad prevalence rate roughly double the HCM cases. Prevalence of ARVC is not extensively explored as multiple clinical evaluations required for diagnosis, but estimated at 1:2000 to 5000. [2]

1.3 Classification of Cardiomyopathies:

Based on the predominant organ affected cardiomyopathies have been classified into two broad categories namely primary and secondary. Primary cardiomyopathies are the ones which are principally confined to heart and have been further classified into genetic (hypertrophic cardiomyopathy (HCM), Left ventricular noncompaction (LVNC), Arrhythmogenic right ventricular cardiomyopathy/dysplasia (ARVC/D), long QT syndrome (LQTS), short QT syndrome (SQTS), Brugada syndrome, and catecholaminergic polymorphic ventricular tachycardia (CPVT)), Acquired (inflammatory cardiomyopathy (myocarditis), stress cardiomyopathy: ("Tako-Tsubo") cardiomyopathy, peripartum cardiomyopathy and mixed category (both genetic and acquired) (Dilated cardiomyopathy (DCM) and restrictive cardiomyopathy). Secondary cardiomyopathies are characterized by abnormal myocardial incrimination in a wide range of widespread systemic (multiorgan) disorder. As the matter of fact that certain cardiomyopathies primarily affect the heart but can have consequent actions on other organs, the distinction between primary and secondary types is contextual and pins one's hope on the assessment of the clinical significance and outcomes of myocardial process.[8]

1.4 Hypertrophic cardiomyopathy:

Hypertrophic cardiomyopathy (HCM) is the most common, autosomal dominant genetic form of cardiomyopathy and major cause of mortality in young individuals resulting from sudden cardiac arrest. Hypertrophic cardiomyopathy (HCM) is defined by the presence of an enlarged and thickened left ventricle (LV) and inter-septal wall, without any other underlying systemic or cardiac condition that might account for the observed degree of wall thickening.[9]

Individuals with a genetic abnormality for hypertrophic cardiomyopathy (HCM) may not always show clinical signs of the condition, such as left ventricular hypertrophy on an echocardiogram, abnormal electrocardiogram (ECG) readings, or symptoms. Additionally, ECG changes might

occur before the onset of hypertrophy. And thus, requires a thorough clinical evaluation for the diagnosis.

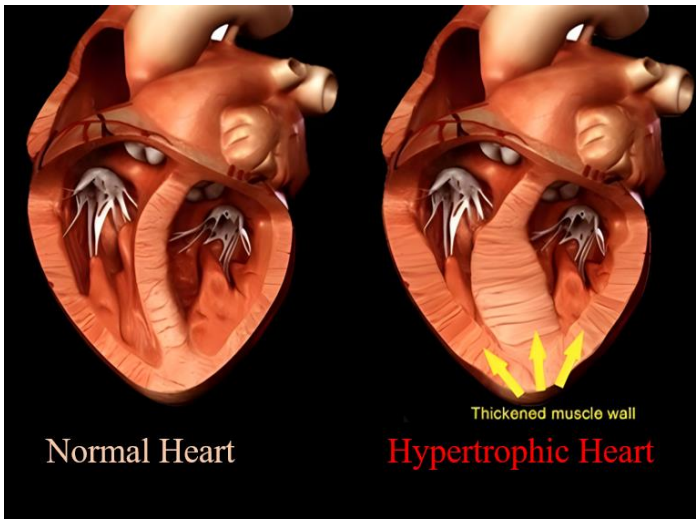

HCM is majorly caused by mutations in genes that encode contractile proteins found in the cardiac sarcomere. To date, there are 11 genes are reported with variants that are linked to hypertrophic cardiomyopathy, with the most often seen ones being β-myosin heavy chain (*MYH7*) and myosin-binding protein C (*MYBPC*). The remaining 9 genes are responsible for a smaller number of instances of HCM, which include troponin T and I (*cTnT, cTnI*), regulatory and essential myosin light chains, titin (*TTN*), α-tropomyosin (*TPM*), α-actin (*ACTA1*), α-myosin heavy chain (*MYH7*), and muscle LIM protein.[10] Among these, the presence of genetic diversity further aggravates significant intragenic heterogeneity, with over 400 distinct mutations identified so far. The most frequent kind of mutations are missense mutations resulting in a single nucleotide which makes HCM a predominantly a monogenic disorder. However, other types of mutations like as insertions, deletions, and splicing mutations that result in the production of truncated sarcomeric proteins are also observed. The wide range of characteristics observed in individuals with HCM can be attributed to the mutations that cause the illness, as well as the potential effect of modifier genes and environmental variables.

Recent reports have identified mutations in two genes related to cardiac metabolism that are responsible for primary cardiac glycogen storage illnesses in older children and adults. The γ-2 regulatory subunit of the AMP-activated protein kinase (*PRKAG2*) is linked to varying levels of left ventricular hypertrophy and ventricular pre-excitation.[11] Another scenario entails the gene responsible for encoding lysosome-associated membrane protein 2 (LAMP-2), leading to the development of Danon-type storage disorder.[12] These mutations can cause clinical symptoms that are similar to or cannot be distinguished from those of sarcomeric hypertrophic cardiomyopathy. These illnesses are now classified as a subset of previously identified infiltrative types of left ventricular hypertrophy, including Pompe disease and Fabry's disease.[13]

LV hypertrophy is linked to other disorders characterized by significant thickening of the LV wall. These cardiomyopathies encompass secondary forms such as Noonan syndrome, mitochondrial myopathies caused by mutations in mitochondrial DNA or mitochondrial proteins linked to ATP electron transport chain enzyme deficiencies, metabolic myopathies characterized by defects in ATP production and utilization related to abnormalities in fatty acid oxidation, and infiltrative myopathies like glycogen storage diseases, Hunter's and Hurler's diseases, as well as transient and nonfamilial cardiomyopathy occurring alongside generalized organomegaly.

1.5 Classification of HCM:

In hypertrophic cardiomyopathy (HCM), there are two main forms: Obstructive HCM and Nonobstructive HCM which differ in their clinical features.

a. **Obstructive HCM** is characterized by heart muscle thickening, especially the septum that separates the ventricles, thereby obstructing or decreasing the flow of blood from the left ventricle to the aorta. These obstructions present symptoms such as shortness of breath, chest pain, tiredness, palpitations, dizziness, fainting spells and increased risk for sudden cardiac death. Heart failure, mitral valve regurgitation, arrhythmias and sudden cardiac death can be complications of Obstructive HCM.[14,15]

b. **Nonobstructive HCM** refers to thickening and stiffening of the left ventricle without impeding blood flow directly. However, this translates into an inadequate ejection of blood with every heartbeat. Signs such as chest pain, dyspnea (shortness of breath), fatigue, arrhythmias (abnormal heart rhythms), dizziness or lightheadedness upon standing up or exertion), fainting episodes due to a drop in BP and swelling in other parts of body could suggest non-obstructive HCM. Over time Nonobstructive HCM may turn into more depressed heart function and quality of life resulting atrial fibrillation and heart failure along with others.[16]

For diagnosis purposes peak gradient across LVOT is usually raised (>30 mmHg at rest or >50 mmHg during provocation) while echocardiography shows high velocity jet across LVOT caused by hypertrophied septum leading systole as well as obstruction.[17] HCM was established as

nonobstructive (<30 mm Hg at rest and stress), labile (<30 mm Hg at rest and ≥30 mm Hg with stress), and obstructive (≥30 mm Hg at rest and stress).[18–20] In addition, it has also been shown that epsilon (ε) (longitudinal strain) value greater than -10.6% has sensitivity 85%, specificity 100%, positive predictive accuracy 91.2% for diagnosis of HCM;[21] on other hand nonobstructive HCM has less significant LVOT obstruction with lower peak gradients. In both types of HCM echocardiography shows increased left ventricular wall thickness but different patterns depending on presence or absence of obstruction. These echocardiographic indices can help differentiate between these cases and guide treatment decisions to ensure optimum management of this complex cardiac condition.

1.6 Clinical manifestation of HCM:

Despite high prevalence rate, clinical diagnosis remains fairly unclear in HCM. Unlike olden times, with the advent of various diagnostic technique, HCM now comes under treatable disease and associated with extended longevity. But only possible with early diagnosis of the pathological condition. The process of diagnosing cardiomyopathy in patients requires a very careful analysis of medical tests and imaging techniques. These tests, including electrocardiograms (ECGs) echocardiograms and cardiac magnetic resonance imaging (MRI) help assess the hearts' structure and function. They also aid in identifying any thickening of the heart muscles and detecting associated complications, like arrhythmias. Additionally genetic testing may be recommended to identify gene mutations linked to cardiomyopathy. By utilizing a combination of these tools' healthcare professionals can accurately monitor the condition in patients.

Presence of hypertrophy in cardiac muscles (hypertrophic cardiomyopathy) many at times goes unnoticed due to absence of symptoms or minimal symptoms. This itself establishes the complexity and variability of disease. Many individuals lifelong may entirely remain asymptomatic and others might attain only mild symptoms that may not impair their normal functioning. This variability is due to adaptability of heart to various stress (workload) situations masking the underlying re-modelling. However, its crucial to recognize the pathological condition, despite the absence of symptoms as individuals with HCM still faces the risk of sudden cardiac arrest. Early detection, extensive clinical evaluation and pertinent management strategies are

essential to mitigate the potential complications associated with this genetic cardiovascular disorder.

Following lined up the most common clinical conditions in an HCM patient:

1.6.1 Diastolic dysfunction:

HCM is a very heterogenous inheritable disease. Despite this heterogeneity in phenotypic expression, most of the affected individuals will show a certain degree of diastolic dysfunction, which is characterized by impaired left ventricle filling.[4] This phenotype is multifaceted and very complex resulting from variety of molecular signaling, myocardial tissue consequently reaching up to global left ventricular level. Degree of ventricular hypertrophy, disarrayed myocardial tissue and interstitial fibrosis are the morphological parameters which defines the level of diastolic dysfunction.[22] Left ventricle filling impairment occurs as a consequence improper relaxation. In diastole ventricle lose the ability to generate force and shortens before returning to an unstressed length and force. Diastolic dysfunction arises when these processes are extended, delayed, or incomplete. Unlike LV end-diastolic pressure volume which is a passive process, left ventricular filling is neither slow nor a passive process. The peak flow rate across the mitral valve is equal to or greater than the peak flow rate across the aortic valve.[23] To be clear about the terms diastolic dysfunction and diastolic heart failure which differs in former being abnormal mechanical property and later being the classified as clinical syndrome.[24] In absence of any single quantitative measurement of filling pressure echo doppler could be used for prognosis of HCM. Trans-mitral doppler E/A ratio (E-wave /A- wave) parameter measure such impairment which measure the relaxation and the mitral deceleration time (DT) resulting in quantification of pulmonary capillary wedge pressure in patients with LV dysfunction.[4] Normal diastolic function in a particular individual ranges from 0.75-1.5 and DT is <220ms. E/A ratio of < 0.75 denotes mild diastolic dysfunction (Grade I, impaired relaxation), Moderate or Grade II DD (pseudo-normal) is distinguished by decreased LV compliance with increased LA pressure, and hence the E/A ratio seems normal, but reversal occurs with the Valsalva technique. In severe or Grade III DD (restrictive filling), there is severely decreased compliance, leading further increase in LA pressure, culminating in a very elevated E wave and low A wave (E/A > 1.5) and substantially reduced DT (< 150ms) and IVRT (Isovolumic relaxation time) (< 70ms).[25]

1.6.2 Left ventricular outflow tract obstruction (LVOTO):

LVOT refers to the passage which conduit blood flow from left ventricle and pumped out of aorta to rest of the body. In HCM dynamic LVOTO is observed in around ~70% of the patients.[26] LVOT obstruction (LVOTO) encompasses a line of stenotic lesions that begin in the anatomical left ventricular outflow tract (LVOT) and stretch to the descending the provisions of the aortic arch. These obstructions could be sub-valvar (structures located below or beneath the valve), valvar (refers to structures associated with or pertaining to the valve itself), or supra-valvar (refers to structures located above or beyond the valve).[27] Hinderances to forward flow can occur alone or in conjunction, as is typical with a bicuspid aortic valve and aortic coarctation. All of these abnormalities can further increase the load on the left ventricle and, if severe and untreated can lead to extreme form of hypertrophy, dilatation, and heart failure.[27] With the advancements in echocardiography technology many patients with HCM are now being diagnosed with dynamic LVOTO, in absence or presence of mild septal hypertrophy.[16, 17] Patients with HCM possess the higher incidences of mitral valve (MV) abnormalities (mitral valve regurgitation) and papillary muscle (PM) abnormalities in contrast to the control subjects that have potential to account for severe LVOTO.[26]

1.6.3 Chest pain:

Patients with HCM typically experience ischemic discomfort in their chests, which could have or might not have the characteristics of angina pectoris and arises due to disparity in myocardial oxygen demand and supply.[9] The reasons for this could be following.

Firstly, the thicker rigid structure in HCM intrudes onto space within hearts chambers precisely the left ventricular outflow tract. The intramural coronary arteries, which supplies the oxygen rich blood to the myocardial tissue becomes squeezed and narrowed within this thickened wall leading to myocardial hypoperfusion. Secondly, the demand of oxygen by hypertrophied cells is much higher because of the size and metabolic needs compared to the normal myocardial cells leading perturbed demand and supply meet.[29] As a result in condition of stress (increased cardiac strain), patients with HCM feel discomfort in chest. This pain may emerge as ischemic chest pain, similar to angina pectoris, which is often experience by patients as tightness, pressure, squeezing, or heaviness in the chest. Nevertheless, these symptoms do not always stick to the conventional

pattern of angina, and many patients describe them differently. Ischemic chest pain and structural defects in HCM patients takes the attention of clinicians and researchers to manage individuals with this combined illness.

1.6.4 Arrhythmias:

Palpitations, presyncope, and fainting (syncope) are prominent signs and symptoms of heart failure (HCM), which is frequently accompanied by persistent non-sustained ventricular tachycardia. Non-sustained ventricular tachycardia (NSVT) is a significant risk factor for stroke given that it can develop to ventricular fibrillation. Syncope (fainting) can also be induced by significant LVOT blockage. The fundamental processes of ventricular arrhythmias in HCM are unknown, although possible causes include cardiac hypertrophy, interstitial fibrosis, myocardial ischemia, and myocyte disarray.

Patients with hypertrophic cardiomyopathy (HCM) combined with left ventricular outflow tract (LVOT) obstruction, often shows the prevalence of atrial fibrillation (AF). An estimated 25% of HCM subtypes are associated with AF, which has an annual incidence rate of around 2-3%.[30,31] In such individuals suffering from this disorder, having AF exacerbates the symptoms and worsens the diastolic left ventricular pressure further impacting cardiac performance. Furthermore, irregularity in heartbeats as in AF may increase risk for thromboembolic events including strokes; blood clots can form in the atrium. The exact process by which atrial fibrillation arises in HCM patients are poorly understood despite of extensive investigations. Some potential mechanisms include enlargement of atria, increased mechanical strain on atria due to thickened ventricular walls, scarring within the atrial myocardium, abnormal production of mutated proteins known to be associated with HCM and modifications in gene expression pattern.[32]

In brief, HCM patients can show symptoms ranging from shortness of breath, chest pain, dizziness and arrhythmias. The hypertrophied muscle consequently impacts the blood flow to myocardial tissue and cab be further enhanced upon strenuous exercise or emotional distress. Therefore, to manage HCM, these symptoms need to be kept in check to avoid any other implications resultant of improper disease management.

1.7 Need for early detection:

Early detection and accurate diagnosis play a pivotal role, in managing the health outcomes of patients with cardiomyopathy ultimately improving their quality of life. Detecting and diagnosing cardiomyopathy at a stage is essential for managing patients' health outcomes and enhancing their overall well-being. By identifying and monitoring symptoms like shortness of breath, chest pain, dizziness and irregular heart rhythms healthcare professionals can intervene quickly and provide appropriate treatment. Timely diagnosis enables the implementation of management plans that include lifestyle adjustments, medications or even invasive procedures if necessary. This proactive approach helps prevent complications such as heart failure, arrhythmias or sudden cardiac death. Additionally early detection empowers patients to make decisions about their health actively participate in shared decision making with healthcare providers. Take preventive measures to optimize their cardiovascular health.

1.8 Challenges in diagnosis:

Numerous challenges or complications may arise during the diagnosis process for hypertrophic cardiomyopathy patients specifically differentiating it from other cardiac conditions or recognizing unusual presentations. Moreover, accurately diagnosing cardiomyopathy can be challenging due, to its clinical manifestations that may overlap with other heart related conditions. Differentiating cardiomyopathy from conditions, like dilated athletes heart requires a thorough assessment of symptoms, medical history and diagnostic test results. It is more challenging to identify presentations of hypertrophic cardiomyopathy particularly in elderly individuals or those with minimal symptoms.

However, with advent of modern advancements in echocardiography like tissue doppler imaging, 2D and 3D speckle tracking echocardiography, M-mode, Pulse wave or continuous-wave Doppler, color doppler and cardiac magnetic resonance (MRI) diagnosis improved the clinical diagnosis.[33] These techniques along with genetic testing have made clinicians to diagnose the disease more precisely.

1.9 Traditional Genetic Approaches for Studying HCM:

Conventional or traditional methods for genetic studies that have been historically used to investigate genetic basis of disease and HCM are outlined as follows:

1.9.1 Linkage Analysis:

A classical genetic tool to locate the gene locus linked to genetic disorders like HCM is linkage analysis, which is based upon the notion of genes located close to each other in chromosome are inherited together more often than by chance expectation.

With respect to HCM, familial studies were often used to discover genomic areas which are inherited with disease manifestation. DNA sequence variation scattered throughout the genome are used as genetic markers for analysis. Pattern of inheritance of these genetic markers cases (affected) and controls (unaffected) family members led researchers to identify chromosomal areas with genes associated with HCM. Benefits of linkage analysis for gene loci discovery comes up even when the underlying genes is unknown. By virtue of linkage analysis genetic variability in affected families can be mapped which helps in revealing HCM's genetic architecture. "14q1" is the first discovered locus associated with HCM was identified using linkage analysis of 96 individuals spanning in 4 generations.[34] Shortly after this discovery led to discovery of defects at locus 14q11-12, establishing two homologous genes *MYH6* and *MYH7*, a potential causal genes for HCM.[35]

Limiting factors for linkage analysis come in context of rare illness like HCM in absence of big pedigrees with several affected family members to have a statistically significant interpretation. Furthermore, linkage mapping identifies the gene loci to broader chromosomal regions rather than individual genes which further needs a detailed mapping and gene identification. Despite this linkage analysis has helped researchers to explain several inherited diseases including HCM and led to discovery of several HCM associated genes to helped to comprehend the disease molecular underpinnings.

1.9.2 Candidate Gene Approach:

This is focused approach of gene variant identification based upon the speculation of certain genes already known to be involved in particular disease or trait.[36] For instance, in case of HCM, gene variant identification will be specifically aimed within the genes that are known to contribute to

development or disease progression. This approach has been widely applied to understand aspects of cardiac anatomy, function and gene regulation in reference to HCM disease manifestation. Based on the biological relevance of the gene with respect to heart structure, contractility, signaling cascades and relevant physiological processes researchers pick the candidate genes. Sarcomeric gene like actin, myosin, troponin etc., cardiac energy metabolism related genes, development related genes, cardiac growth and hypertrophy related genes, channel protein are often taken into consideration. Candidate gene analysis is indispensable for positional cloning of QTLs controlling the significant genetic variation of interested traits.[36] After identification of variant p.Arg403Glu (p.R403Q) mutation in the *MYH7* gene (beta myosin heavy chain) using linkage analysis and co-segregation studies led researchers to identify various other gene variants in the same gene using candidate gene approach.[35] Identification of *MYBPC3* (cardiac myosin-binding protein C3),[37] *TNNT2* (cardiac troponin T)[38] and *TNNI3* (cardiac troponin I)[39] variants have been discovered as causal gene variants for HCM using candidate gene approach.

Limitation of candidate gene approach it requires a prior knowledge about the gens implicated in the disease and thus can miss out on the genes which are unexplored for the disease.

Thorough genetic analysis of HCM disease manifestation needs method like genome wide association studies (GWAS) and next generation sequencing (NGS) to identify novel genes and novel gene variants.

1.10. Next Generation Sequencing in Genetic Studies of HCM:

HCM is a complex disease and potentially life-threatening situation and demands for careful monitoring and proper disease management. By utilizing NGS a thorough genetic screen of each individual is now possible which could help healthcare providers to better understand the risk associated with the disease and could suggest a treatment plans accordingly. This approach will help not only the affected individuals but also the family members who might be at risk of the disease. Early detection can also help healthcare providers and genetic counsellors to direct patients' families to provide valuable insights of genetic predisposition for HCM and can be informed to be proactive with respect to health. It is only through proper education and support patients and their families could be navigated through the challenges of living with the heart disease.

In contrast to conventional sequencing methods, higher sensitivity in low frequency allele detection, sample multiplexing and tremendous pace of turnover for larger sample size and cost effectiveness of new age NGS technology bring forth the abilities of novel gene discovery at a unimaginable scale.[40]

In present world NGS has become integrated part of personalized medicine (genomic medicine) field with its broad applicability in laboratory medicine. Discovery of novel gene variants in association with disease have spiked exponentially with cutting edge NGS technology. Most commonly used approaches for disease associated gene discovery can briefly be categorized into 1) WES (whole exome sequencing) or WGS (whole genome sequencing) where a patient cohort of similar clinical condition is analyzed and rare variants are filtered out, and 2) Tri-Exome sequencing, where a proband and its family members are taken into account and variants are filtered out on the basis of disease inheritance for identification of causal gene.[40]

1.10.1 Advantages of exome in identifying novel gene variants:

WES is cost-effective because it focuses only on protein coding regions of the genome therefore reducing expenses. This facilitates quick interpretation of data in clinical settings where only clinically relevant sequences are needed. Additionally, several HCM causing mutations, which are clinically actionable are located within exonic regions.

For this study we have employed **Tri-Exome sequencing** for the gene identification. Tri-exome technique requires the exomes of a trio, usually consisting of two parents and an affected child, to be sequenced and this has been identified as one the best genetic analysis approaches for several reasons.

- Firstly, it helps in identifying de novo mutations which are necessary for understanding the genetic mechanism of sporadic or familial diseases. By comparing the exomes of parents and the affected child, tri-exome sequencing makes it easier for clinicians to identify therapeutically relevant variants.
- Additionally, this approach enables the detection of compound heterozygosity which can be useful in diagnosing recessive genetic disorders. The incorporation of family data improves precision in gene diagnosis thus distinguishing pathogenic from benign variants required for personalized treatment planning.

- Lastly, knowledge on inheritance patterns acquired from tri-exome sequencing is very important in genetic counseling and family planning. Thus, tri-exome sequencing is a powerful tool in clinical diagnostics and genomic research that provides comprehensive insights into the genetics behind diseased states with great potential to revolutionize medical practice.

1.11 Molecular basis of HCM:

Cardiomyopathies are very heterogenous in nature can and the penetrance varies across different individuals mainly characterized overall heart enlargement, thickened, or rigid and thus leading to complications such as heart failure. Among various factors, genetic factors are the primary causes of hypertrophic cardiomyopathies. This includes protein abnormalities in sarcomeres which make up the contractile units of muscle cells (as shown in reference figure above).

Sarcomeres which form part of the basic structure and functional unit of muscles (reference figure) including the heart muscle contain different proteins organized into thick and thin filaments; there are few major proteins coded by genes namely ***MHY7, MYBPC3, TTN, TNNT2, TNNI3, ACTA1, TPM1*** and several minor ones. Generating force during muscular contraction is mainly done by myosin heavy and light chains found in most thick filaments. Among these major proteins Myh7 and MyBPC3 alone accounts for 70 percent of sarcomeric gene related cardiomyopathies.

Sometimes any mutation may arise from both these proteins especially those concerned with sarcomere building blocks hence causing abnormal cardiac muscle contractions thereby leading to cardiomyopathy. The clinical manifestations related to this genetic predisposition creates a heterogeneous nature for cardiomyopathies. Consequently, there is need to understand the role played by these proteins in combination with their genetic basis since it would be helpful while trying to comprehend how myocardium could be damaged resulting in various diagnostic and treatment modalities being adopted henceforth.

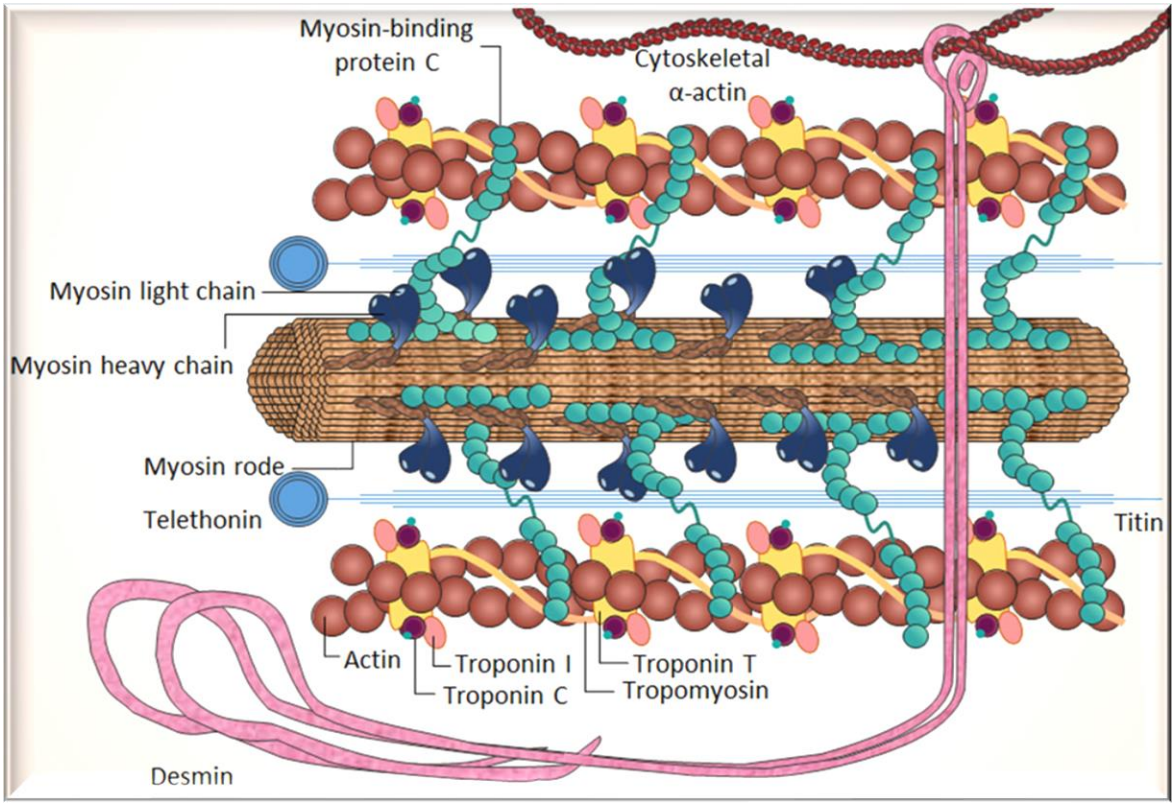

Figure1.1: Structural cardiac sarcomeric elements involved in HCM pathogenesis

(Adapted from Babken Asatryan & Argelia Medeiros-Domingo, Journal of Molecular Medicine, review, 2018.

The predominant thin filament composition in cardiac cells consists of actin and other regulatory proteins such as tropomyosin and troponin. During muscle relaxation, the blockage of active sites on actin is done by tropomyosin molecules, which therefore, prevent interaction between myosin and actin, hence inhibiting muscle contraction. When calcium ions are released from the sarcoplasmic reticulum within cardiac muscle cells and then muscle contraction begins. These calcium ions bind to troponin resulting into changes on the shape that dislodges tropomyosin molecules from their inhibitory positions in actin thus exposing myosin binding sites. Consequently, adenosine triphosphate (ATP), molecules associated with myosin are acted upon by the enzyme adenosine triphosphatase (ATPase) to produce an energized myosin molecule. Later, this energized myosin molecule attaches itself to actins leading to the release of stored energy by the head of myosin. Bound crossbridge movement during this process resembles that of

rowing. This forces the actins molecules towards the middle of sarcomere hence causing muscle contraction. Muscle contraction occurs in a normal way when adenosine triphosphate (ATP) attaches to myosin, detaching it from actin and enabling it to be ready for another binding cycle as per calcium availability in sarcomere. Yet, mutations in sarcomeric proteins interfere with the whole process. Earlier this disease has been recognized as "Diseases of Sarcomere". However, with around 50% cases being idiopathic led researchers to investigate the non-canonical reasons behind the disease pathogenesis and consequently some signaling genes have come in front so far like:

ALKP3 - a pseudokinase, loss of function of which leads to mis-localization of key M-band proteins like myomesin proteins (involved in force buffering) resulting in overall dysregulation of crucial sarcomeric protein turnover.[41]

RAF1- a RAS-MAPK family member, Noonan syndrome associated variants in RAF1 have shown to cause heart failure via activated MEK1/2 signaling in absence of ERK1/2 signaling but rather activation of ERK5.[42,43]

ADIPOR1- a member of progestin and adipo-receptor family. Variants in this gene have now been reported to cause HCM via p38/mammalian target of rapamycin (mTOR) and/or ERK1/2 pathway.[44]

RPS6KB1 (this study)- a serine threonine kinase, a downstream target of mTORC1, involved in regulating protein synthesis. Variants in the gene reported in present study are implicated in HCM via upregulation of protein synthesis rate (increased phosphorylation of ribosomal protein S6) in the cells and activation of ERK1/2.[45]

These discoveries signify the importance of signaling gene variants involved in HCM pathogenesis and opens the much anticipated but underexplored research void. The identification of signaling genes has revolutionized our understanding of hypertrophic cardiomyopathy (HCM), which was previously thought to be solely caused by sarcomeric gene abnormalities. This discovery also partially explains the broad spectrum of disease abnormalities observed in patients.

1.12 Genes implicated in HCM:

Listed below are the genes known to cause HCM so far with their ClinGen evaluation as definitive, moderate, limited, disputed and not curated.[46]

ClinGen evaluation:

Definitive: A substantial body of research and clinical diagnostic findings consistently demonstrate the gene's involvement in disease, with robust genetic evidence and corroborating experimental data confirming its causal connection.

Moderate: The gene is likely associated with a disease, with supportive evidence including convincing genetic data. There is no contradictory evidence to suggest otherwise.

Limited: Indicates that the gene-disease relationship is plausible but not sufficient to meet the criteria for Moderate evidence. Examples include moderate cases with consistent phenotypes, small cases with well-defined presentations, rare cases with distinct phenotypes, or single cases with bi-allelic loss of function variants.

Disputed: A few cases involve non-specific, genetically heterogeneous phenotypes and missense variants, with no experimental data available. All reported cases scored 0 or below 1 after GCEP review, with initially reported variants being too high to be consistent with the disease.

Table 1.1 Genes known for HCM

S.no	Gene	Function	Gene type	ClinGen	reference
1	MHY7 (β-myosin heavy chain)	Contractile force generation	Sarcomeric	Definitive	35
2	MYBPC3 (myosin binding protein C3)	Cardiac muscle contraction	Sarcomeric	Definitive	47
3	TNNT2 (Cardiac troponin T2)	Cardiac muscle contraction	Sarcomeric	Definitive	38
4	TNNI3 (Cardiac troponin I3)	Cardiac muscle contraction	Sarcomeric	Definitive	39
5	TPM1 (α-Tropomyosin)	regulating muscle contraction by controlling the interaction between actin and myosin	Sarcomeric	Definitive	38
6	ACTC1 (Cardiac alpha actin)	facilitating the generation of contractile force during cardiac muscle contraction.	Sarcomeric	Definitive	48
7	MYL2 (Regulatory myosin light chain 2)	regulating muscle contraction by controlling the interaction between actin and myosin	Sarcomeric	Definitive	49
8	MYL3 (Essential myosin light chain 3)	muscle contraction and relaxation	Sarcomeric	Definitive	49
9	CSRP3 (Cysteine and glycine rich protein 3)	structural integrity, mechano-transduction signaling pathways	Non-sarcomeric	Definitive	50
10	FHL1 (Four-and-a-half LIM domains 1)	muscle development and function, cellular homeostasis	Non-sarcomeric	(NA)	51,52

11	***MYOZ2 (Myozenin 2) (Calsarcin 1)***	*regulation of muscle contraction*	*Sarcomeric*	*Disputed*	[53]
12	***PLN (Phospholamban)***	*modulating cardiac muscle contraction and relaxation by regulating calcium uptake and release*	*Non-sarcomeric*	*Definitive*	[54]
13	***TCAP (Tcap (telethonin))***	*anchoring titin to the Z-disc*	*Sarcomeric*	*Disputed*	[55]
14	***TRIM63/MuRF1 (Muscle Ring finger protein 1)***	*muscle-specific E3 ubiquitin ligase, regulates protein degradation, particularly during conditions such as muscle atrophy and remodeling.*	*Non-sarcomeric*	*Moderate*	[56]
15	***TTN (titin)***	*molecular spring, maintaining the structural integrity of sarcomeres*	*Sarcomeric*	*Limited*	[57]
16	***ACTN2 (a-2 Actinin)***	*organizing the cytoskeleton and anchoring actin filaments to the Z-discs, muscle contraction and integrity.*	*Non-sarcomeric*	*Definitive*	[58]
17	***ANKRD1 (Ankyrin repeat domain 1)***	*transcriptional regulation, sarcomere assembly, and mechano-sensing in cardiac muscle cells*	*Non-sarcomeric*	*Disputed*	[59]
18	***CASQ2 (Calsequesterin-2)***	*calcium storage and release within the sarcoplasmic reticulum, cardiac muscle contraction and relaxation.*	*Non-sarcomeric*	*Disputed*	[54]
19	***CAV3 (Caveolin 3)***	*formation of caveolae, maintains cell membrane integrity and regulating signal transduction*	*Non-sarcomeric*	*Limited*	[60]

20	***JPH2 (Junctophilin-2)***	*Junctophilin-2 maintains the structure of junctional complexes between the sarcoplasmic reticulum and the cell membrane, facilitating efficient calcium signaling and excitation-contraction coupling*	*Non-sarcomeric*	*Moderate*	[61]
21	***LDB3 (Lim domain binding protein 3)***	*maintains structural integrity of the sarcomere and regulates gene expression*	*Sarcomeric*	*Disputed*	[62]
22	***MYH6 (Myosin heavy chain a)***	*generates contractile force during cardiac muscle contraction*	*Sarcomeric*	*Limited*	[63]
23	***MYLK2 (Myosin Light chain kinase 2)***	*regulates the interaction between actin and myosin in smooth muscle cells. mediates smooth muscle contraction*	*Non-sarcomeric*	*Disputed*	[64]
24	***NEXN (Nexilin)***	*maintains the structural integrity of the sarcomere*	*Sarcomeric*	*Limited*	[65]
25	***TNNC1 (Cardiac troponin C1)***	*regulates the interaction between actin and myosin filaments and regulates contraction cycle*	*Sarcomeric*	*Definitive*	[66]
26	***VCL (vinculin)***	*maintains the structural integrity of intercalated discs and facilitating cell-cell adhesion*	*Non-sarcomeric*	*Disputed*	[67]
27	***ALPK3 (Alpha kinase 3)***	*signal transduction, cell cycle regulation, and cytoskeletal organization*	*Non-sarcomeric*	*Definitive*	[68]
28	***FLNC (filamin C)***	*sarcomere organization, mechano-sensing, ion channel regulation, cell adhesion and migration, and signaling pathway regulation*	*Non-sarcomeric*	*Definitive*	[69]

FHOD3 (Formin Homology 2 Domain-Containing 3)	*regulates sarcomere organization, myofibrillogenesis, and cardiac contractility*	*Non-sarcomeric*	*Not curated so far*	[70]	

1.13 Multi-model approaches in understanding HCM mechanisms:

Understanding how disease is caused at the molecular level is crucial in the search for cure, prevention and better outcomes. To understand the fundamental molecular signaling pathways involved in HCM pathogenesis, we employed different model systems towards discovering disease-relevant mechanisms. We aim to dissect these pathways with a view to discovering novel targets or biomarkers for diagnosing and treating these diseases. Moreover, deciphering disease mechanisms could help unlock phenotypic heterogeneity amongst patients as well as differential treatment responses allowing personalized medicine approaches.

Our approach will involve a combination of patient specific pluripotent stem cell-derived cardiomyocytes and various other cellular models.

Cellular Models (H9C2, HL-1):

H9C2 and HL-1 are commonly used cell lines for studying cardiac physiology and pathology. These models permit examination of cellular response to diverse stimuli as well as characterizing molecular changes associated with diseased condition.

These models were employed to explore central issues in relation to gene expression dysregulation, protein signaling perturbation, as well as cellular functional impairment during disease pathogenesis. So, through visualizations using microscopy techniques and by doing quantitative assays at both genetic and protein levels we were able to demonstrate the disease progression over time through deregulated signaling pathways in HCM.

Patient-Specific iPSCs-derived Cardiomyocytes:

Induced pluripotent stem cells (iPSCs) allow modeling of diseases at a patient-specific level. Henceforth by using adult somatic cells (PBMCs) were obtained from patients suffering from the

proband being studied; re-programmed them into iPSCs and differentiating them into cardiomyocytes which would be provide a fully representative models of the patient specific diseased tissue.

We therefore created iPSC lines from patients' PBMCs and differentiate these into cardiomyocytes cells for studying the molecular characteristics of the diseases. Ultimately, we determined disease-specific signatures as well as abnormal signal transduction pathways that underlying HCM by comparing the molecular profiles of patient-derived iPSC-cardiomyocytes with matched controls. This strategy allows us to explore HCM from different perspective, maximizing the chances of identifying key genetic factors contributing to its disease progression.

1.14 Conclusion:

Hypertrophic cardiomyopathy (HCM), is a complex disorder involving myocardial hypertrophy and an inclination towards adverse cardiac events. The presence of genetic heterogeneity is a significant obstacle to fully comprehend the intricate connections between genotype and phenotype in hypertrophic cardiomyopathy. The diagnostic hurdles raised by HCM which include its diverse clinical presentation plus elusive genetic basis necessitate the adoption of superior ways to characterize and control diseases.

The next generation sequencing (NGS) technology in conjunction with multi-model approach has transformative effects on genetic diseases comprehension and precision medicine. The use of NGS to systemically probe into genome landscapes has discovered several new gene loci linked to HCM thereby providing unprecedented understanding of disease etiology and pathogenesis. History have mainly revealed the implications of sarcomeric gene variants in the disease but still 50% of cases being idiopathic, demands the need to explore other genetic factors involved such as signaling gene variants and mechanism associated with them**.** In addition, Indian subcontinent despite the presence of such diverse ethnicities, HCM genetic understanding remains elusive.

1.15 RESEARCH GAP

A comprehensive understanding of hypertrophic cardiomyopathy (HCM) related genes, especially in India is still missing leading to a significant void in HCM research. Although many of sarcomeric gene variants are known to imply in HCM, less is known about 'signaling gene variants' contributing to the disease. As of now we know that many HCM cases are linked to mutations in sarcomeric or sarcomeric-associated genes. But with around 50% cases still having unexplained genetic causes (idiopathic in nature), it is expected that other new HCM causing genes are yet to be discovered. This lacuna limits our ability to understand the complex molecular mechanisms behind HCM and hinders our potential to develop precise diagnoses and treatments.

In addition, most of the therapies present in the market are not the cure and targets the disease symptoms rather than the cause that plays direct role in cardiac pathology. Only few exceptions, for instance, 'Mavacampten' targets the S2 domain of MYH7 and cardiac contractility. This helps only the subset of HCM patients (NHYA II and NHYA III).[71] Moreover, in context to the patients with signaling gene variants such medications may not be the best target of the disease. Thus, it is apparent, that there is a need for gene identification and potential therapeutic targets based on disease mechanism.

CHAPTER: 2

OBJECTIVES

The research gap highlights the need for new gene discoveries, related mechanism and associated therapeutic. To achieve this, we took advantage of a multi-model approach involving human genetics and cellular models including stem cell models. In addition, the Indian population, which is ethnically very diverse, are poorly studied for HCM new gene identification. This study intends to bring us closer to understanding HCM genetics while laying down a platform for designing more effective diagnostic as well as therapeutic interventions specifically targeting individual patients. Based upon which following are the objectives of my thesis:

1) Discovery of novel gene loci through Next -Generation Sequencing for HCM.

2) Deciphering the key molecular mechanisms pertaining disease pathogenesis.

CHAPTER: 3

MATERIALS AND METHODS

3.1 Recruited patients' hospital information:

A set of 401 hospitalized registered individuals, unrelated and along with their written informed consent, were recruited from Government Medical College in Kozhikode, Kerala, Sivagangai Medical College in Sivagangai, Tamil Nadu, and Sri Jayadeva Institute of Cardiovascular Sciences and Research in Bengaluru, Karnataka.[72] The study protocols were approved by the institutional review boards of the study centers.

3.2 Criteria for diagnosing Indian patients and controls:

The patients were diagnosed using an established global norms, as previously detailed.[72] The specific information regarding the baseline characteristics of the Indian patients may be found in table below:

Table 3.1: Baseline characteristics of Indian HCM patients.

Variables	Cohort 1 (n=101)-Exomes	Cohort 2 (n=300)-Targeted
Age, year (mean ±SO)	43.25±13.44	44.90±12.10
Male, n (%)	54 (53)	174 (58)
Female, n (%)	47 (47)	126 (42)
Chest pain, n (%)	71 (70)	204 (68)
Dyspnea, n (%)	50 (50)	234 (78)
Syncope, n (%)	66 (65)	213 (71)
NYHA (1-111), n (%)	96 (95)	267 (89)
Hyperlipidemia, n (%)	8 (8%)	0 (0)
CAD, n (%)	None	None
AF, n (%)	16 (16)	78(26)
Abnormal ECG, n (%)	93(92)	237 (79)
Alcohol	None	None
Smoking	None	None
HTN	None	None
LVIDd, cm	4.7 ± 0.81	4.3± 0.70

LVOT, cm	53.22±10.11	55.83±16.12
LVIDs. cm	2.61±0 77	2.34±0.18
IVSd, cm	1.79±0 33	1.1±0.5
LVEF(%)	60.12±3.8	56.56±5.2

The clinical diagnosis of the study individuals was confirmed by two independent cardiologists. The Indian control groups consist of a total of 3521 participants (n=7042 alleles), which includes population stratified 1800 healthy Indians,[42,72,73] 1029 healthy Indian genomes from the IndiGenomes database,[74] 94 healthy aging Indians over the age of 80 from www.idhans.org,[72] and 598 Indian exomes from the Genome Asia 100K database.[75] Population stratification analysis was conducted utilizing 50 ancestry-informative markers, following the described procedure.[73] The controls consisted of healthy volunteers who did not have any family history or symptoms of cardiovascular disorders. They had routine ECG and echocardiography tests, as detailed in our earlier work[42,72,73]. It is important to note that these controls were not related to the patients with cardiomyopathy.

3.3 Whole-exome sequencing, target re-sequencing and analysis:

The study's specific exome analysis process, developed in-house at inStem, is described in detail in the figure 1. Accordingly, genomic DNA from the corresponding study participants was extracted from peripheral blood lymphocytes using standard methods.[73] The DNA libraries were generated and accompanied by capture probes specific to targeted regions, implementing the techniques outlined in the SureSelect V5 Target Enrichment kit (Agilent Genomics).Four The libraries obtained were enhanced and are subsequently amplified using polymerase chain reaction (PCR). The sequencing was conducted by the respective service providers and the institutional sequencing facility at inStem, post elimination of patient information. Paired-end 100–base pair reads (with 100X coverage) were utilized for each exome, resulting in the acquisition of 6 gigabytes of information. The mean coverage of the target region of the capture kit was 88, with 85% of the region having a coverage of at least 30X and 98% of the region having a coverage of at least 10X. Poor-quality and adapter sequences were eliminated using Trimmomatic software. The exomes were initially aligned to the human reference genome (GRCh38) using Burrows-Wheeler aligner version 0.7 (BWA-MEM). The process of identifying genetic variations was carried out using the Haplotype-Caller tool from the Genome Analysis Tool Kit (GATKv.3.4)

software, which can be accessed at software.broadinstitute.org/gatk/. The variants were annotated using the web interface of the ANNOVAR software (wannovar.wglab.org/). The identification of pathogenic or deleterious variants were carried out utilizing in silico tools such as Polymorphism Phenotyping v2 (PolyPhen2), Sorting Intolerant From Tolerant (SIFT), Position-Specific Evolutionary Preservation (PANTHER-PSEP), the algorithm used for protein analysis through evolutionary links.[76] MetaDome,[77] Combined Annotation Dependent Depletion (CADD),[78] Mutation Taster, and Mendelian Clinically Applicable Pathogenicity (M-CAP).[79] In order for a variant to be considered pathogenic or deleterious, it should be predicted as such by the majority of in silico techniques (at least 4 out of 7) and then were reviewed according to the standards set forth by the American College of Medical Genetics (ACMG).

The primary parameters used to prioritize pathogenic variants were as follows: (1) coding regions, (2) rare variants with a minor allele frequency (MAF) of ≤ 0.1% (0.001), (3) ultrarare variants with a MAF of ≤ 0.01% (0.0001), and (4) novel variants; in public human population genome reference datasets with diverse ethnicities. The reference datasets utilized include:

i) Genome Aggregation Consortium (gnomAD), the 1000 Genomes Project, the Korean Variant Archive (KOVA), Iranome, the Tohoku Medical Megabank Organization 8.3K Japan (ToMMo 8.3KJPN), and the Han Chinese Genomes Database (PGG. Han).

ii) The disease datasets used in this study include Trans-Omics for Precision Medicine (TOPMed), Genotype to Mendelian Phenotype (Geno2MP v2.4), the NHLBI Exome Sequencing Project (ESP), Exome Variant Server, Swedish datasets (SweGen and ACpop Variant Frequency Datasets).

iii) Additionally, Indian and Caucasian wellderly control datasets were included, which consist of healthy aging Indian exomes from www.idhans.org and the Wellderly dataset.[79]

iv) Furthermore, South-Asian specific Indian control datasets were utilized, including Genome Asia 100K, Indigenomes, and South Asian (Indian) healthy controls.[72,73] The cardiac-specific expressing genes have been obtained from the human protein atlas[80] and single cell genomics data[81] which encompasses all the well-established genes linked with heart development, physiology, and cardiomyopathy. The other genes were classified as non-cardiac genes for the purpose of our analysis. The identification and analysis of pathogenic mutations in all of these genes were filtered and examined.[42]

3.4 Protein-protein interactions (PPI) network analysis:

A structure for network analysis was created using established HCM genest[82], incorporating physical, co-expression, co-localization, pathway, and genetic interactions. Each mutated gene in proband 1 (P1) exome was uniquely included in the network. The network was constructed using STRING (Search Tool for the Retrieval of Interacting Genes)[83], which provided information on both predicted and experimental protein interactions. In order to construct the network model, the commonly used minimum interaction score of ≥ 0.4 was chosen. The network module, consisting of a group of genes that participate in the same biological function, was identified from the protein-protein interaction (PPI) network using the MCODE algorithm, which is a plugin of Cytoscape [2]. The study employed the following parameters: a node density cutoff of 0.1, a node score cutoff of 0.2, a K-score of 2, and a maximum depth of 100.

Ultimately, a comprehensive examination of the chosen genes was acquired by conducting a literature search using the PUBMED database.

To do resequencing and confirm the specific disease-causing mutations, we amplified the exons and the adjacent intronic boundaries of gene from genomic DNA. The amplified PCR products underwent purification using a QIAGEN PCR purification kit, followed by sequencing and subsequent analysis. The examination of amino acid conservation among species involved the comparison of protein sequences from different vertebrate species using the ClustalW2 program.

3.5 Replication association studies:

The UK Biobank dataset (approval number 67095) included 190 patient exomes diagnosed with hypertrophic cardiomyopathy (HCM) according to the International Classification of Diseases (ICD) codes 42.1 and 42.2. Additionally, it contained 16,479 individual exomes with corresponding ICD codes (C01-14, D10-12,17,22,23 and 25, G-47 and 51-58, I11-13, 25 and 44-49, J-09-13,15, 18, 21,22, 39, 40, 43-45 and 47, I11-13, 25 and 44-49) serving as controls. These controls were obtained from the OQFE pipeline, as previously described.[84] The VCF files were acquired and the same variant filtering methods (Figure 4.1) The Arab patient provided written informed permission, which was obtained from Partners Healthcare in Boston with approval from the institutional review board.

3.6 *S6K1* plasmids:

The *S6K1* variant was introduced into a GFP- tagged construct containing human full-length *S6K1* gene by site-directed mutagenesis (QuikChange Site-Directed Mutagenesis Kit, Stratagene).

3.7 HL-1 cardiomyocytes and HEK-293T culture maintenance:

Both cell lines (HL-1 and HEK293T) were cultured at 37°C in a humidified atmosphere of 5% CO2. For HL1 line, the complete medium consisted of 87% Claycomb medium (Sigma-Aldrich catalog #51800C), 10% fetal bovine serum (FBS, Sigma- Aldrich catalog #F2442), 1% glutamine (2mM) and norepinephrine (100µM norepinephrine in 30mM L-ascorbic acid), and 1% penicillin/streptomycin (100 U/mL: 100µg/mL). For HEK-293T cell line, DMEM F-12 with 10% FBS and 1% penicillin/streptomycin was used. Cells were transfected with S6K1 wild-type (WT) or mutant constructs for 24hrs by jetPRIME (Polyplus transfection, USA Catalog #55-250) in 6-well plates. Twenty-four to forty-eight hours after transfection, HEK-293T cells were switched to serum-starvation medium for 6-8 hrs. After stimulation with PMA (500 nmol/ml) (Sigma-Aldrich catalog #P8139) for the indicated intervals at 37 °C, the cells were lysed for further analysis.

3.8 Immunocytochemical staining for HL-1 and H9C2 cellular model and microscopy:

For immunofluorescence studies, HL-1 cardiomyocytes cultured on coverslips were washed with 1× phosphate-buffered saline (PBS) (Gibco) twice, 5 min each on mild shaking. Cells were fixed in 4% paraformaldehyde (Sigma-Aldrich catalog # 158127) for 20 min at room temperature, again washed with 1× PBS, and permeabilized with 0.1% Triton X-100 (Sigma-Aldrich catalog # 93443) in PBS for 15 min at room temperature. Blocking was performed using 1% bovine serum albumin (HiMedia catalog # GRM3151) and 1% normal goat serum (Thermofisher scientific catalog # 50197Z) in PBS for 1 hour at room temperature. Cells were incubated with antibody against cardiac troponin T (Cell Signaling Technology catalog #5593) overnight at 4°C. After washing cells with 1× PBS, three times, and cells were incubated with secondary antibody (Alexa Fluor 555 catalog #A-21422) for 1 hour at room temperature. After washing three times, cells were incubated with phalloidin 488 (Thermofisher Scientific catalog #A12379) as per the manufacturer's protocol for 1 hour at room temperature. Nuclear staining was performed using

Hoechst dye (Thermofisher Scientific catalog # 62249). After washing cells twice, coverslips were mounted using VECTASHIELD antifade mounting medium (Vector Laboratories catalog #H-1000-10). Images were collected using Olympus IX73 inverted fluorescence microscope system and then analyzed using ImageJ (Fiji) software.

3.9 Immunocytochemical staining for iPSC derived cardiomyocytes:

iPSCs derived-cardiomyocytes from patient and isogenic line were dissociated and seeded on Matrigel coated ibidi confocal dishes (catalog #81156). Cells on dishes were properly washed with PBS thrice and then fixed with 4% paraformaldehyde (Sigma-Aldrich catalog # 158127) for 15 mins at room temperature (RT). Again, coverslips are washed thoroughly with PBS thrice, and permeabilized afterwards with 0.3% triton-X100 (Sigma-Aldrich catalog # 93443) for 15 mins at RT. Cells were then blocked with 3% BSA, 1% NGS, 0.3% triton-X100 for one hour at RT. Primary antibody, alpha-sarcomeric actinin (Invitrogen, MA1-22863,dilution 1:500), de-tyrosinated α-tubulin (Abcam catalog #ab48389, dilution 1:500) and desmin (Thermofisher scientific catalog #MA5-32068, dilution 1:500) were added onto dishes for overnight at 4°C with respect to experiments requirements. Next day dishes were washed thrice with PBST (PBS+0.1% Tween20) and then secondary antibody was added to the dishes (Alexa Fluor 488, 647 in accordance with required experiment) for one hour at RT and then washed thrice with PBST. After this phalloidin 546 (Thermofisher scientific catalog #A22283, dilution 1:400) along with Hoechst (Thermofisher Scientific catalog # 62249, dilution 1:10,000) was added to the dishes for one hour at RT, and then washed with PBST thrice and imaged on Olympus FV3000, 20X/60X NA 1.40 oil immersion objective.

3.10 Cell size analysis:

For the aim of elucidating cell size, the ImageJ software was employed. In order to retrieve pertinent cellular information from the confocal pictures, the captured multi-stack images were stacked into one image and the projection with the highest intensity was recovered, which resulted in an improvement in the visibility of cellular structures and then all the channels were made to split away. Noise was removed up to 2-pixel size and 50µm range. After that, a particle analysis was carried out in order to accurately quantify of cell surface area. The effective tracking of regions of interest was made possible by the administration of segmented cells through the ROI Manager.

Following the completion of the data collection process, stringent quality control procedures were put into place in order to validate the precision of the measurements.

3.11 Reactive oxygen species (ROS) measurement and analysis:

Before staining, the cardiomyocytes are seeded on suitable culture dishes and allowed to adhere and grow into the ideal morphology. To measure ROS, dihydroethidium (DHE) (Sigma-Aldrich catalog #309800) is employed. The DHE powder is dissolved in dimethyl sulfoxide (DMSO) to form a stock solution. This stock solution is prepared at a concentration of 5mM. To get a working concentration of 5μM, the stock solution is diluted in either PBS or cell culture medium. The cells were initially rinsed with PBS and then exposed to the DHE staining solution at a temperature of 37°C in a dark environment for a duration of 30 minutes. This incubation period allows the DHE to penetrate the cells and undergo oxidation by reactive oxygen species (ROS).

After the incubation period for staining, the staining solution is cautiously pipetted out and the cells are gently rinsed with PBS to eliminate any surplus dye. The cells were subsequently treated with a 4% paraformaldehyde solution for 5 minutes at room temperature in order to maintain the integrity of the staining pattern. The stained cells are imaged using a confocal microscope that has the necessary filter sets for DHE, with excitation/emission wavelengths of 488/610 nm. Optimal exposure settings were employed to capture a balanced range of fluorescence intensity, avoiding overexposure. These parameters were maintained consistently for all samples.

3.12 Intensity measurement of confocal images:

In order to measure the intensity of certain biomolecules in the cell upon staining and confocal imaging firstly a selection is made using ImageJ. Then by going at “Analyze” dropdown option “set measurements” option was picked and then “area integrated density” and “mean grey value” is selected. After this “measure” option is selected, which gives the intensity of the area selected. Then similarly a region near to cell with no fluorescence was selected and the intensity is measured. This will give us the “background”. With these two measurements corrected total fluorescence is calculated (CTCF) using the following formula:

CTCF= Integrated density- (Area of selected cell x mean fluorescence of the background)

3.13 Quantitative Real time PCR:

The extraction of total RNA was performed using TRIzol (Invitrogen catalog #15596026), adhering to the manufacturer's extraction technique, the RNA samples were cleansed to remove any impurities that could potentially disrupt subsequent procedures. For the next stage, the RNA that had been isolated was converted into complementary DNA (cDNA) using the Verso cDNA synthesis kit from Thermofisher Scientific (catalog #AB1453A). It guarantees a highly effective and precise transformation of RNA into cDNA, while maintaining the integrity of the genetic information.

Following the completion of cDNA synthesis, the quantification of the generated cDNA was assessed using real-time PCR, a sensitive method that enables accurate measurement of nucleic acids. The PCR experiment utilized PowerUp™ SYBR™ Green Master Mix for real-time qPCR (Applied Biosystems catalog # A25743), which provided a reliable and efficient method for analyzing gene expression.

The real-time PCR study was conducted using a 7500 real-time PCR equipment from Applied Biosystems. This phase yielded quantitative data regarding the abundance of certain mRNA transcripts within the samples.

In order to evaluate alterations in gene expression levels, the fold change was determined via the relative comparison approach. Gene expression levels are quantified by measuring the cycle threshold (Ct) values acquired during PCR amplification. Smaller Ct values correspond to more gene expression, whereas larger Ct values correspond to reduced expression. The results entail normalizing the Ct values of the target gene with respect to an internal reference gene, such as 18S or U6 rRNA, in order to derive the ΔCt value. The disparity in ΔCt values between the experimental and control samples (ΔΔCt) signifies the magnitude of the alteration in gene expression. A fold change above 1 implies upregulation, whereas a fold change below 1 indicates downregulation. This approach offers a quantitative evaluation of gene expression levels, assisting researchers in comprehending gene regulation across various experimental settings.

Table 3.2: qRT-PCR primer list

Gene	**species**	**Forward primer**	**Reverse primer**
ACTA1	*Homo Sapiens*	**TCTCACCGACTACCTGATGAA**	**AGCACAGCTTCTCCTTGATG**
PLN	*Homo Sapiens*	**CTCACTCGCTCAGCTATAAGAAG**	**AGAGAAGCATCACGATGATACAG**

BNP	*Homo Sapiens*	**TCCTGCTCTTCTTGCATCTG**	**GTAACCCGGACGTTTCCAA**
ANP	*Homo Sapiens*	**TTGCTGGACCATTTGGAAGA**	**GCTTCTTCATTCGGCTCACT**
BMHC	*Homo Sapiens*	**TGAAGGAGGACCAGGTGAT**	**GTAGCGATCCTTGAGGTTGTAG**
U6	*Homo Sapiens/Rattus/Mus musculus*	**ATTGGAACGATACAGAGAAGATTAG**	**AATATGGAACGCTTCACGAAT**
18S	*Rattus novergicus*	**GGAACTGAGGCCATGATTAAGA**	**CAAATGCTTTCGCTCTGGTTC**
BNP	*Rattus novergicus*	**AGATGATTCTGCTCCTGCTTT**	**ATCGTGGATTGTTCTGGAGAC**
MYH6	*Rattus novergicus*	**CAGCAGAACCCTCCGAAAT**	**CATAGCGCTCCTTGAGATTGTA**
Acta1	*Rattus novergicus*	**CCTGGACTTCGAGAATGAGATG**	**CGATAAAGGAAGGCTGGAAGAG**
Pln	*Rattus novergicus*	**AGAGCCTCGACTATTGAAATGC**	**GCAGACATATCAAGATGAGACAGAA**
ANP	*Rattus novergicus*	**ATTTCAAGAACCTGCTAGACC**	**TTTTCAAGAGGGCAGATCTAT**
BMHC	*Rattus novergicus*	**CCTCGCAATATCAAGGGAAA**	**TACAGGTGCATCAGCTCCAG**
BNP	*Mus musculus*	**GACAGCTCTTGAAGGACCAAG**	**GCCCAAAGCAGCTTGAGATA**
Myh6	*Mus musculus*	**GTGCTGTACAACCTCAAGGA**	**ACACAGGCAGCCACTTATAG**
Pln	*Mus musculus*	**CACGTCAGAATCTCCAGAAC**	**TCACAGAAGCATCACAATGA**
Acta1	*Mus musculus*	**GCTCTTCCAGCCTTCCTTTAT**	**CATACAGGTCCTTCCTGATGTC**
ANP	*Mus musculus*	**TCCGATAGATCTGCCCTCTT**	**CTCCAATCCTGTCAATCCTACC**
BMHC	*Mus musculus*	**GCATTGAGTGGACCTTCATAGA**	**GAACATGCACTCCTCCTCAA**
18S	*Mus musculus/Homo sapienns*	**GTAACCCGTTGAACCCCATT**	**CCATCCAATCGGTAGTAGCG**
GAPDH	*Mus musculus*	**AACAGCAACTCCCACTCTTC**	**CCTGTTGCTGTAGCCGTATT**
Cyba	*Homo Sapiens*	**TTCACCCAGTGGTACTTTGG**	**GTCATGTACTTCTGTCCCCAG**
Cybb	*Homo Sapiens*	**AGGAGTTTCAAGATGCGTGG**	**TTGAGAATGGATGCGAAGGG**

Nrf2	*Homo Sapiens*	**GTTGCCCACATTCCCAAATC**	**CGTAGCCGAAGAAACCTCAT**
NOX4	*Homo Sapiens*	**TCACAGAAGGTTCCAAGCAG**	**ACTGAGAAGTTGAGGGCATTC**
Desmin	*Homo Sapiens*	**GGTACAAGTCGAAGGTGTCAG**	**GGTGTCGGTATTCCATCATCTC**
GCLC	*Homo Sapiens*	**CCCAAACCATCCTACCCTTT**	**CATGTTGGCCTCAACTGTATTG**
ATP2A1	*Homo Sapiens*	**TGGTTTGAGGAAGGTGAAGAG**	**CATCTCTGGCTCATACTCCTTC**
ATP2A2	*Homo Sapiens*	**GAAATGTGTAACGCCCTCAAC**	**CGACATAGAGGATCAGGAAGTG**
ATP2A3	*Homo Sapiens*	**GGGACCTCACATCAACTTCTAC**	**GCACATTTCAATGGTCACGAG**
Pln	*Homo Sapiens*	**CCAATACCTCACTCGCTCAG**	**GATTCTGTAGCTTTTGACGTGC**
Nqo1	*Homo Sapiens*	**GGGATGAGACACCACTGTATTT**	**TCTCCTCATCCTGTACCTCTTT**
GSR	*Homo Sapiens*	**GGGACTTGGGTGTGATGAAA**	**CTTCTGAAGAGGTAGGGTGAATG**

We were able to precisely measure the levels of gene expression while understanding more about the molecular mechanisms behind biological processes of interest by utilizing this all-inclusive procedure.

3.14 Immunoblotting analysis and antibodies:

RPS6KB1 study:

Experimental HL-1 cardiomyocytes or HEK-293T were homogenized in radioimmunoprecipitation assay buffer containing protease (Roche) and phosphatase (Sigma-Aldrich) inhibitors. Thirty micrograms of protein were applied to SDS–polyacrylamide gel electrophoresis and transferred onto nitrocellulose membrane. The following antibodies obtained from Cell Signaling Technology were used: ERK1/2, phospho-ERK1/2(Thr202/Tyr204), phospho-S6K1 (Thr389), S6K1, rpS6, phospho-rpS6 (Ser235/236), phospho-rpS6 (Ser240/244), eEF2, DAP5, phospho-4EBP1(Thr37/46), phospho-eIF4E (Ser209), phospho-eIF4G (Ser1108) and glyceraldehyde-3-phosphate dehydrogenase (GAPDH). The membranes were incubated with appropriate secondary antibodies, and signal intensities were visualized with enhanced chemiluminescence (Pierce catalog #32106). Total protein contents of the corresponding proteins

were analyzed after stripping the phospho-blots to verify protein loading. GAPDH was used as internal loading control.

Table 3.3: List of Antibodies used in current research

RPS6KB1 study:

S.no	Name of Antibody	Company	Catalog no.
1	Anti-ERK1/2	CST	4695
2	Anti-phospho-ERK1/2(Thr202/Tyr204)	CST	4370
3	Anti-S6K1	Invitrogen	MA5-15141
4	Anti-phospho-S6K1 (Thr389)	Invitrogen	MA5-15202
5	Anti-rpS6	Invitrogen	701374
6	Anti-phospho-rpS6 (Ser235/236)	Invitrogen	17-9007-42
7	Anti-phospho-rpS6 (Ser240/244)	Invitrogen	44-923G
8	Anti-phospho-eEF2(Thr-56)	CST	2331
9	Anti-pEIF4G2/p97 (DAP5)	CST	5169
10	Anti-phospho-4EBP1(Thr37/46)	CST	2855
11	Anti-phospho-eIF4E (Ser209)	CST	9741
12	Anti- phospho-eIF4G (Ser1108)	CST	2441
13	GAPDH	Invitrogen	MA5-15738

TTL study:

S.no	Name of Antibody	Company	Catalog no.
1	Anti-ERK1/2	CST	4695
2	Anti-phospho-ERK1/2(Thr202/Tyr204)	CST	4370
3	Anti -De-tyrosinated alpha tubulin	Abcam	ab48389
4	Anti -tyrosinated alpha tubulin (YL1/2)	Abcam	ab6160
5	Anti - alpha tubulin (DM1A)	Abcam	ab7291
6	Anti-Desmin	Sigma-Aldrich (mouse)	D1033
7	Anti-Desmin	Invitrogen(rabbit)	MA5-32068
8	Anti-Nrf2	CST	12721
9	Anti-GCLC	CST	52183

10	Anti-SOD1	Invitrogen	8B10
11	Anti-NQOI	Invitrogen	A180
12	Anti-phospho-AKT (Ser 473)	CST	4060
13	Pan-AKT	CST	4691
14	GAPDH	Invitrogen	MA5-15738

3.15 Generation of induced pluripotent stem cells (iPSCs):

Patient specific peripheral blood mononuclear cells (PBMCs) were isolated using density gradient method using Histopaque (sigma catalog#1077). iPSCs are generated using Cytotune2.0 Sendai virus kit (Invitrogen catalog#A16517). Initially cells were seeded in a well of 24 well plate at cell count of $3.5x10^5$ per microliter with 95% viability on day -4, in complete PBMC media. PBMC medium consists of complete StemPro™-34 medium (Invitrogen catalog #10639011) supplemented with the appropriate cytokines (SCF c-kit 100 ng/mL (Invitrogen catalog #PHC2115), FLT-3 100 ng/mL (Invitrogen catalog #PHC9414), IL-3 20 ng/mL (Invitrogen catalog #PHC0034), IL-6 20 ng/mL (Invitrogen catalog # PHC0064) at their final concentration). At day 0, cells were transduced by Sendai reprogramming vectors at appropriate MOIs. Volume of virus used is calculated by following equation:

V= [MOI (CIU/cell) x number of cells] / titer of virus (CIU/cell) x 10^{-3} (ml/µl)

Volume of virus used for reprogramming:

Klf4 = $(3x(1x10^5)/1.1x10^{-3}x10^{-5}$= **2.7µl,**

c-myc = $(5x(1x10^5)/1x10^8x10^{-3}$= **5µl**

KOS= $(5x(1x10^5)/9.8x10^7x10^{-3}$=**5.1µl**

On day 1 medium was replaced with PBMC medium to remove the viral titer. On day 3 cells were plated onto vitronectin coated plate in complete StemPro™-34 medium without cytokines. On day 7, transitioning started in Essential-8^{TM} medium. From day 8 till day 28 medium was changed every-day and was checked for iPSCs colony emergence. After stable proliferation of iPSCs colony, cells were passaged and expanded for characterization and differentiation. Wild type, *MYBPC3*$^{\Delta 25bp}$ lines were obtained from our own lab resource and SHOC2 p.S2G initial line was a kind gift by Prof. Maria I Kontaridis and has been characterized in our own lab.

3.16 Embryoid body formation:

Embryoid bodies are the aggregates of embryonic stem cells (ESCs) or iPSCs allowed to form a 3D structure in a differentiated manner. Over the course of two to four days, all three germ layers ectoderm (outer layer), mesoderm (middle layer) and endoderm (inner layer) shall be present in a differentiated embryoid bodies. For the embryoid formation, after passaging iPSCs with ReleSR (Catalog #100-0484) for 3 minutes cells were taken out by gentle pipetting into a 15ml falcon tube, containing 5ml of iPSCs culture media, stemflex (Catalog #A3349401) and pelleted down at 200 rcf for 5 minutes. Supernatant was removed and cell pellet was resuspended in 1ml of stemflex medium and 10µl of cells were taken out for cell counting. Cells were mixed with 10µl of trypan blue and counted using Countess 3 automated cell counter. Approximately 30,000 cells were seeded into each well of ultra-low attachment 24-well plate with 500µl of stemflex media. Cells were then allowed to form aggregates for next 24-48 hours and then these were taken out for RNA isolation.

3.17 Germ layer marker analysis:

Isolated RNA from fully formed embryoid bodies were converted to cDNA using Verso cDNA synthesis kit (Thermofisher scientific catalog #AB1453A) and the generated cDNA were subjected to PCR as template against different germ layers markers like GATA4 (mesoderm), Nodal (endoderm), Sox2 and Nestin (ectoderm) and U6 (house-keeping gene).

PCR reaction composition:

Forward primer	0.5µl
Reverse primer	0.5µl
Emerald Taq mastermix (2X)	5µl
Nuclease free water	3µl
Template cDNA	1µl (1:500 diluted sample)
Total	10µl

3.18 Karyotyping:

Generated iPSCs at fifty percent confluency were given for karyotyping to "Neuberg Anand diagnostic laboratories" at Sahakarnagar, Bengaluru and giemsa (G-banding) cytogenetic staining technique was applied to detect condensed chromosome.

3.19 Pluripotency characterization:

Pluripotency status of the generated iPSCs were checked using immunocytochemical staining against different pluripotency markers like Oct3/4 (Santacruz catalog #sc-5279), SSEA3 (Santacruz catalog # sc-21703), SSEA4 (Santacruz catalog #sc-21704), Tra 1-60 (Santacruz catalog #sc-21705), Tra 1-81 (Santacruz catalog #sc-21706). The protocol mentioned above for immunocytochemical staining is exactly followed for this experiment too.

3.20 Cardiac differentiation:

Initially patient specific iPSCs and isogenic line (wild type) were acclimatized to mTeSr medium (Stem cell technologies, catalog # 100-0276) and cells were seeded in Matrigel (Merck Corning #CLS354234) coated 12 well plate for differentiation. After reaching 70-80% confluency differentiation was started with induction by 4μM CHIR99021 (Sigma Aldrich #SML1046) for 48 hours followed by 5μM IWP2 (Wnt inhibitor) (Sigma Aldrich #I0536) for two days in cardiac differentiation medium (RPMI1640 with Glutamax (Thermofisher Scientific # 61870036), 213μg/ml ascorbic acid (Sigma Aldrich catalog #A92902), 500μg/ml human serum albumin (Sigma-Aldrich catalog # A1887) and B27 minus insulin (Gibco catalog # A1895601) Cells were maintained till day 7 in cardiac differentiation media and was then replaced with cardiac maintenance media (RPMI1640 with Glutamax and B27 supplement (Gibco catalog # 17504044)) for next 20 days. On day 27 cells were transitioned to lactate medium (Sodium L-lactate (Sigma-Aldrich catalog # 71718), RPMI1640 minus Glucose (Gibco catalog #11879020), 213μg/ml ascorbic acid, 500μg/ml human serum albumin) for 4 days for purification of cardiomyocytes. After recovery of cells in cardiac maintenance media for 4 days, cells were passaged and plated onto freshly coated Matrigel plates/ dishes and with cardiac maintenance media (RPMI1640 with Glutamax, B27 supplement and 5% Knock out serum (KOSR)).

3.21 Muscle motion analysis:

The muscle motion analysis procedure has been performed using the plugin called Muscle Motion Analysis available in ImageJ. The first step is to import video files that include muscles movement data into ImageJ. In order to reduce the effects of motion artifacts, some pre-processing was conducted such as brightness/contrast adjustment and stabilization of videos by use of stabilizer. After this step, the Muscle Motion Analysis plugin was installed and activated through the Plugins menu. Within these iPSC-CMs are defined regions of interests (ROIs) while frame rate and analysis method were set according to how experimental setup was done. This thereafter ran the plugin for tracking ROIs that got chosen throughout all video sequences. Results were generated and evaluated which included motion trajectories as well as displacement maps. The analysis results also provided quantitative data like displacement values and velocity profiles that could be extracted from the experiment's outcome. Consequently, these findings were interpreted within the ambit of research objectives with a view to understanding their significance in terms of physiological function or experimental outcomes. To ensure reliability and accuracy regarding both methodology and results, validation procedures were carried out.

3.22 Cell lysate preparation:

Cells were lysed in RIPA buffer (50mM Tris (pH 8.0), 150mM NaCl, 10 mM EDTA, 10% glycerol, 1% Triton X-100, 0.1% SDS, 1× protease inhibitor cocktail). Protein concentrations for cell lysates were measured using the BCA method, and approximately 15-20µg of total protein was loaded onto gels, separated by SDS-PAGE.

3.23 Western Blotting:

Protein gels (SDS-PAGE) are transferred onto poly-vinylidene difluoride (PVDF) membranes (Bio-Rad). Membranes were blocked in 3% BSA and incubated with primary antibodies overnight at 4 °C. Membranes were then incubated with appropriate secondary antibodies conjugated to horseradish peroxidase (Invitrogen), and signal intensities were visualized by chemiluminescence.

3.24 Purification of recombinant TTL proteins:

Human tubulin tyrosine ligase (hTTL) variants (Wild type and G219S) with C-terminal 6XHis-tag were overexpressed in *E.coli* (bl21)cells and purified as described previously with some

modifications. Transformed *E.coli* cells were induced with 0.5mM IPTG overnight at 27°C to initiate protein expression. After induction, cells were harvested by centrifugation at 100000x g for 10 min at 4°C and the resulting cell pellet was washed twice with PBS. The pellet was then resuspended in cold lysis buffer and sonicated on ice for 10 cycles. The soluble cell lysate was purified using His Trap column. The soluble fraction was equilibrated to a final concentration of 10mM imidazole before loading on to the column. The column was thoroughly washed using wash buffer and the bound hTTL was eluted with elution buffer containing 500mM Imidazole. Following elution, enriched hTTL fractions were pooled and was further purified using Sephadex200 16/60 column connected to an Akta purification system. The purity and concentration of the protein was determined using SDS page.

3.24.1 Buffer compositions:

Lysis buffer	Wash buffer	Elution buffer
50mM Tris-Cl (pH 7.5)	50mM Tris-Cl (pH 7.5)	50mM Tris-Cl (pH 7.5)
10mM BME	10mM BME	10mM BME
2.5mM MgC12	2.5mM MgC12	2.5mM MgC12
10% Glycerol	10% Glycerol	10% Glycerol
1M NaCl	1M NaCl	1M NaCl
1mM PMSF	20mM Imidazole	500 mM Imidazole

3.25 CPA treatment and tyrosination assay:

Tubulin was purified from goat brain using two cycles of polymerization and depolymerization. Carboxypeptidase A (CPA) treatment of purified goat brain tubulin was carried out as described previously. A reaction mixture containing purified goat brain tubulin with 20% glycerol, 2 mm GTP, and 2.5-µg/ml of pancreatic CPA was prepared in 1x BRB80. Briefly, the mixture was incubated on ice for 10 min and the reaction was initiated by incubating at 37°C for 20 min. After incubation, the reaction was immediately stopped by adding 20 mm DTT and the microtubules were further allowed to polymerize for 10 min at 37°C. Polymerized microtubules were then pelleted at 100,000*g* for 40 min at 37°C and was further resuspended using ice cold BRB80.

A reaction mixture (10ul) containing CPA treated tubulin(2.5µM) in 50mM MES/K, 100mM KCl, 10mM MgCl2, 5mM DTT, 2.5mM ATP, 0.2 mm L-tyrosine was used to analyze the tyrosination abilities of TTL variants. The mixture was incubated with TTL at a molar ratio of 1:0.0002 for different time points (0, 5, 10, 15, 20, 30 min) at 37°C in a circulating water bath. The enzymatic

reaction was stopped using 2x SDS-PAGE Sample Buffer. The resulting samples were subsequently analyzed using Western blotting and were probed using anti-Tyr-α-tubulin (1:5000) or anti-α-tubulin (1:5000), followed by anti-mouse or rabbit peroxidase-conjugated secondary antibody (1:5000). Image J (NIH) was utilized to quantify the relative intensities of western blot bands.

3.26 Molecular dynamics simulation:

The molecular dynamics (MD) simulations of tubulin-TTL complexes (both wild type (PDB ID 4IHJ) and G219S mutant) were performed using Charmm36 force field within the GROMACS 2019 framework. All the simulations involved positioning of tubulin-TTL complexes at the center of an octahedral box with a distance of 15A^{o} from the boundary walls surrounded by TIP3P water molecules for solvation under periodic boundary condition. The neutralization of the complexes was carried out by adding appropriate amount of sodium and chlorine ions and the topology file was generated. The model systems were subjected to energy minimization and subsequent equilibration using canonical ensemble (NVT) followed by isothermal-isobaric ensemble (NPT). Finally, the simulation was carried out for 100 ns.

3.27 RNA-Sequencing:

RNA was isolated from 40 days old cardiomyocytes using a Trizol RNA extraction method. The Next-Generation Sequencing facility at the National Centre for Biological Sciences (NCBS) conducted sample quality control, library preparation, and RNA-seq. RNA integrity was checked using Bioanalyzer and samples with RIN (RNA integrity number) above 9 were used for analysis. cDNA preparation was done in accordance with manufacturer's instructions by NEBNext® Ultra™ Directional RNA Library Prep Kit for Illumina®. (catalog #NEB-E7760). For mRNA enrichment, polyA selection method was employed. Next-generation sequencing of libraries was performed on the Illumina HiSeq 2500 platform for 1 × 100 base-pairs at ~30 to 35 million reads per sample.

3.28 RNA Sequencing analysis:

Sequencing data was trimmed for adaptor sequences and low-quality reads (~15bp) using Trim Galore! and was mapped to GRCh38 using Top hat. Paired-end reads obtained from both ends of the same RNA fragment, examined and paired reads ≥ 35 base pairs (bp) were retained. Differentially expressed genes (DEGs) between the samples were identified using Cufflinks/Cuffdiff software with parameters: Log_2fold change ±1.0 and adjusted *P*-value 0.05. Gene ontology of biological processes (using Enrichr) was used to show the network of significantly enriched biological processes and pathways.

3.29 Statistical analysis:

Statistical significance analysis was determined by two-tailed Student's t test, Fisher's exact test and one-way analysis of variance (ANOVA) with appropriate post hoc analysis. $P < 0.05$ was considered to be statistically significant.

CHAPTER: 4

RESULTS AND DISCUSSION

Ribosomal protein S6 kinase beta-1 gene variants cause hypertrophic cardiomyopathy

Publication:

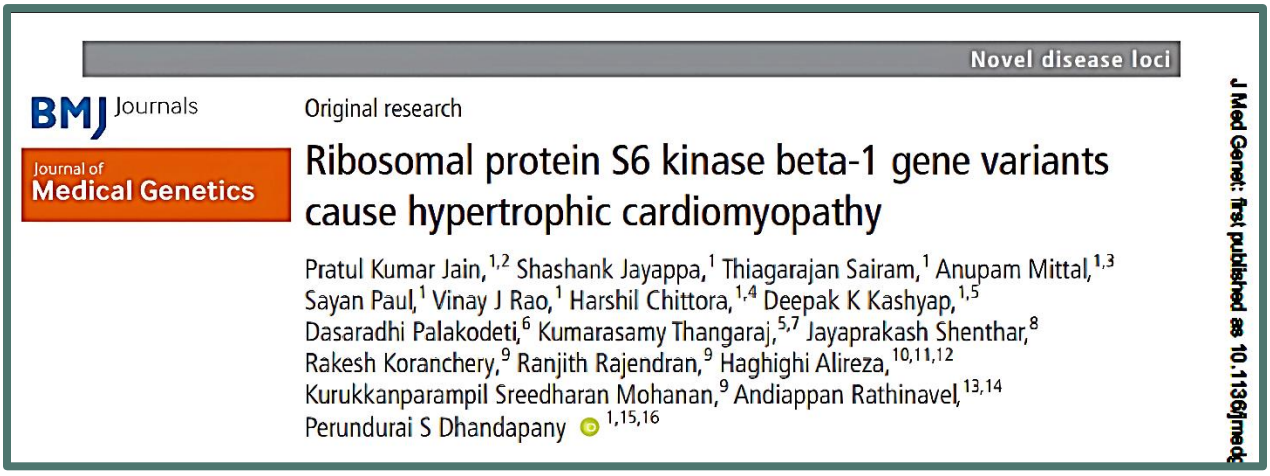

Novel disease loci

BMJ Journals

Journal of Medical Genetics

Original research

Ribosomal protein S6 kinase beta-1 gene variants cause hypertrophic cardiomyopathy

Pratul Kumar Jain,[1,2] Shashank Jayappa,[1] Thiagarajan Sairam,[1] Anupam Mittal,[1,3] Sayan Paul,[1] Vinay J Rao,[1] Harshil Chittora,[1,4] Deepak K Kashyap,[1,5] Dasaradhi Palakodeti,[6] Kumarasamy Thangaraj,[5,7] Jayaprakash Shenthar,[8] Rakesh Koranchery,[9] Ranjith Rajendran,[9] Haghighi Alireza,[10,11,12] Kurukkanparampil Sreedharan Mohanan,[9] Andiappan Rathinavel,[13,14] Perundurai S Dhandapany [1,15,16]

J Med Genet: first published as 10.1136/jmedg

4.1 INTRODUCTION:

Hypertrophic cardiomyopathy (HCM) is a cardiac muscle disorder characterized by increased ventricular wall thickness and diastolic dysfunction. HCM is primarily caused by mutations in genes encoding sarcomeric and signaling-associated proteins.[85,86] However, genetic studies reveal the absence of reported cardiomyopathy-related pathogenic gene mutation in a significant number of patients (~50%), suggesting that novel disease associated genes remain to be discovered.

Among the various hypertrophy-associated signaling pathways, p70 ribosomal protein S6 kinase beta-1 (S6K1) is critical in compensatory hypertrophy. S6K1 is a primary downstream substrate of the mechanistic target of rapamycin complex 1 (mTORC1) and has crucial roles in ribosome biogenesis and translation.[87] S6K1 regulates protein synthesis by phosphorylating the 40S ribosomal S6 protein (rpS6). On persistent activation, this signaling pathway progresses towards the maladaptive stage.[87] To the best of our knowledge, the S6K1 variant has not been reported in patients with HCM. In this study, we describe novel and ultra-rare S6K1 heterozygous variants in South Asian, European and Middle Eastern patients with HCM. Using functional studies, we established the potential disease-causing nature of the S6K1 variants and provided direct evidence of S6K1 activation in a genotype-positive patient biopsy sample.

4.2 RESULTS:

4.2.1 Discovery of S6K1 as a novel HCM gene:

For this study initially we analyzed a total of 300 patients with HCM exomes of South Asian (Indian) origin and selected 101 unexplained cases without any causal sarcomeric gene mutations (Cohort 1, Figure 4.2). The details of the baseline characteristics of the patients are outlined in material and methods chapter.

The identified *S6K1* variant is located in the N-terminal region of the protein (Figure 4.4B), and in the respective variant, an evolutionarily conserved glycine was changed to tryptophan at the 47th amino acid position (NM_003161.4:c.139G>T, p.G47W) (Figure 4.4C). Also, the variant is predicted to be pathogenic, as suggested by most in silico analyses (Figure 4.4D).

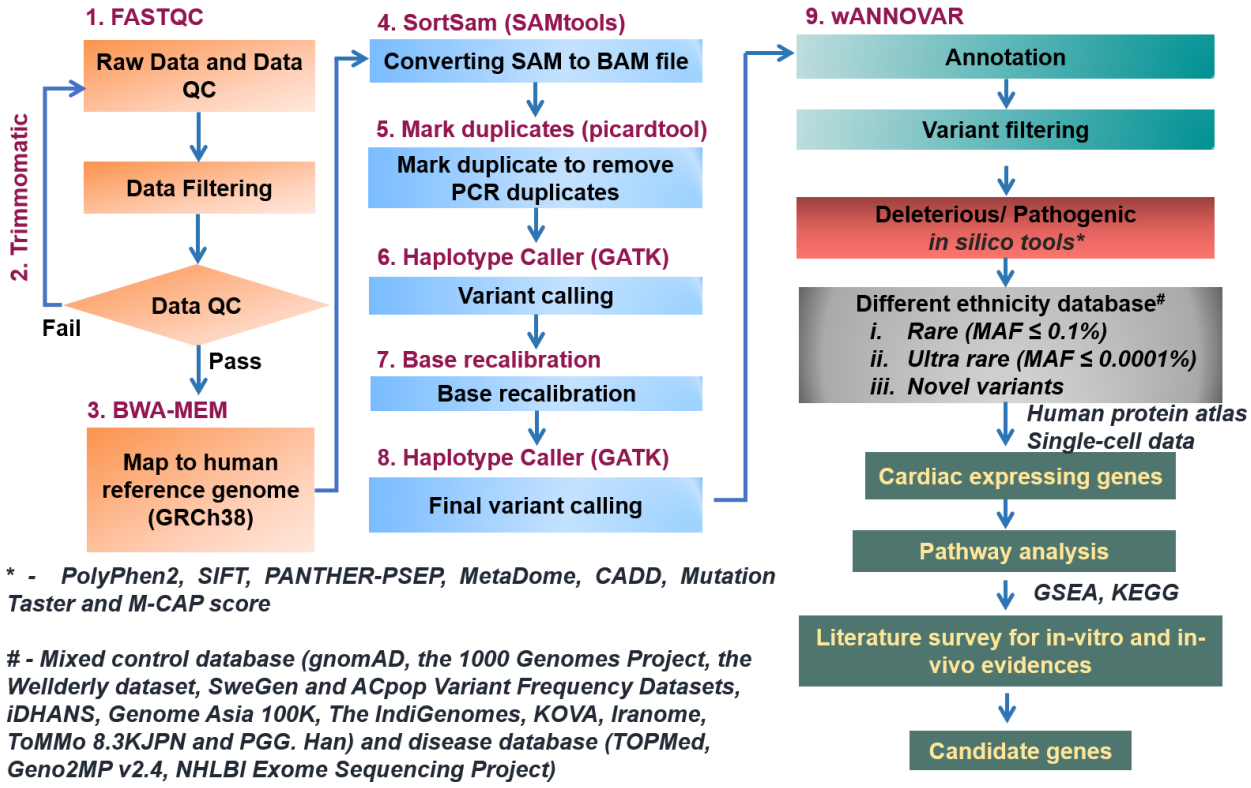

Figure 4.1: Whole exome pipeline for candidate gene selection.

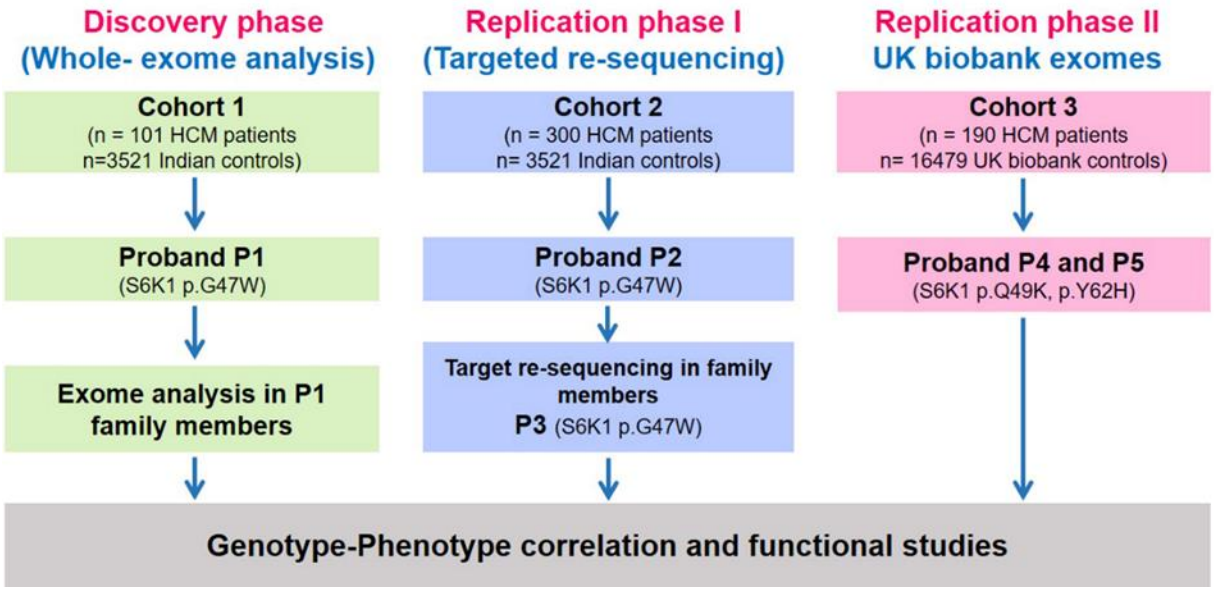

Figure 4.2: Overall study design.

The S6K1 amino acid alteration was absent in various available human exome and genome databases of different ethnicities (n=430864 individuals) outlined in methods. Notably, the variant was also absent in the 3521 Indians, including 1800 healthy Indians (60% male and 40.02±28 years, respectively),[42,72,73] 1029 healthy Indian genomes from IndiGenomes,[88] 94 healthy ageing Indians over the age of 80 years (www.idhans.org)4 and 598 Indian exomes from Genome Asia 100K.[75]

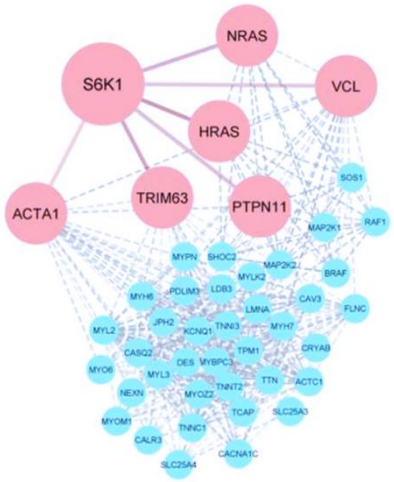

node1	node2	combined_score
ACTA1	S6K1	0.522
HRAS	S6K1	0.701
NRAS	S6K1	0.573
PTPN11	S6K1	0.434
VCL	S6K1	0.402
S6K1	TRIM63	0.614

Figure 4.3: Protein-protein interaction Protein-protein interaction (PP-I) networks showing direct network interaction of the S6K1 gene with other HCM associated genes.

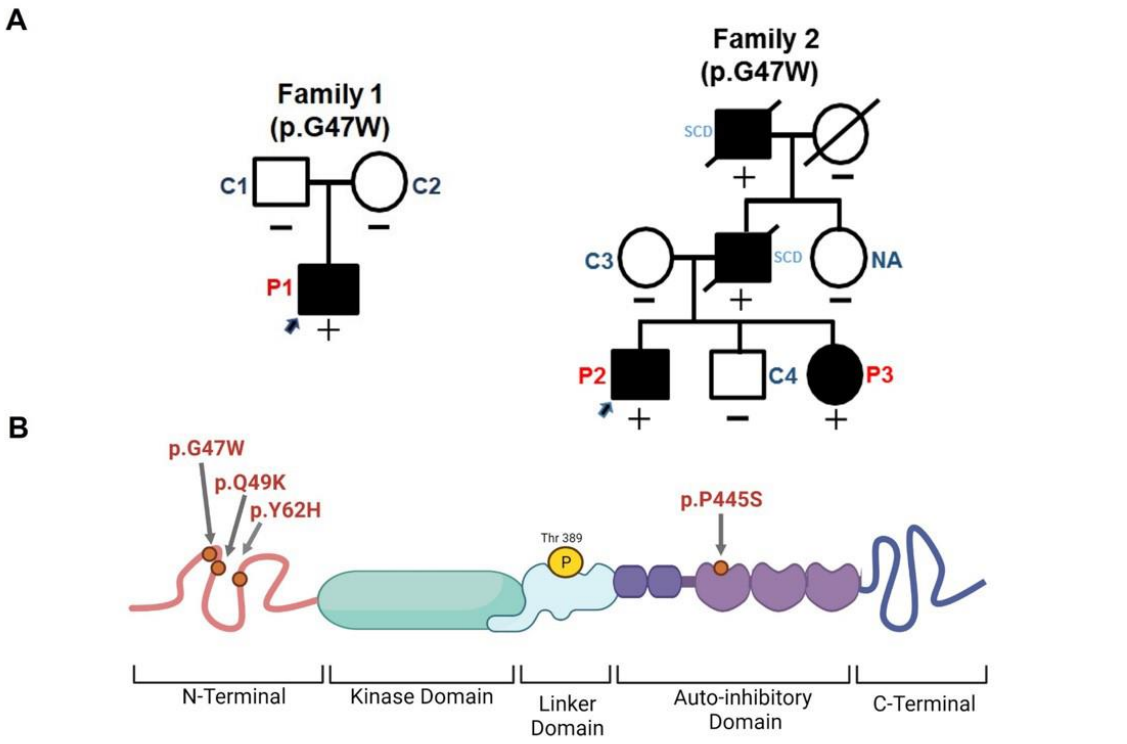

D

In silico tools	Prediction (Score)			
	p.G47W	p.Q49K	p.Y62H	p.P445S
Mutation Taster	Disease causing	Disease causing	Disease causing	Disease causing
PANTHER-PSEP	Possibly damaging	Possibly damaging	Possibly damaging	Possibly damaging
CADD	Disease causing (33)	Disease causing (22.4)	Disease causing (20)	Disease causing (24.4)
MetaDome	Intolerant (0.42)	Intolerant (0.68)	Intolerant (0.93)	Intolerant (0.58)
SIFT	Damaging (0.004)	Tolerated (0.759)	Tolerated (0.418)	Damaging (0.014)
PolyPhen-2	Possibly damaging (0.948)	Benign (0.000)	Benign (0.426)	Possibly damaging (0.467)
M-CAP	Possibly pathogenic (0.192)	Likely Benign (0.013)	Likely Benign (0.018)	Likely Benign (0.020)

Figure 4.4: Molecular genetic analysis of S6K1 variants.

(A) Pedigree of the Indian HCM family 1 and 2. Filled symbols indicate individuals affected with HCM. Arrow indicates the proband. Presence and absence of the S6K1 variant is indicated by the symbols + and −, respectively. **(B)** Schematic representation of the S6K1 structure and location of residues altered in patients with HCM. Regulatory threonine residue is shown in yellow. **(C)** Alignment of S6K1 protein sequences from various species with the amino acid change altered in the probands shown in highlight. **(D)** *In silico* analysis using various software for the S6K1 amino acid changes showing predicted pathological nature.

S6K1 is strongly implicated in cardiac physiology and disease.[87] Various models of cardiac hypertrophy have suggested that S6K1 plays a crucial role in protein synthesis and organ size.[89,90] In these models, S6K1 signals through its downstream pathway members, including rpS6.[83,84] These data suggest the *S6K1* variant (p.G47W) as a potential candidate for HCM in P1.

Next, we target 300 re-sequenced patients with HCM in an independent Indian cohort (Cohort 2, Figure 2 and Table 1) for the S6K1 gene and identified the same variant in another unrelated patient (P2) (Family 2, Figure 4.4A). P2 was screened negative for sarcomeric genes in our previous study.[42,72]

Table 4.1: The baseline characteristics of genotype-positive Indian patients

	Patients		
	P1 (p.G47W)	**P2 (p.G47W)**	**P3 (p.G47W)**
Age	**Late adolescence**	**Adult**	**Adult**
BMI (kg/m^2)	**21**	**24**	**25**
BP (mmHg)	**90/50**	**90/70**	**120/70**
HTN	**No**	**No**	**No**
LVEF, %	**65**	**69**	**71**
IVSd, mm	**22**	**20**	**18**
IVSs, mm	**24**	**21**	**22**
TGL (mg/dL)	**100**	**151**	**160**
HDL (mg/dL)	**40**	**24**	**38**
LDL (mg/dL)	**60**	**72**	**84**
CAD	**None**	**None**	**None**
AF	**None**	**None**	**None**

Table legend: NYHA, New York Heart Association; CAD, Coronary artery disease; AF, Atrial Fibrillation ECG, Electrocardiogram; HTN, Hypertension; LVIDd Left Ventricular Internal Diameter in End Diastole; LVOT Left Ventricular Outflow Tract; LVIDs, Left Ventricular Internal Diameter in End Systole; IVSd, Intraventricular Septal thickness in diastole; LVEF, Left Ventricular Ejection Fraction; BMI, Body Mass Index; BP, Blood Pressure; IVSs, Intraventricular Septal thickness in systole; TGL, Triglycerides; HDL, High-Density Lipoprotein; LDL, Low-Density Lipoprotein.

4.2.2 S6K1 variants in the UK Biobank cardiomyopathy cohort:

Next, we analyzed Cohort 3, comprising 190 cardiomyopathy exomes from the UK Biobank (Figure 4.2). The details of the baseline characteristics of the UK Biobank patients are outlined in Table 4.3. We identified two additional heterozygous variants in *S6K1* (NM_003161.4: c.145C>A, p.Q49K and NM_003161.4: c.184T>C, p.Y62H) in two unexplained probands with no disease-

causative variants in other genes previously linked to HCM. The probands are Caucasians (Table 4.4), and the variants were absent in 16479 UK Biobank controls.

4.2.3 High frequency of N-terminal S6K1 variants in Indian and UK Biobank cardiomyopathy cohorts:

Strikingly, the disease-causing pathogenic missense variants were clustered in the N-terminal domain (amino acids 1 to 90) of S6K1 protein; the OR for the N-terminal pathological missense variants in Indian cases (3/401) were 13 versus Indian controls (2/3521) (95% CI 2.2 to 79.6; $p<0.001$). The OR for N-terminal pathological missense variants in UK Biobank cases (2/190) were 43.8 versus UK Biobank controls (4/16479) (95% CI 7.9 to 240; $p<0.0001$).

Table 4.2: Segregation analysis of S6K1 variant c.139G>T p.G47W) in Indian families (1 & 2)

S.No.	Family member	Age/ Sex	Sequence	Status
1	C1	XX/XX	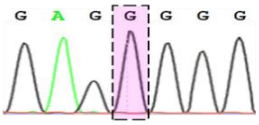	Normal
2	C2	XX/XX	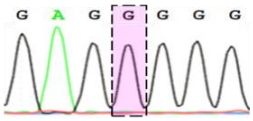	Normal
3	P1	XX/XX	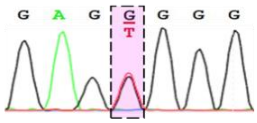	HCM
4	C3	XX/XX	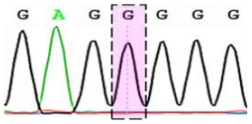	Normal
5	C4	XX/XX	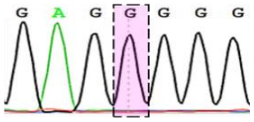	Normal
6	P2	XX/XX	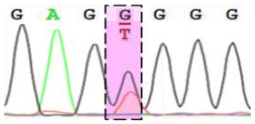	HCM
7	P3	XX/XX	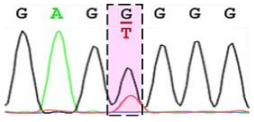	HCM

Table 4.3: The baseline characteristics of UK-biobank cardiomyopathy samples. (n=190)

Characteristic features	Values
Age, mean (SD), year	72.41 (6.5)
Male, n (%)	119 (62.6)
Female, n (%)	71 (37.4)
Race/ ethnicity, n (%)	
British	169 (88.9)
Other white background	9 (4.7)
Caribbean	5 (2.6)
Irish	3 (1.5)
African	1 (0.52)
Indian	1 (0.52)
Unknown	2 (1.05)
BMI, mean (SD), kg/m^2	28.65 (5.5)
Body surface area, m^2	1.94 (0.20)
Dyslipidemia	80 (42.10)
Cardiac parameter, mean (SD)	
Ejection fraction, %	47.12 (11.32)
Left ventricle end diastolic volume, mL	174.25 (56.77)
Left ventricle end systolic volume, mL	96.5 (56.62)
Left ventricle stroke volume, mL	77.875 (16.47)
Cardiac output, litres/min	4.95 (1.09)
Cardiac index, litres/min/m^2	2.54 (0.52)
Average heart rate, bpm	64.5 (10.71)
Estimated wall thickness, mean (SD), mm	≤ 13

The OR for combined (UK Biobank and Indian) N-terminal pathological missense variants in cases (5/591) was 42 versus respective combined controls (UK Biobank and Indian) (4/20000) (95% CI 11 to 159; $p<0.0001$) and 164 against gnomAD subjects (13/282314) (95% CI 58.54 to 463.5; $p<0.0001$). These data support *S6K1* variants as a new candidate for HCM.

4.2.4 Autoinhibitory S6K1 variant in an Arab patient with HCM:

We also found a deleterious heterozygous variant in *S6K1* (NM_003161.4:c 1333C>T, p.P445S) in an unsolved Arab patient with HCM without any known cardiomyopathy gene variants. (P6, Table 5).

Table 4.4: Detailed characteristics of genotype-positive UK biobank HCM patients

	Patients	
	P4 (p.Q49K)	**P5 (p.Y62H)**
Age	Adult	Adult
Sex	Female	Male
Body Mass index, kg/m^2	23.63	30.06
Blood Pressure, mmHg	121/72	158/87
Body surface area, m^2	1.78	*Not revealed*
Hypertension	No	Yes
Ejection fraction, %	63	*Not revealed*
Left ventricle end diastolic volume, mL	153	*Not revealed*
Left ventricle end systolic volume, mL	56	*Not revealed*
Left ventricle stroke volume, mL	97	*Not revealed*
Cardiac output, litres/min	6.6	*Not revealed*
Cardiac index, litres/min/m^2	3.7	*Not revealed*
Average heart rate, bpm	68	*Not revealed*
Estimated wall thickness, mm	14	*Not revealed*
Triglycerides, mmol/L	1.049	1.157
High-Density Lipoprotein, mmol/L	1.832	1.145
Low-Density Lipoprotein, mmol/L	3.084	3.313
Atrial Fibrillation	No	Yes
Final diagnosis	Obstructive hypertrophic cardiomyopathy (I42)	Hypertrophic cardiomyopathy (I42)

This variant affected an evolutionarily conserved proline in the autoinhibitory domain and was predicted to be pathological (Figure 4.4B–D). Notably, the autoinhibitory domain interacts with the N-terminal domain for S6K1 activation. The p.P445S is ultrarare or absent (MAF of 0.0001–0) among various populations and has a rare MAF of 0.004 among the Ashkenazi Jewish subpopulation in gnomAD.

4.2.5 Genotype-phenotype correlation:

The genotype positive P1 from Family 1 was in his early adolescence, and his medical records suggested a mild neurodevelopmental delay. The parents of P1 were paternity-confirmed, healthy and negative for this particular variant, suggesting its de novo origin (Table 4.2). However, in Family 2, multiple family members were affected with HCM (P2 and P3) with no obvious extracardiac findings.

Table 4.5: The baseline characteristics of the Arab HCM patient.

	Patient
	P6 (p.P445S)
Age	Adult
Sex	Male
Body Mass index, kg/m^2	26.6
Blood Pressure, mmHg	125/70
Body surface area, m^2	NA
Hypertension	No
Ejection fraction, %	65%
Left Ventricle end diastolic volume, mL	123
Left Ventricle end systolic volume, mL	44
Average heart rate, bpm	68
Estimated wall thickness, mm	15.3
Triglycerides, mmol/L	6.6
High-Density Lipoprotein, mmol/L	2.1
Low-Density Lipoprotein, mmol/L	3.8
Atrial Fibrillation	None
Final diagnosis	HCM

Targeted sequencing of the respective *S6K1* variant in various members of Family 2 suggests that the variant is present only in affected family members (Table 4.2). Also, a high incidence of sudden cardiac deaths was documented in Family 2 (Figure 4.4A). Clinical presentations for all the genotype-positive patients are given in Table 4.1,4.4 and 4.5.

Table 4.6: Inclusion Exclusion criteria

S.No.	Gene Name/mutation	Pathogenicity (Polyphen)	Function	GnomAd frequency	Gene Expression in Heart		Protein-protein interaction (PPI) and network analysis* (3)	Cardiomyopathy related literature (4)	Criteria for exclusion
					Tissue (1)	Single cell (2)			
1.	AGPAT5: p.H136Y	Damaging	Acyltransferase activity	0.00	Yes	Yes	No direct interaction	No	3 and 4
2.	AGR3: p.P61Q	Damaging	Dystroglycan binding	0.00	Yes	No	No interaction	No	2, 3 and 4
3.	ANKRD31: p.D905del	Damaging	Involved_in homologous chromosome pairing at meiosis	0.00	Yes	No	No interaction	No	2, 3 and 4
5.	CHPF: p.N272T	Damaging	Acetylgalactosaminyltransferase activity	0.00	Yes	Yes	No interaction	No	3 and 4
6.	COL4A6: p.A1553D	Damaging	Extracellular matrix structural constituent	0.00	Yes	Yes	No interaction	No	3 and 4
7.	EXT1: p.M215K	Damaging	Acetylglucosaminyltransferase activity	0.00	Yes	Yes	No interaction	No	3 and 4

8.	FKBP9: p.G230R	Damaging	Calcium ion binding and peptidyl-prolyl cis-trans isomerase activity	0.00	Yes	Yes	No interaction	No	3 and 4
9.	HAUS7: p.A12V	Damaging	Microtubule minus-end binding and thioesterase binding	0.00	Yes	No	No interaction	No	2, 3 and 4
10.	IFT80: p.D316Y	Damaging	Involved in articular cartilage development	0.00	Yes	Yes	No interaction	No	3 and 4
11.	KIF7: p.L1167F	Damaging	ATP binding and ATP hydrolysis activity	0.000004134	Yes	No	No interaction	No	2, 3 and 4
12.	**RPS6KB1: p.G47W**	**Damaging**	**Protein serine/threonine/tyrosine kinase activity**	**0.00**	**Yes**	**Yes**	**Direct interaction with other CM genes**	**Yes**	**Selected**
13.	MAFB: p.E4G	Damaging	DNA-binding transcription activator activity, RNA polymerase II-specific	0.00	Yes	No	No interaction	No	2, 3 and 4
14.	MFSD10: p.L346del	Damaging	Organic anion transmembrane transporter activity	0.00	Yes	Yes	No interaction	No	3 and 4
15.	MUC16: p.A12383_G12384insA	Damaging	Role in forming a barrier, protecting epithelial cells from pathogens	0.00	Yes	No	No interaction	No	2,3 and 4
16.	MUC16: p.I12380_A12382del	Damaging	Role in forming a barrier, protecting epithelial cells from pathogens	0.00	Yes	No	No interaction	No	2, 3 and 4
17.	MYO1G:p.R462C	Damaging	ATP binding, actin filament binding, calmodulin binding and microfilament motor activity	0.00002488	Yes	No	No interaction	No	2, 3 and 4
18.	PCDHGA12: p.G82A	Damaging	Calcium ion binding	0.00	Yes	No	No interaction	No	2, 3 and 4
19.	PTGDR2: p.I221T	Damaging	G protein-coupled receptor activity and neuropeptide binding	0.000005145	Yes	No	No interaction	No	2, 3 and 4
20.	SERP2: p.A10D	Damaging	Protein binding	0.00	Yes	Yes	No interaction	No	3 and 4
21.	STON2: p.G51R	Damaging	Clathrin adaptor activity and protein binding	0.000007976	Yes	Yes	No interaction	No	3 and 4
22.	STXBP3:p.C501Y	Damaging	Protein binding, protein-containing complex binding and syntaxin binding	0.000003981	Yes	Yes	No interaction	No	3 and 4
23.	TCEA3: p.N317S	Damaging	DNA binding, protein binding and Zinc ion binding	0.00	Yes	No	No interaction	No	2, 3 and 4
24.	TCHH: p.E1340K	Damaging	Calcium ion binding and transition metal ion binding	0.000004007	Yes	No	No interaction	No	2, 3 and 4
25.	TTI2: p.V278L	Damaging	Involved in cellular resistance to DNA damage stresses and may act as a	0.00001193	Yes	Yes	No interaction	No	1, 2, 3 and 4

			regulator of phosphoinositide-3-kinase-related protein kinase (PIKK) abundance						
26.	AOC2:p.P722T	Damaging	Aliphatic-amine oxidase activity, aminoacetone:oxygen oxidoreductase(deaminating) activity, copper ion binding and electron transfer activity	0.002355	Yes	No	No interaction	No	2, 3 and 4
27.	CCDC18:p.L448P	Damaging	Nucleotide binding	0.001386	Yes	Yes	No interaction	No	3 and 4
28.	CCDC51:p.R165C	Damaging	Mitochondrial ATP-gated potassium channel activity and protein binding	0.004855	Yes	No	No interaction	No	2, 3 and 4
29.	MELTF:p.T240M	Damaging	Iron ion binding and protein binding	0.001605	Yes	No	No interaction	No	2, 3 and 4
30.	NUMA1:p.R311C	Damaging	Disordered domain specific binding, dynein complex binding and microtubule binding	0.0004136[@]	Yes	Yes	No interaction	No	2 and 3
32.	THADA:p.R1353S	Damaging	Involved_in lipid homeostasis and adaptive thermogenesis	0.006408	Yes	No	No interaction	No	2, 3 and 4
33.	ZFHX4:p.A1003T	Damaging	DNA-binding transcription factor activity, RNA polymerase II-specific	0.000352	Yes	Yes	No interaction	No	3 and 4

4.2.6 S6K1 variants cause cardiac hypertrophy:

To understand the functional significance of S6K1 variants, we transiently expressed the GFP-tagged full-length S6K1 WT and a representative mutant (p.G47W) constructs individually in the HL-1 (mouse cardiomyocytes) cells. Subsequent immunofluorescence analysis demonstrated that transient expression of the variant protein (p.G47W) was associated with a significant increase in cell size compared with S6K1 WT-expressing cardiomyocytes (Figure 4.5A). Next, we quantified the mRNA levels of various bona fide hypertrophic markers, such as atrial natriuretic peptide (*Nppa*), brain natriuretic peptide (*Nppb*), skeletal muscle alpha-actin (*Acta1*) and myosin heavy chain ratio (*Myh6/Myh7*), in HL-1 cardiomyocytes expressing S6K1 WT and p.G47W, respectively. We observed a significant upregulation and a shift in the *Myh6/Myh7* ratio of hypertrophic markers in S6K1 p.G47W-expressing cardiomyocytes compared with controls (Figure 4.5B). These results suggest that the S6K1 variant induces cardiac hypertrophy.

4.2.7 S6K1 variants activate rpS6/ERK related signaling:

Activation of S6K1 is a complex process but requires phosphorylation of T389, leading to the release of its interaction between the C-terminal autoinhibitory and N-terminal domains. Strikingly, the majority of the cardiomyopathy-related S6K1 variants (p.G47W, p.Q49K and p.Y62H) are located in the N-terminal domain of S6K1 (1-90AA) (Figure 4.4B) and activates S6K1 by hyper-phosphorylating T389 (Figure 4.5C). Activated S6K1 is known to phosphorylate the 40S rpS6 at the S235/236 and S240/244 sites and reduce phospho-eEF2 at the threonine 56 (T56) site.[89–91] These modifications are crucial for hypertrophy related protein synthesis, serving primarily to regulate translation initiation and elongation processes. Immunoblot analysis of lysates obtained from representative S6K1 p.G47W-expressing HL-1 cardiomyocytes showed significantly increased phosphorylation of pS6K1T389 and rpS6S240/244 with no alterations in the rpS6S235/236 site. Accordingly, there was a substantial reduction in peEF2T56 compared with WT-expressing cells (Figure 4.5C). A similar pattern was observed for other S6K1 mutants (p.Q49K or p.Y62H) expressing cells (Figure 4.6). These results indicate that the *S6K1* variants are gain-of-function variants that induce S6K1 activity through rpS6S240/244 along with a corresponding decrease in peEF2T56 levels.

Recently, the N-terminal domain of S6K1 was also shown to interact with the eukaryotic initiation factor 4E (eIF4E).[92] Notably, elF4E binds to the elF4E-binding protein 1 (4EBP1), and subsequent phosphorylation at 4EBP1 dissociates this binding, leading to active eIF4F complex formation. These events eventually affect the other downstream effectors, and DAP5, to enhance the translation process.[93,94]

These proteins were observed to be hyperphosphorylated in the S6K1 mutant-expressing cells compared with the cells expressing WT (Figures 4.3 and 4.4). In addition, the representative S6K1 p.G47W variant significantly increased the phosphorylation of ERK1/2 compared with S6K1 WT (Figure 4.5D). Sustained ERK1/2 activation was reported in patients with pathological cardiac hypertrophy.[95]

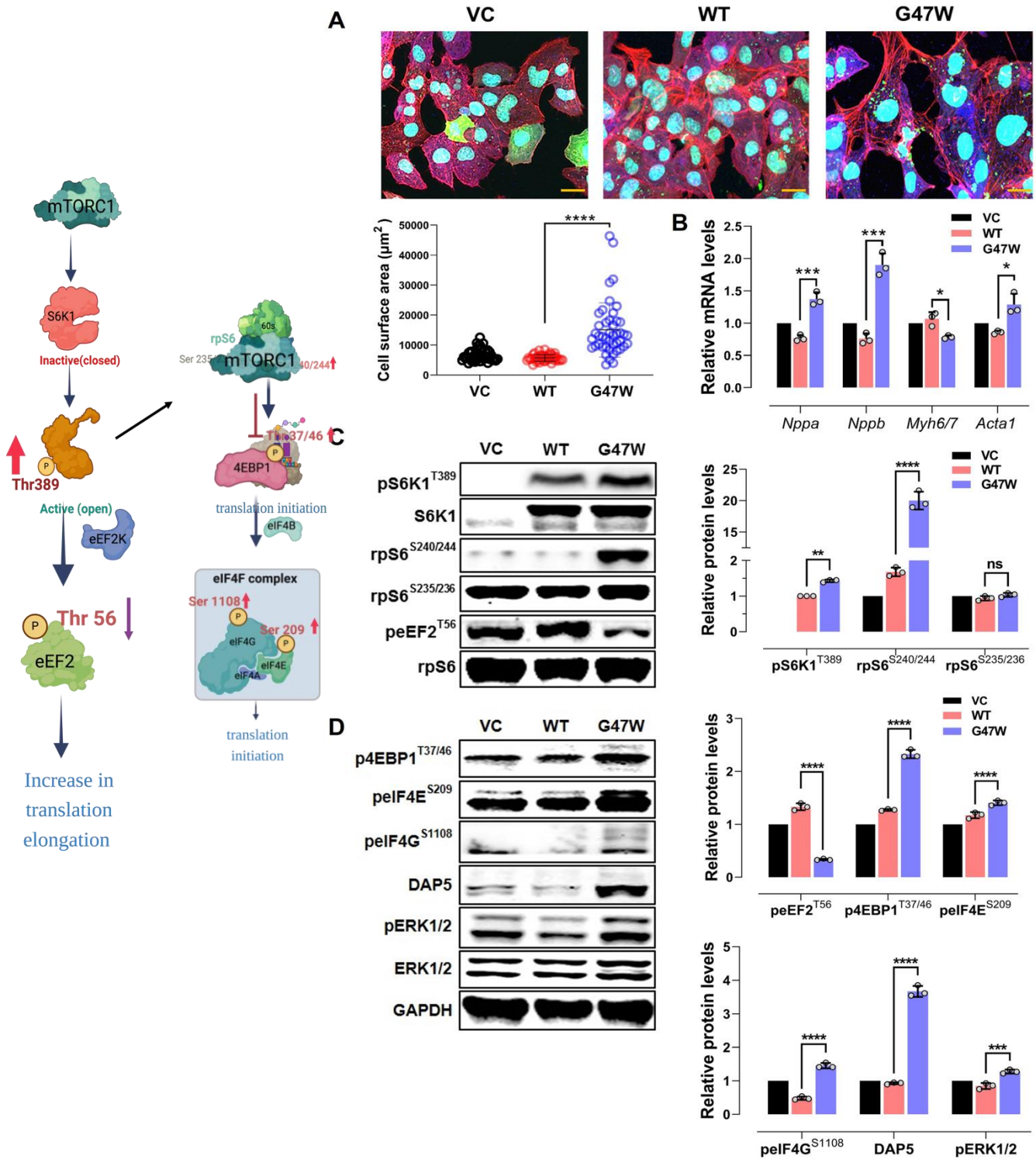

Figure 4.5: S6K1 p. G47W variant induces cardiac hypertrophy and rpS6/ERK pathways.

On the left, schematic showing the activation of S6K1 followed by rpS6 and eIF4A complex. **(A)** Representative images and cell surface area measurements in cardiomyocytes expressing with a vector control (VC), wild type S6K1 (WT) or variant p.G47W (G47W) for 24 hours and stained with phalloidin (actin), cardiac troponin T (cTnT), or Hoechst (nuclei). scale bars, 10 µm. Results presented as relative cell area compared with VC (n=30 to 40 cells in five

different fields). **(B)** Quantitative real-time PCR analysis of hypertrophic markers *Nppa, Nppb, Myh6/Myh7* ratio and *Acta1* in the HL-1 cardiomyocytes expressing VC, WT and G47W, respectively. mRNA levels were normalised to 18 s rRNA and presented as relative expression levels compared with the level in the vector control cardiomyocytes. Values are shown as mean±SEM with each experiment performed in triplicate (n=3). **(C, D)** Representative immunoblots with indicated proteins from the total lysates of HL-1 cardiomyocytes expressing VC, WT and G47W, respectively. Expression levels were normalised to total proteins and presented as relative expression levels compared with the level in VC expressing HL-1 cardiomyocytes. Glyceraldehyde-3-phosphate dehydrogenase (GAPDH) levels were used as a loading control. Values are shown as means±SEM with each experiment performed in triplicate (n=3). Significance was evaluated by Student's t-test or one-way analysis of variance (ANOVA) with post hoc Tukey's test, respectively. *p<0.05, ***p<0.001 and ****p<0.0001.

As a piece of direct evidence, we obtained an endomyocardial biopsy from a patient (P1) with the p.G47W variant. The lysates from the genotype-positive patient tissue sample showed enhanced S6K1 and rpS6 activity by hyper-phosphorylating T389 and S240/244 sites compared with controls (Figure 4.7). Finally, these results suggest that the *S6K1* variants are activating through pathways involving rpS6 to induce cardiac hypertrophy (Figure 4.7).

4.3 DISCUSSION

Here, we screened a total of 592 HCM cases and identified six missense *S6K1* variants in six unexplained cases (three Indians, two Europeans and an Arab). Each allele identified in our cardiomyopathy probands, including Indian and UK Biobank patients, was novel (except Arabian). The overall burden of pathological missense variants in S6K1 in cardiomyopathy cohorts (6/592) was highly enriched compared with those among more than 280000 alleles in gnomAD (148/282314) (OR=19.5, 95% CI 8.6 to 44; p<0.0001). This OR is higher than those obtained by other groups using a similar exome strategy for missense variants in predominant HCM causing sarcomeric genes such as MYBPC3 (OR=5.7) or MYH7 (OR=12).[96] Computational analyses predicted that the identified *S6K1* missense variants cause significant damage to and potential pathological effects on protein structure and function. These data strongly support S6K1 variants as a new candidate for HCM.

S6K1 belongs to family of kinases that plays a crucial role in protein synthesis,[97–99] cell growth regulation,[100] cell cycle progression,[101,102] adipose differentiation,[103] synaptic plasticity[104] and maintaining homeostasis[105] etc. Among plethora of functions, protein synthesis is the major function of RPS6KB1 which is imparted upon the phosphorylation of small subunit (40s) of ribosome at two major phosphorylation sites Ser235/236 and Ser240/244 thus regulating the protein biogenesis.

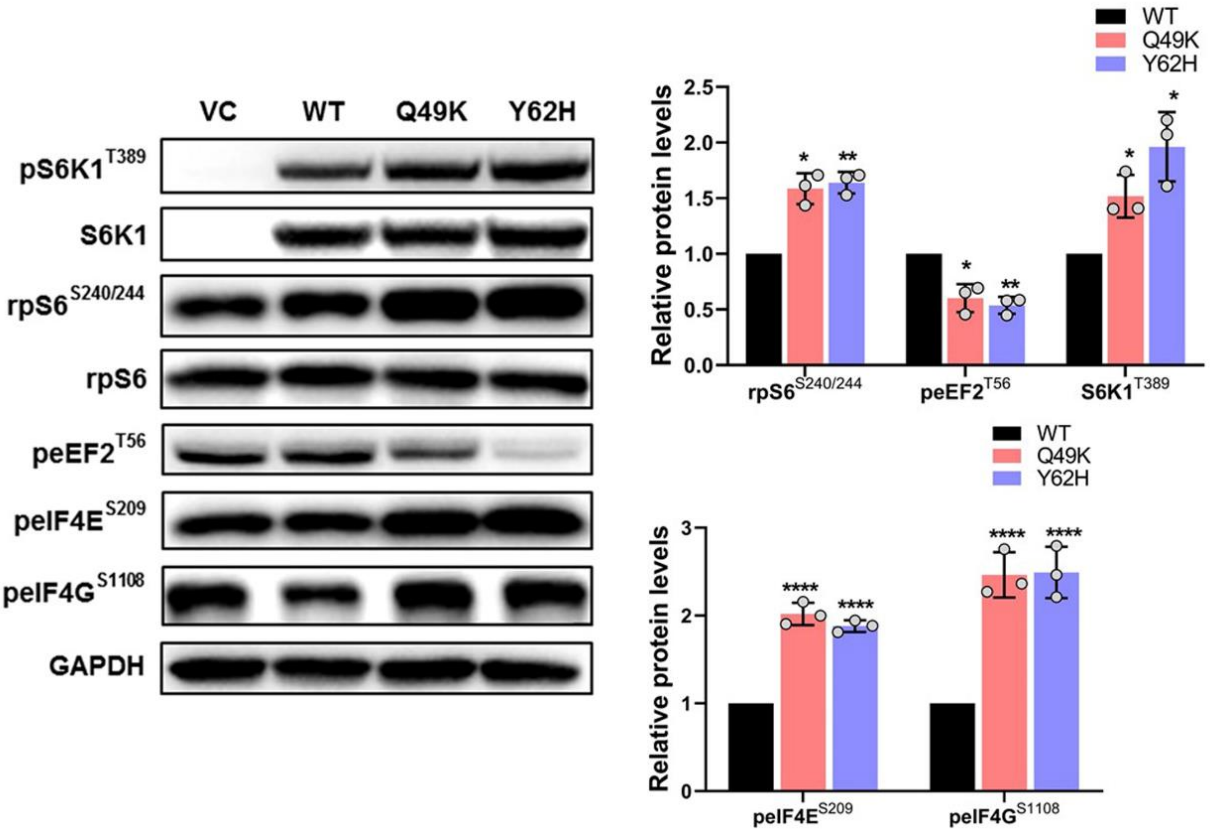

Figure 4.6: UK Biobank cardiomyopathy-associated S6K1 variants (p.Q49K and p.Y62H) activate S6K1/rpS6 and its associated pathways.

Representative immunoblots with indicated proteins from the total lysates of HEK293T expressing vector control (VC), wild type (WT), Q49K and Y62H treated with Phorbol 12- myristate 13-acetate (PMA) for 30 min or 60 min (peIF4E and peIF4G). Expression levels were normalized to total proteins and presented as relative expression levels compared with the level in VC expressing HEK293T. Glyceraldehyde-3-phosphate dehydrogenase (GAPDH) levels were used as a loading control. Values are shown as means±SEM with each experiment performed in triplicate (n=3). Significance was evaluated by Student's t-test or one-way analysis of variance (ANOVA) with post hoc Tukey's test, respectively. *p<0.05, **p<0.01 and ****p<0.0001.

S6K1 is downstream of mechanistic target of rapamycin complex 1 (mTORC1) and its activation is regulated by phosphorylation by mTORC1 on at least 8 mapped sites with 3 major critical sites. First is Threonine 229 in T-loop site activation loop, second one at Serine 371 in turn motif site in

linker domain and most important third one at Threonine 389 in hydrophobic motif.[106] mTORC1 itself is regulated by a complex signaling pathways and environmental cues like i) nutrient availability particularly amino acids like leucine, ii) growth factors and hormones like insulin-like growth factor (IGF-1) can activate mTORC1 via phosphoinositide 3-kinase (PI3K/Akt) pathway. Activation of Akt results in inhibition of tuberous sclerosis complex (TSC); a negative regulator of mTORC1.[107] Inactivated TSC relieves the inhibitory effect on Rheb (Ras homolog enriched in brain) allowing it to activate mTORC1 and subsequently S6K1 iii) stress and cellular damages

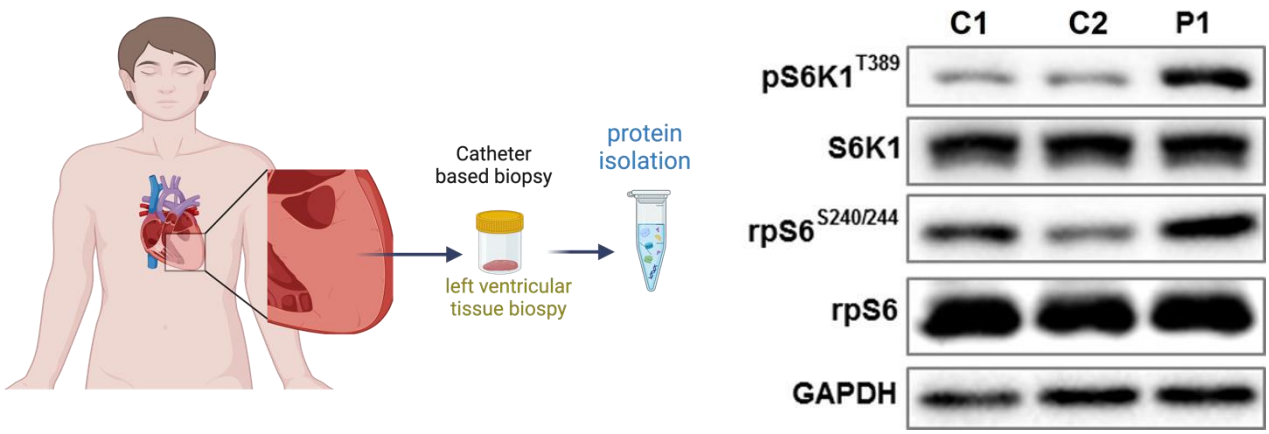

Figure 4.7: S6K1/rpS6 activation in a genotype-positive patient heart tissue sample

S6K1/ rpS6 status in endomyocardial biopsy lysates from P1 and control subjects. Representative immunoblots with indicated proteins from the endomyocardial biopsy lysates from P1 and control subjects (C1and C2) without cardiomyopathy, respectively.

can activate p53 and MAP kinases which can either inhibit or activate mTORC1 in a context and severity dependent manner iv) regulatory proteins which directly interacts with the complex like Rag GTPases which resident of lysosomal membrane can act as molecular switches that control the recruitment of mTORC1 to its activator Rheb.[107]

S6K1 in general remains in closed confirmation; an auto-inhibitory state with its N-terminal domain interaction with auto-inhibitory domain (Figure 4.1B). Upon phosphorylation by mTORC1 at Thr389 position, conformational change leads to opening of S6K1 and consequently increase in activity (Figure 4.1E).

S6K1 is an integral part of the translational initiation and elongation process of protein synthesis.[98,99] Of note, an increase in protein synthesis and subsequent cell size is a hallmark of HCM. The relationship between S6K1 and cardiac hypertrophy has been recently explored in

feline and mice models.[90,108] Accordingly, in a pressure overload model of feline cardiomyocytes, S6K1 is known to activate hypertrophy through ERK1/2 and rpS6 pathways.[108] Transgenic mice overexpressing S6K1 displayed increased heart size and showed evidence of cardiac hypertrophy through phosphorylation of rpS6 kinase.[90] In line with these, we demonstrate that the representative patient-specific *S6K1* mutant constitutively stimulates cardiac hypertrophy in cultured cardiomyocytes by increasing cell size and DAP5, reactivating the fetal gene program, and activating the rpS6 and ERK1/2 pathways.

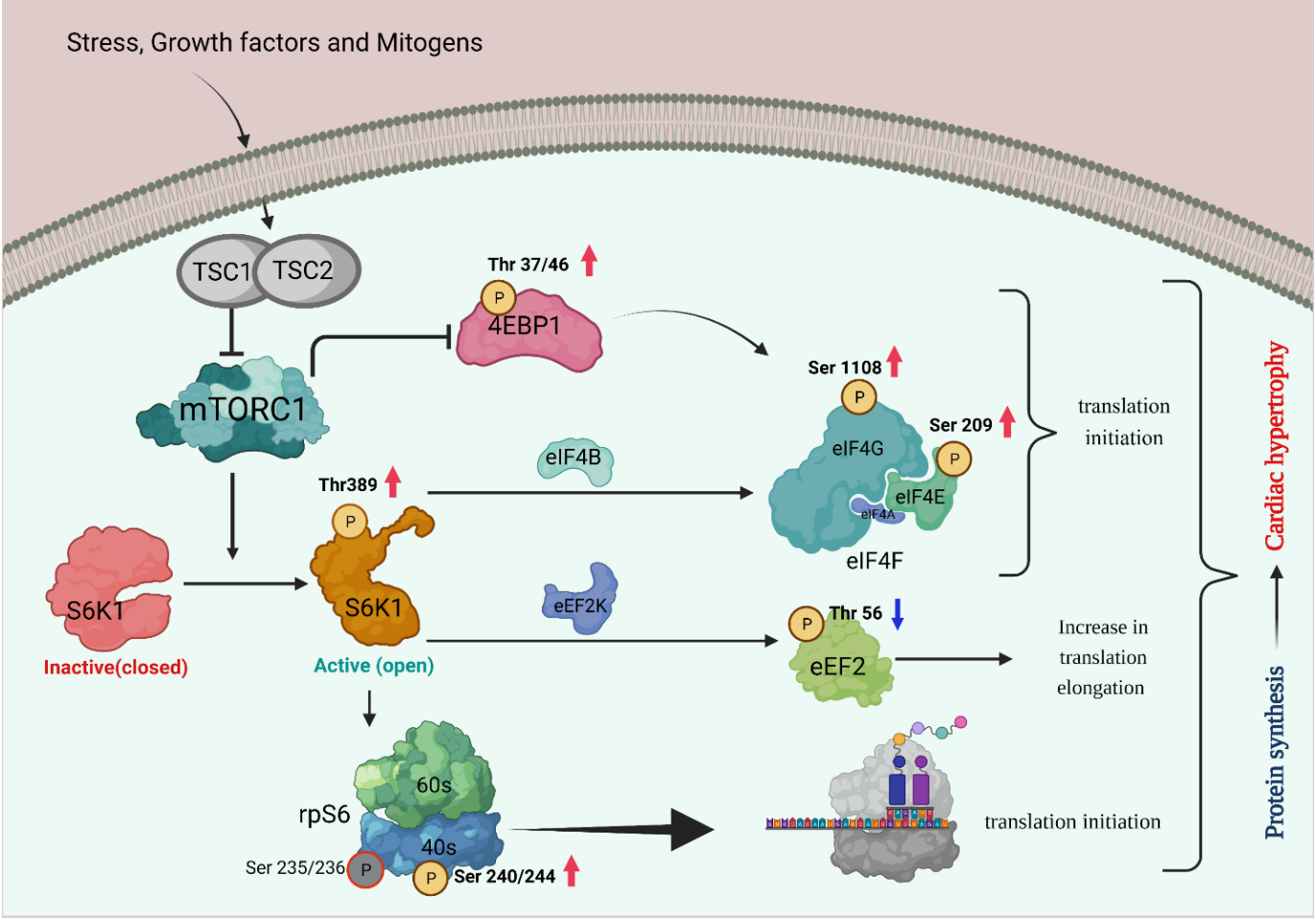

Figure 4.8: Proposed mechanism of S6K1 mutants leading to cardiomyopathy

Under basal conditions, the S6K1 protein exists in an autoinhibited state due to the interaction between its N-terminal and the autoinhibitory domain. The phosphorylation of specific residues located in the linker region, including 389T by the mTOR pathway, results in the release of interaction between the N-terminal and the autoinhibitory domain, allowing the S6K1 protein to

be activated.[89] The activated S6K1 results in phosphorylation of rpS6 and eIF4F complex members, including eIF4G and eIF4E.[89,90] Of note, most HCM mutations are in the *S6K1* N-terminal region that hyperphosphorylated specific sites of S6K1, rpS6 and eIF4F complex members. These results provide potential mechanistic insights of S6K1 mutants in enhancing protein synthesis and causing cardiac hypertrophy.

Taken together, we identified variants in *S6K1* in patients with HCM with different ancestry and demonstrated that these are gain-of-function variants in cellular models and patient tissue samples (P1). Additional screening in a large cohort of patients with HCM and a detailed mechanistic study may enable these findings to be corroborated further.

CHAPTER: 5

RESULTS AND DISCUSSION

TTL $^{p.G219S}$ causes HCM in patient-specific iPSC-derived cardiomyocytes by inducing oxidative stress

5.1 Introduction:

Cardiac function is contingent upon the harmonious operation of molecular mechanisms that ensure optimal function in various physiological circumstances. One such mechanism is the de-tyrosination/tyrosination cycle, which is a vital regulator of microtubule dynamics involved in cellular processes.[109]

The post-translational modification of α-tubulin, which comprises microtubules, by the de-tyrosination/tyrosination cycle occurs through alternating removal and addition of tyrosine at its carboxyl terminus. This process, which is mediated by tubulin tyrosine ligase (TTL) and tubulin carboxypeptidase (TCP), among others, governs the stability and dynamics of microtubules required for intracellular trafficking, cell division, and organelle positioning.[110]

Heart failure patients including HCM are shown to be exhibiting disruption in the balance of the de-tyrosination/tyrosination cycle of microtubules.[111] Additionally, alterations in signaling pathways e.g. Calcium/Calmodulin-dependent protein kinase II (CaMKII), contribute to the instability of microtubules and the development of HCM. It is now acknowledged as a significant regulatory mechanism controlling microtubule dynamics, which are vital for normal cardiac function, and is therefore considered a crucial determinant of the contractile properties and responsiveness of heart tissue.[112]

In our research, we discovered a novel, heterozygous mutation in the Tubulin tyrosine ligase (TTL) gene in a South Indian cohort. To understand the role of this TTL variant in hypertrophic cardiomyopathy (HCM), we employed protein biochemistry, molecular dynamic simulations, and patient-specific induced pluripotent stem cell-derived cardiomyocytes. Our findings provide direct evidence that the TTL variant leads to decreased activity and increased accumulation of de-tyrosinated tubulin in cardiomyocytes, ultimately resulting in oxidative stress. As far as we know, this is the first time a mutation in TTL has been implicated in causing HCM.

5.2 RESULTS

5.2.1 TTL as a novel gene for hypertrophic cardiomyopathy:

Using the cohort of 101 HCM exomes (refer Figure 4.2), we identified a novel and potentially pathogenic gene variant in the coding sequence of the Tubulin tyrosine ligase gene in a patient named P7. Based upon the inclusion and exclusion criteria as explained in (Table 4.6), we selected TTL as a potential candidate. In brief, the other genes are excluded because either they are not expressed in the heart (tissue specific or single cell data) or failed to have direct interaction with already known genes (protein-protein interaction network analysis). The patient's healthy family members, P7a and P7b, tested negative for the specific variant, suggesting a de novo origin in the individual with the TTL variant (Figure 5.1 A). In the patient with the TTL variant, the glycine residue at position 219 was replaced with a serine residue (p.G219S). This position is highly conserved across the species (Figure 5.1B) and various in silico tools have predicted it to be damaging or deleterious in nature (Figure 5.1C). The variant was not observed in any of the publicly accessible databases from various global population datasets, including the Single-Nucleotide Polymorphism Database (dbSNP), 1000 Genomes Project, National Heart Lung and Blood Institute- Grand Opportunity (NHLBI-GO) Exome Sequencing Project (ESP), Korean exomes database (KOVA), Exome Aggregation Consortium (ExAC), Genome Aggregation Consortium (gnomAD), Trans-Omics for Precision Medicine (TOPMed), Iranome, the Tohoku Medical Megabank Organization 8.3K Japan, the Han Chinese Genomes Database (PGG. Han), Genotype to Mendelian Phenotype (Geno2MP v2.2) cohorts, which comprise approximately 426,060 alleles, the NHLBI Exome Sequencing Project, Exome Variant Server, Swedish data sets (SweGen and ACpop Variant Frequency data sets), Indian and Caucasian elderly control data sets including healthy ageing Indian exomes (www.idhans.org) and the Wellderly data set, as well as the South Asia-specific Indian control data (N=3521) sets such as Genome Asia 100K, Indigenomes, and South Asian (Indian) healthy controls.

5.2.2 TTL p.G219S variant shows perturbed conformational dynamics than wild type:

To further investigate the impact of the mutation in the TTL protein on its interaction with the alpha tubulin C terminal tail (CTT), we performed MD simulation of the wild type and mutant

TTL enzyme with CTT using GROMACS.[113] TTL bound tubulin CTT structure was prepared from the crystal structure of the tubulin-stathmin-TTL ADP complex (PDB ID: 4IHJ) by removing the stathmin bound tubulin dimers using UCSF Chimera.[114] A single amino acid substitution at the glycine 213 position to serine was introduced in the wild type protein using UCSF Chimera to generate the mutated version of the protein (Figure 5.2A). The deviation in the structural characteristics, spatial displacement and stability of the protein was monitored during the course of the 100 ns simulation and was represented using Root-Mean Square Deviation (RMSD), Root Mean Square Fluctuation (RMSF) and change in radius of gyration (Figure 5.2B). The RMSD fluctuation of the alpha carbons (Cα) backbone shown in figure 5.2B indicated that even though fluctuations were evident throughout the simulation, the wild type system reached its equilibrium after approximately 8ns with structure maintaining at level of around 1.5Å till the end of the simulation. In contrast, the mutant TTL system reached its equilibrium after 20ns and showed a higher average displacement among atoms with structure maintaining at level above 2Å. The change in root mean square fluctuation was used to identify the protein regions with greater flexibility. In comparison to wild type, the mutant exhibited higher flexibility in residues near to 219th site, which are in close proximity to the highly conserved nucleotide binding site.[115] The measure of radius of gyration (Rg) reflects the overall compactness of the protein that correlates with the stability of the protein.[116] The overall changes in the Rg value of wild type and mutant during the course of simulation is shown in (Figure 5.2D) . Our result suggested that the mutant protein has a higher degree of Rg as compared to wild type, indicating a reduction in compactness in the mutant TTL variant.

5.2.3 TTL p.G219S variant displayed delayed activity:

MD simulation suggested that variant site of TTL (G219S) induces a conformational change near the beta loop and the nucleotide binding site and alters its interacting ability with the tubulin C-ter tail. To validate this observation, we conducted an *in vitro* tyrosination assay using purified recombinant wild type and mutant TTL protein (Figure 5.1C) with carboxypeptidase-treated goat brain tubulin as substrate. The enzymatic activity of both wild type and mutant TTL was captured by immunoblotting for different time points. Our findings revealed that the rate of tyrosine addition to the tubulin substrate by the mutant TTL protein was notably delayed than that of the wild type TTL protein (Figure 5.1D).

A

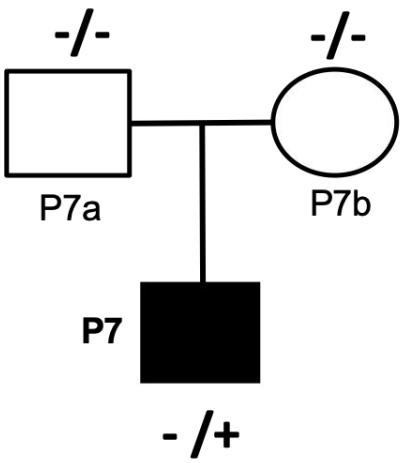

B

Software	Score	Prediction
CADD_Phred	24.8	Damaging
Polyphen	0.999	Damaging
Mutation taster	1	Damaging
PROVEAN	-5.3	Damaging
SIFT	0.052	Tolerated
Mutation Taster	1	Deleterious
MetaIR	0.059	Tolerated
DANN	0.928	Deleterious
M-Cap	0.025	Tolerated
Fathmm-MKL	0.978	Damaging

C

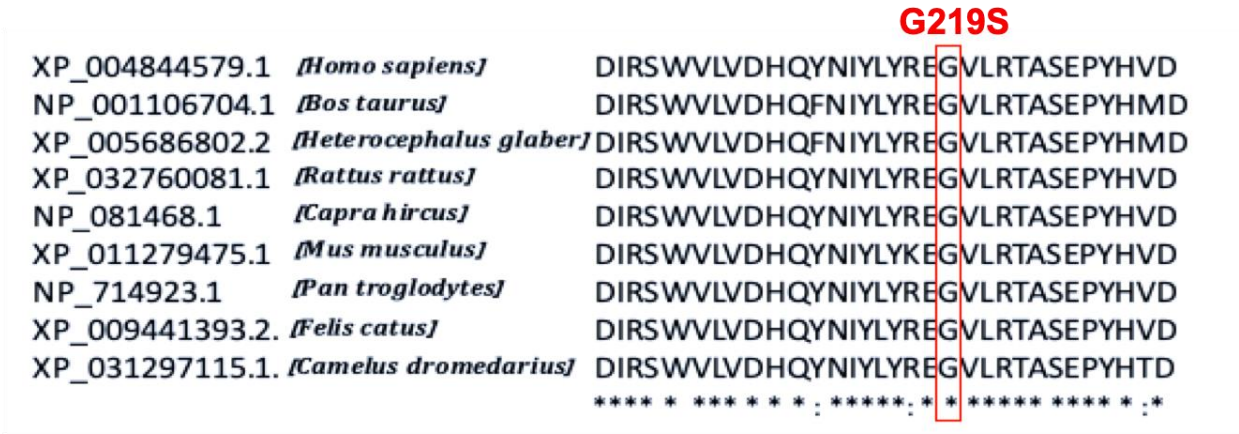

D

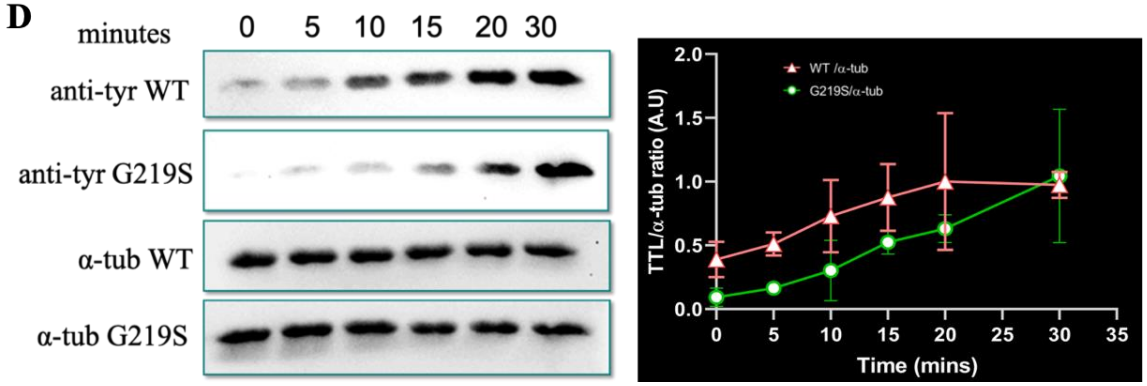

Figure 5.1: Molecular genetic analysis of TTL and its activity assay.

(A) Pedigree of HCM family with TTL p.G219S variant. Black shaded boxes represent the affected individual. (+) and (-) represents the presence and absence of variant in the individual respectively, (-/+) represents the presence of heterozygous condition with respect to variant. **(B)** In silico analysis of TTL gene using various pathogenicity determining tools. **(C)** Multiple sequence alignment of the protein region across different species with the amino acid conservation at 219th position is shown in red box. **(D)** Immunoblot of *in vitro* tyrosination assay with purified TTL WT and TTL p.G219S and quantification of the same on the right side (n=3).

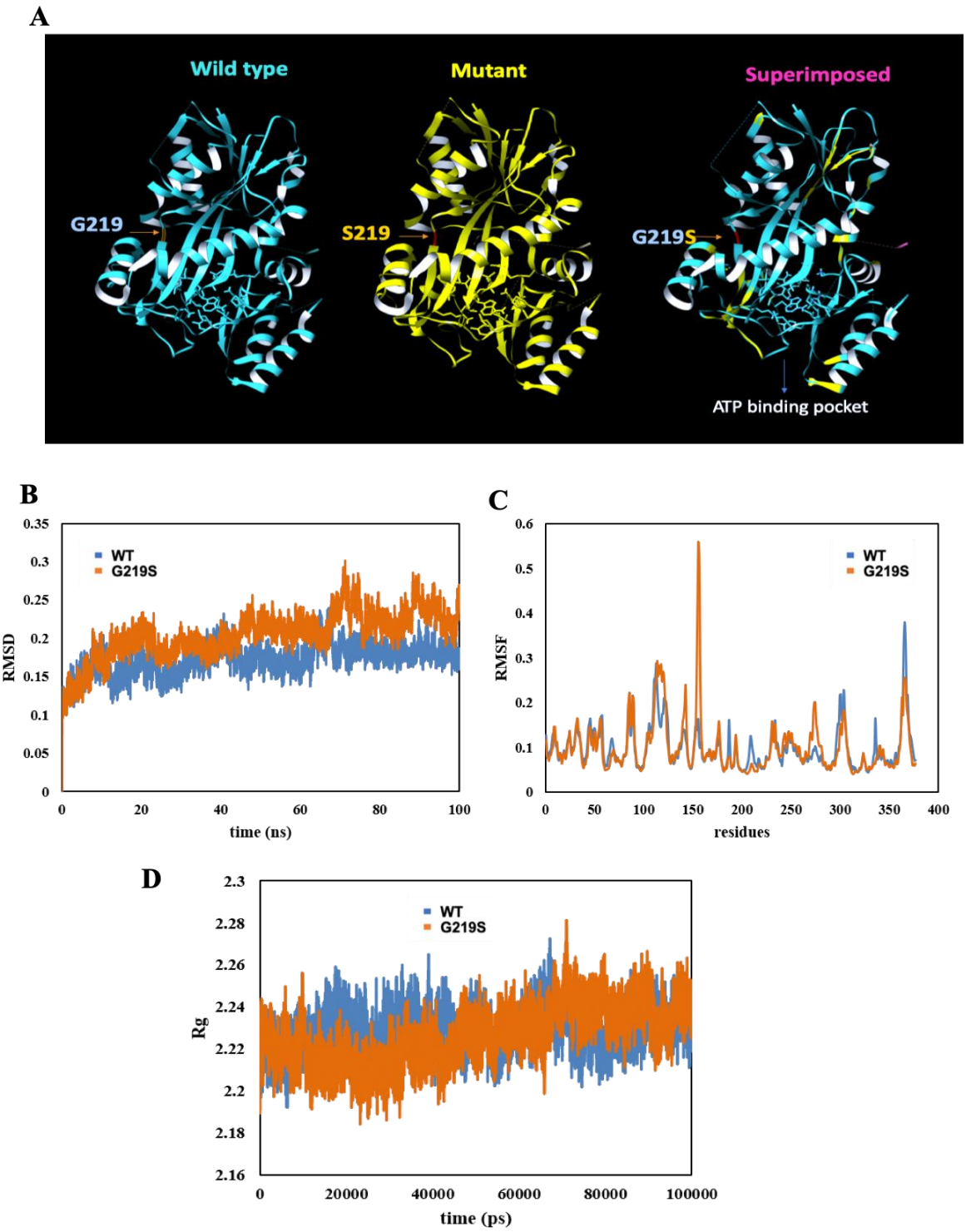

Figure 5.2: Molecular dynamics (MD) simulation of Wild type TTL and p.G219S TTL.

(A) MD simulation of wild type and mutant TTL (PDBID: 4IHJ) (bound to C terminal tail of α/β-tubulin heterodimer and ATP) showing multiple regions not overlapping upon the complex formation. **(B)** Root mean square deviation (RMSD) of WT versus TTL p.G219S. **(C)** Root mean square fluctuations (RMSF) of WT versus TTL p.G219S. **(D)** Radius of gyration (Rg) of WT versus TTL p.G219S.

5.2.4 Generation and characterization of TTL patient specific -iPSCs:

The generation of an induced pluripotent stem cell (iPSC) line from a 40-year-old male patient carrying the TTL p.G219S variant is a critical component in understanding the progression of hypertrophic cardiomyopathy (HCM). In order to separate the peripheral blood mononuclear cells (PBMCs) from whole blood, a SepMate tube and histopaque 1077 were used to perform density gradient centrifugation. The non-integrative Sendai virus vectors expressing c-Myc, Klf4, Oct3/4, and Sox2 were used to reprogram the PBMCs into iPSCs (Figue5.3A). On the 10th day of transduction, the iPSC colonies displayed human embryonic stem cell morphology (Figure 5.3B) and genotyping of the established iPSC line showed the presence of a heterozygous G219Spoint mutation (Figure 5.3E). The high-level expression of pluripotency markers, including OCT3/4, NANOG, and SSEA4, was observed using immunofluorescence staining of iPSC (Figure 5.3F).

The iPSC colonies were allowed to form embryoid bodies (Figure 5.3C) to validate the differentiation potential, and the expression of ectoderm (SOX2 and NESTIN), mesoderm (GATA4), and endoderm (Nodal and GATA4) markers was assessed using quantitative reverse transcriptase PCR (Figure 5.3D). Karyotyping analysis using the Giemsa-banding technique revealed that the iPSC line had a diploid 46, XY karyotype without any chromosomal anomalies (Figure 5.3G). Regular monitoring of Mycoplasma contamination revealed the absence of contamination in the cultured iPSC line.

5.2.5 Cardiomyocytes derived from TTL p.G219S patient specific iPSCs displays HCM phenotypes:

To elucidate the fundamental pathophysiology, TTL p.G219S induced pluripotent stem cell (iPSC) lines were differentiated into cardiomyocytes (iPSC-CMs) by modulating the Wnt/β-catenin pathway,[117] followed by lactate-based selection and purification to achieve a high yield of cardiomyocytes (≥90%) (Figure 5.4A). After differentiation, the cell surface area of TTL p.G219S iPSC-CMs, as revealed by α-sarcomeric actinin (ACTN2), phalloidin, and Hoechst staining, showed a marked increase in the cell surface area in comparison to its wild type (Figure 5.4A).

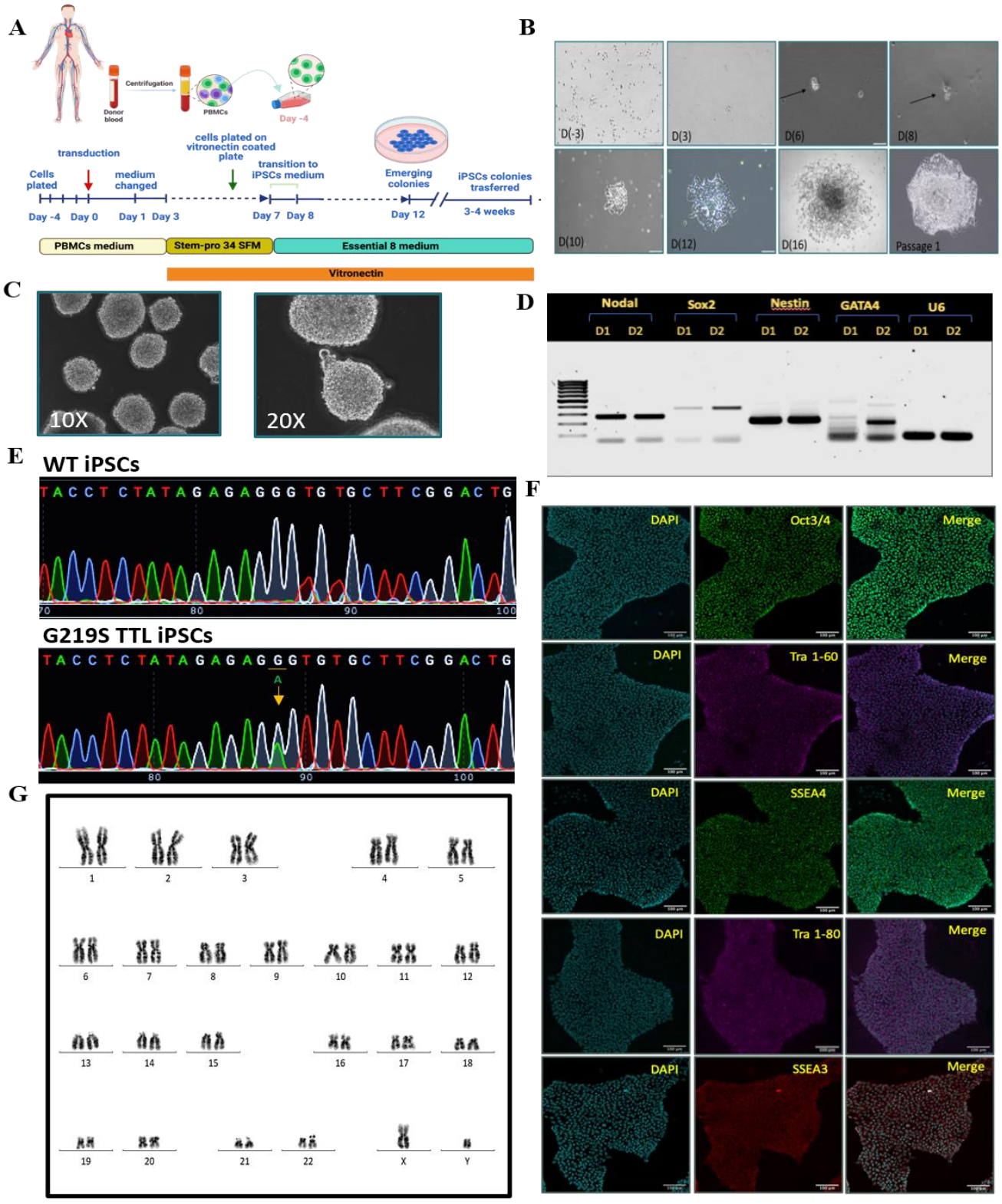

Figure 5.3: Patient specific iPSCs generation and characterization.

(A) Schematic diagram displaying iPSC generation from TTL p.G219S patient specific peripheral blood mononuclear cells (PBMCs) **(B)** Representative images at different stages of iPSC generation. **(C)** Representative images of embryoid body formation. **(D)** Agarose gel image of amplified germ layer markers from total RNA isolated from day

1 and day 2 of embryoid bodies. (**E)** Sanger sequencing results from WT and TTL p.G219S iPSCs amplicon. (**F)** iPSC showing normal stem cell morphology and stemness markers including Oct3/4, Tra 1-60, SSEA4, Tra 1-80 and SSEA3. (**G)** Karyotype analysis of TTL p.G219S iPSCs.

We subsequently analyzed the organization of the myofibrils in both the induced pluripotent stem cell-derived cardiomyocytes (iPSCs-CMs). The myofibrillar system is crucial for cardiac contraction and undergoes significant intrinsic changes during the development of HCM.[118] To study myofibrillar organization and sarcomeric integrity, we utilized ACTN2 immunofluorescence staining as a marker. Our findings revealed a significant increase in sarcomeric organization at day 30 and subsequent increase in sarcomeric disorganization at day 40 in the cardiomyocytes derived from TTL (p.G219S) compared to WT. The increased sarcomeric organization might be due to an adaptive response to increased force production in stressed cells, which subsequently leads to disorganization supporting the disease phenotype (Figure 5.4B).

Along with this, the relative mRNA levels of bona-fide hypertrophy markers like ANP (atrial natriuretic peptide), BNP (brain natriuretic peptide), MHC (alpha myosin heavy chain/ Myh6)/MHC (beta myosin heavy chain/Myh7) ratio and ACTA1 (Actin Alpha 1, Skeletal Muscle), have shown significantly upregulation in TTL p.G219S iPSC-CMs in comparison with its WT (Figure 5.5A). Immunoblot analysis was performed to examine the level of extracellular regulated kinase (ERK1/2), a hallmark of pathological hypertrophy.[95] Persistent ERK1/2 stimulation was observed in TTL p.G219S iPSC-CMs (Figure 5.5B), which can result in hypertrophy, which can ultimately lead to heart failure. In summary, upregulation of hypertrophy markers, increase in cell size, myofibrillar disarray, increased levels of ERK1/2, suggests that TTL (p.G219S) variant can lead to pathological cardiac hypertrophy.

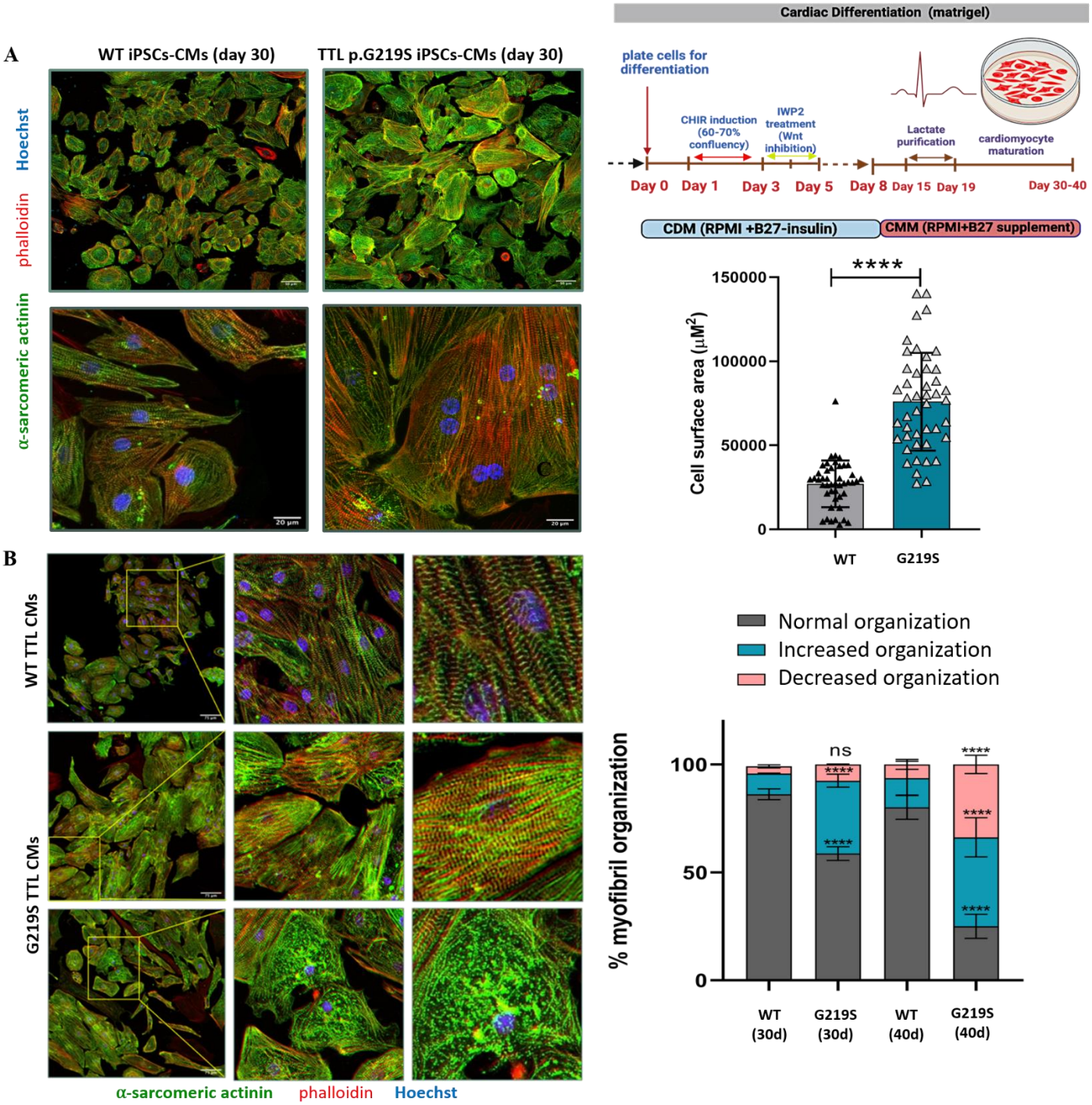

Figure 5.4: Patient specific iPSCs derived cardiomyocytes shows hypertrophic phenotypes.

(A) Representative images of iPSC-CMs stained for alpha-sarcomeric actinin, phalloidin and Hoechst. Schematic showing the cardiomyocyte differentiation using Wnt perturbation pathway and quantification of cell surface area in WT and TTL p.G219S iPSC-CMs on the right-side. **(B)** Quantification of percentage of cells with increased organization and decreased disorganization arrangement at day 30 and day 40 of differentiation. Values are shown as means ± SEM with each experiment performed in triplicate (n=3). (****P<0.0001, Student's t-test (60-90 cells per group)).

5.2.6 TTL p.G219S iPSCs derived cardiomyocytes displays contractile dysfunction:

During the diastolic phase, the heart muscle expands, resulting in the release of calcium ions (Ca2+), which leads to an increase in intracellular free Ca2+ levels and the propagation of Ca2+ waves throughout the cell.[119] However, in abnormal conditions, the excessive accumulation of Ca2+ in the sarcoplasmic reticulum and increased sensitivity of ryanodine receptors (RyR2s) can result in more significant increases in intracellular Ca2+ levels.[120] We observed a decrease in SERCA2 (a sarcoplasmic reticulum Ca2+ ATPase, ATP2A2) expression in the mutant CMs compared to the wild type, which suggests reduced reuptake of cytosolic Ca2+ into the sarcoplasmic reticulum, leading to contractile defect and relaxation as shown in (Figure 5.5D). Phospholamban (PLN) regulates the function of SERCA by inhibiting it in its unphosphorylated form and relinquishing this inhibition when phosphorylated.[121] The ratio of SERCA2 to PLN is very crucial for the appropriate contraction cycle. Any imbalance to this may lead to systolic (inappropriate contraction) or diastolic dysfunction (inappropriate relaxation).[122] Our findings indicated that the ratio of SERCA2 to PLN levels had also significantly diminished in both qPCR and immunoblots Figure 5.5D, E), suggesting left ventricular remodeling. Notably, the contractile amplitude was observed to be higher in mutant CMs compared to WT CMs suggesting an increased force of contraction as a consequence of hypertrophy (Figure 5.5C).

5.2.7 TTL p.G219S iPSC-CMs displayed increased de-tyrosinated tubulin:

The process of de-tyrosination is facilitated by a tubulin carboxypeptidase (TCP) and can be reversed by the action of tubulin tyrosine ligase (TTL). To investigate whether a decrease in TTL p.G219S gene variant activity may result in an accumulation of de-tyrosinated tubulin within cardiomyocytes, we utilized immunofluorescence images and immunoblots to target the de-tyrosinated alpha tubulin protein in wild-type and mutant cardiomyocytes. Our findings revealed a substantial increase in the levels of de-tyrosinated tubulin in mutant cardiomyocytes compared to wild-type cardiomyocytes, as depicted in the accompanying figure (Figure 5.6A and C). Our immunoblots data suggest the same (Figure 5.6D). This accumulation of modified microtubules disrupts the balance between de-tyrosinated and tyrosinated tubulin, which in turn influences the structural and functional dynamics of microtubules, ultimately leading to altered mechanical properties by increasing the overall stiffness and binding interactions of the microtubules in cardio-

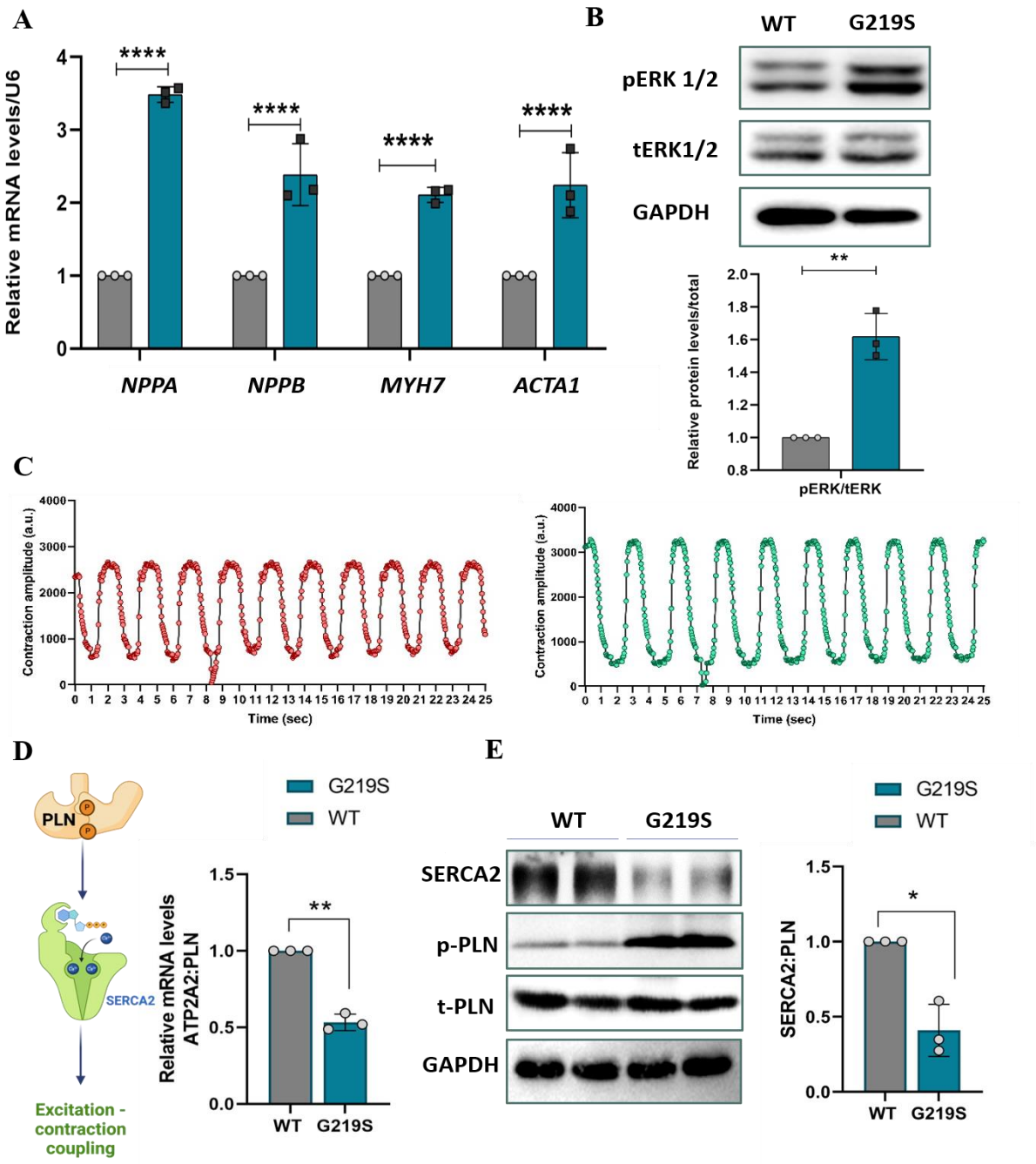

Figure 5.5: Patient specific iPSCs derived cardiomyocytes showing activation of fetal gene markers, ERK1/2 and contractile defects.

(A) Quantitative real time PCR (qRT-PCR) analysis for hypertrophic markers (*NPPA, NPPB, MYH7* and *ACTA1*). mRNA levels were normalized to U6. **(B)** Representative immunoblot images from the total lysates of WT and TTL p.G219S iPSCs-CMs, quantification on the right side. **(C)** Comparison of iPSCs-CMs contractile physiology compared with respect to time using muscle motion plugin in ImageJ. **(D)** qRT-PCR analysis of SERCA2 (ATP2A): PLN (Phospholamban), involved in calcium regulation in sarcomere. **(E)** Representative immunoblots of SERCA2 and PLN levels in iPSC-CMs and its quantification on the right side. Values are shown as means±SEM with each experiment performed in triplicate (n=3). Significance was evaluated by Student's t test or one-way analysis of variance (ANOVA) with post hoc Tukey's test, respectively. *P < 0.05, **P < 0.01, and ****P < 0.0001.

-myocytes.[123] In order to investigate the impact of elevated de-tyrosinated tubulin on intermediate filament proteins, such as desmin, we conducted a study using WT and mutant cells. Desmin is primarily located at the Z-discs, where it forms a striated pattern and plays a critical role in the mechanical stability of cardiomyocytes.[124] Our results showed that desmin levels were higher in both immunoblots (Figure 5.6D) and immunofluorescence in the mutant cells (Figure 5.6B and C). These findings suggest that the mutant cardiomyocytes experience impaired stability and altered mechano-transduction processes.

5.2.8 De-tyrosination is higher in TTL p.G219S iPSC-CMs compared to other known HCM iPSCs-CMs:

To verify the role of the TTL variant in causing the disease, we utilized two different types of iPSC-derived cardiomyocytes that had known variants for hypertrophic cardiomyopathy, specifically *MyBPC3*$^{\Delta 25bp}$ (which affects a sarcomeric gene)[73] and SHOC2 p.S2G (which affects a signaling gene)[125]. Our results demonstrated that the ratio of de-tyrosinated alpha tubulin to tyrosinated alpha tubulin was higher in the lysates of TTL p.G219S variant cardiomyocytes compared to both the other sarcomeric (*MyBPC3*$^{\Delta 25bp}$) and signaling (SHOC2 p.S2G) gene variants, as shown in the figure (Figure 5.7A). This data suggests our finding that the pathological condition because of de-tyrosination in TTL p.G219S iPSC-CMs is greater than known HCM variants.

5.2.9 RNA-Seq analysis shown perturbed redox and calcium handling genes:

To gain a deeper understanding of the molecular mechanisms underlying the disease pathology, we performed bulk RNA-Seq on wild-type (WT) and TTL p.G219S induced pluripotent stem cell-derived cardiomyocytes (iPSC-CMs). Our RNA-Seq analysis revealed differential expression patterns of genes involved in the organization of sarcomeres, myofibrils and the assembly and redox metabolism related to contractile function of the heart (Figure 5.8 A).

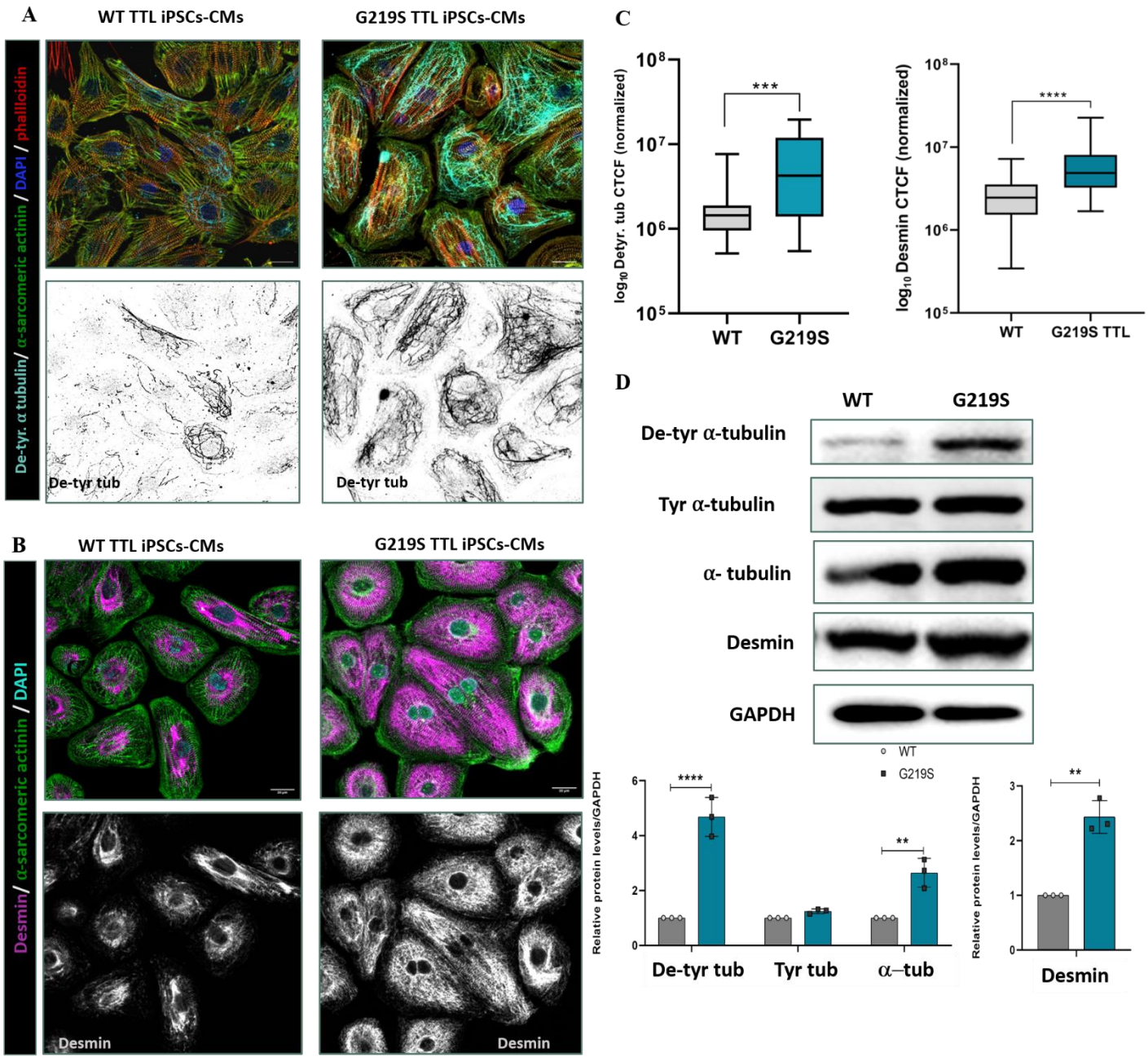

Figure 5.6: TTL variant iPSCs-CMs showing increase in the levels of de-tyrosinated α-tubulin and intermediate filament protein (Desmin).

Representative **(A)** Immunofluorescence images of de-tyrosinated a-tubulin (cyan), a-sarcomeric actinin (green), phalloidin (red) and Hoechst (blue) in wild type and mutant TTL iPSCs derived cardiomyocytes. Shown below is the grey scale of de-tyrosinated a-tubulin form of the same image. **(B)** Immunofluorescence images of desmin (magenta), a-sarcomeric actinin (green), and Hoechst (cyan) in wild type and mutant TTL iPSCs-CMs. Shown below is the grey scale of desmin of the same image. **(C)** Quantification of (A) and (B) resp. **(D)** Immunoblots from the lysates from WT and TTL p.G219S iPSCs-CMs, with quantifications on the right side. Levels of de-tyrosinated a-tubulin form and desmin have been quantified based on intensity and corrected total cell fluorescence have been calculated as shown on right side. Values are shown as means±SEM with each experiment performed in triplicate (n=3). Significance was evaluated by Student's t test. (n=50-60 cells per group)) $^{**}P < 0.01$, $^{***}P < 0.001$, and $^{****}P < 0.0001$.

Our results showed that genes associated with hypertrophic cardiomyopathy, such as NPPA, NPPB, TNNC1, and desmin, were markedly upregulated in the mutant compared to WT (Figure 5.8B top panel). Furthermore, we found that genes involved in maintaining redox homeostasis, including CYBB (p91-phox), NCF2 (p67-phox), COX7A1, COX7B, CYBB, TRPC5, and CHCHD2 were dysregulated (Figure 5.8B middle panel). Additionally, genes associated with calcium handling in cardiomyocytes, such as PLN, RyR2, CAMK2B, CASQ and CACNA1C, were also found to be dysregulated in the mutant iPSC-CMs (Figure 5.8B bottom panel). Given that optimal calcium and reactive oxygen species (ROS) levels are essential for maintaining the balance of cellular signaling networks, the disturbed calcium handling and redox-related genes in the mutant iPSC-CMs suggest a pathological condition (Figure 5.8C).

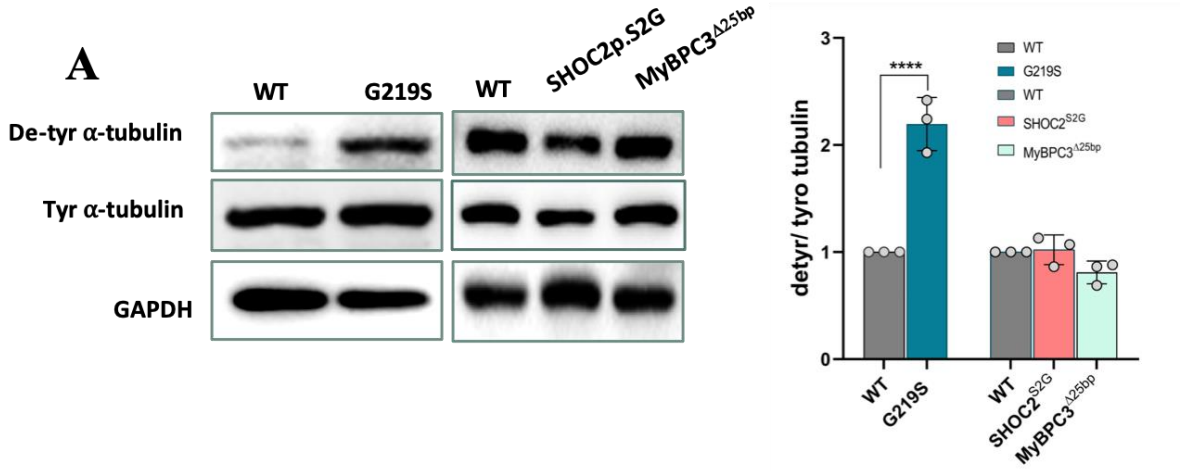

Figure 5.7: De-tyrosination levels were higher in TTL p.G219S iPSC-CMs compared to other HCM gene variant iPSC-CMs.

(A) Representative immunoblot analysis from lysates obtained from iPSC-CMs (day 30) of TTL variant and two other HCM gene variants (SHOC2 p.S2G and *MyBPC3*$^{\Delta 25bp}$). Ratios of de-tyrosinated to tyrosinated α-tubulin is increased only in TTL variants compared to WT and other HCM iPSC-CMs. Values are shown as means±SEM with each experiment performed in triplicate (n=3). Significance was evaluated by ****p<0.0001, one-way ANOVA.

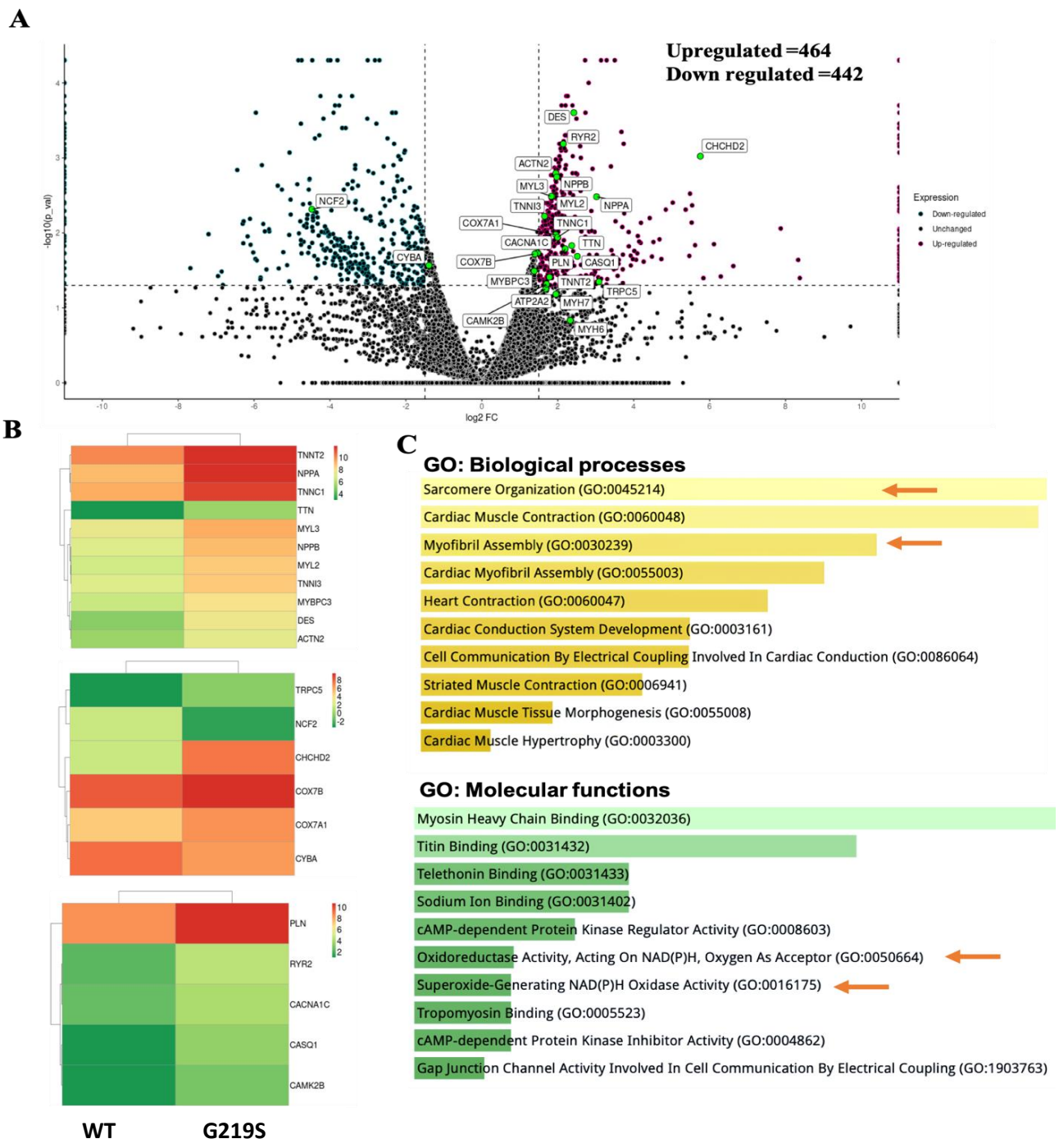

Figure 5.8: RNA-Seq analysis of WT versus TTL p.G219S iPSC-CMs.

(A) Volcano plot showing the differentially expressed genes in WT versus TTL p.G219S iPSC-CMs (p-value <0.05), FC denotes fold change**. (B)** A heat map illustrates the genes that are dysregulated in TTL p.G219S iPSC-CMs compared to WT iPSC-CMs, with a FC greater than 2. The heat map is divided into three sections, with the top section representing hypertrophy-related and structural genes, the middle section representing redox homeostasis-related genes, and the bottom section representing calcium-related genes. **(C)** The dysregulated genes are further analyzed using gene ontology (GO) to identify the biological processes and molecular functions that are significantly affected, with a p-value less than 0.05. The top section of the GO analysis shows the biological processes, and the bottom section shows the molecular functions.

5.2.10 TTL p.G219S iPSCs-CMs exhibits oxidative stress:

TTL plays an important role in tyrosination process of microtubules. Specifically de-tyrosinated microtubules have been shown to exert a significant influence on mechano-transduction within the heart and skeletal muscle by enhancing stiffness, which consequently results in aberrant contractile properties.[123] This dysfunctional contractility, coupled with abnormal calcium handling and ROS is linked to heart failure.[126]

To evaluate the role of ROS in disease pathogenesis, we performed a live cell staining assay using Dihydroethidium (DHE) to assess the levels of reactive oxygen species (ROS) in wild-type (WT) and TTL p.G219S iPSC-CMs. DHE reacts with free O^{2-} to form two red fluorescent products, ethidium (E^+) and 2-Hydroxyethidium (2-OH-E^+), which are indicative of ROS. The immunofluorescence images showed a higher intensity of (E^+) and (2-OH-E^+) in the TTL p.G219S variant iPSC-CMs compared to the WT iPSC-CMs, indicating increased ROS generation in the mutant iPSC-CMs and suggesting an oxidative stress condition (Figure 5.9A).

Increased ROS production is shown to be associated with NADPH oxidase 4 (NOX4) and CYBA (p22phox, a component of NOX4 complex) expression.[127] Similarly, our qRT-PCR data shown an increase in the mutant compared to the wildtype (Figure 5.9C). The connection between ROS-mediated oxidative stress and disrupted calcium handling, which exacerbates cardiac pathology, is well-known.[128] Our RNA-Seq data indicates that the upregulation of genes involved in calcium handling, such as CAMK2B, CACNA1C, SERCA2, RYR2, and CASQ, along with perturbed redox signaling, is indicative of improper calcium handling mediated by ROS.

We subsequently analyzed the levels of NRF2-AKT (a master regulator of the redox pathway), which activates the Antioxidant Response Element (ARE) genes.[129] Our analysis revealed a significant increase in the expression levels of NRF2, AKT, and ARE in TTL p.G219S cardiomyocytes compared to wild-

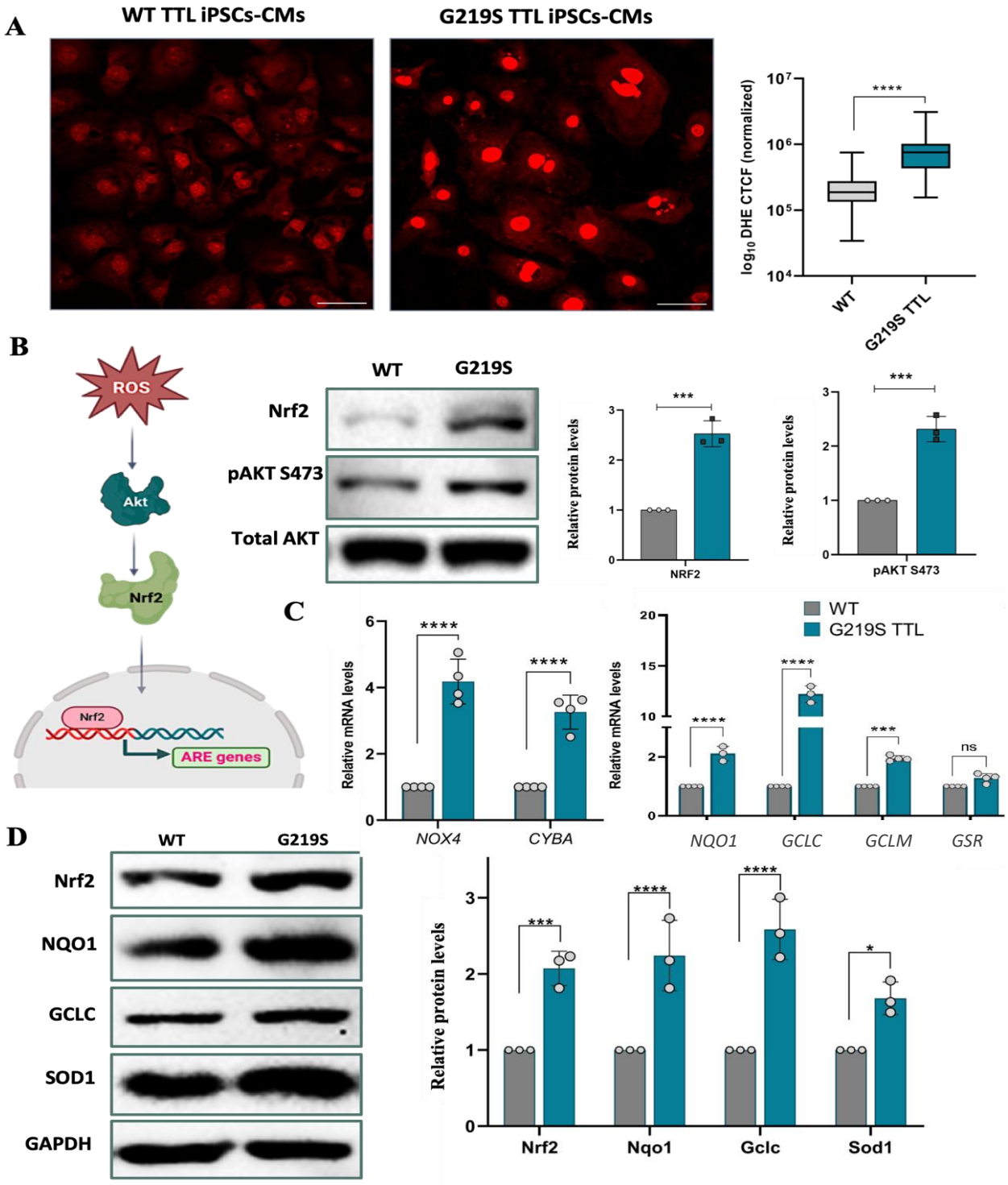

Figure 5.9: TTL p.G219S iPSCs-CMs shows increased ROS levels and induction of antioxidant response element genes.

(A) Representative immunofluorescence of reactive oxygen species (ROS) by dihyrdoethidium (DHE) in wild type and mutant iPSC-CMs (live cell staining). **(B)** Schematic depicting the ROS induced NRF2/AKT pathway and induction of antioxidant response element genes. Representative immunoblots from the lysates from WT and TTL p.G219S iPSCs-CMs probed for p-AKT (S473) and Nrf2. **(C)** qRT-PCR analysis of antioxidant response element

genes like (*NQO1, GCLC, GCLM*). **(D)** Representative immunoblots from the lysates from WT and TTL p.G219S iPSCs-CMs probed for NRF2 and antioxidant response element proteins NQO1, SOD1 and GCLC quantified on the right. Levels of ROS have been quantified based on intensity and corrected total cell fluorescence have been calculated as shown on right side. Values are shown as means±SEM with each experiment performed in triplicate (n=3). Significance was evaluated by Student's t test (for DHE staining, n=80-90 cells per group)) *P < 0.05, ***P < 0.001, ****P < 0.0001 and ns=not significant.

type cardiomyocytes, as demonstrated in the figure (Figure 5.9B). Moreover, we found that genes involved in the antioxidant response element, such as GCLC (Glutamate-cysteine ligase catalytic subunit), NQO1 (NAD(P)H dehydrogenase (quinone 1)), GCLM (Glutamate-cysteine ligase modified subunit), and GSR (Glutathione reductase), were upregulated in TTL p.G219S relative to WT iPSCs-CMs as shown in qRT-PCR and immunoblots (Figure 5.9C and D). These findings confirm the presence of oxidative stress in the respective cells.

5.2.11 Parthenolide rescues TTL p.G219S iPSC-CMs associated de-tyrosinated tubulin and ROS levels:

To ascertain whether the reduction in de-tyrosinated tubulin levels due to decreased TTL activity, we treated WT and TTL p.G219S iPSC-CMs with parthenolide (PTL, an inhibitor of Tubulin carboxy peptidases).[130] Following the treatment of PTL (10uM), we observed a substantial decrease in de-tyrosinated tubulin levels in the immunostaining and immunoblots of TTL p.G219S compared to WT iPSC-CMs (Figure5.10A, C and D). Consequently, as expected, there was also a significant decrease in levels of the intermediate filament protein desmin, indicating that the increased amount of de-tyrosinated alpha tubulin as a result of a reduction in TTL p.G219S variant activity (Figure 5.10B, C and D). We also observed a significant decrease in expression of hypertrophy markers upon PTL treatment in TTL p.G219S versus WT iPSCs-CMs (Figure 5.10E). Following the PTL treatment we observed a significant reduction in DHE staining and expression levels of NRF2 and ARE genes as shown by immunofluorescence, qRT-PCR and immunoblots. (Figure 5.11A and B). These findings strongly suggest that de-tyrosinated alpha tubulin plays a significant role in the oxidative stress.

5.3 Discussion:

More than half of HCM cases have unknown causes, and the South Asian population is understudied. To address this, we aimed to identify a new gene and discovered a novel gene variant, p.G219S, in the tubulin tyrosine ligase gene (TTL). Interestingly, neither of the proband's parents carried the mutation, suggesting that the variant arose de novo. The region containing the variation is highly conserved across various species.

TTL codes for the tubulin tyrosine ligase, which catalyzes the addition of a tyrosine residue to the C-terminal tail of de-tyrosinated alpha-tubulin in an ATP-dependent manner.[109] This modification is a reversible post-translational modification (PTM) of alpha-tubulin and is essential for maintaining microtubule dynamics. The process of tyrosination is involved in the regulation of specific microtubule-associated protein (MAP) recruitment, which in turn regulates cytoskeletal integrity and imparts context-dependent functions in cells.[131] Various tubulin isotypes and their associated PTMs regulate microtubule dynamics, properties, and functions, collectively known as the "tubulin code".[122] These tubulin codes act as specific fine regulators rather than a binary switch for microtubule functions. Since the discovery of TTL as the enzyme responsible for tyrosination of tubulin, the multiple roles of this cycle have been studied and found to be extremely crucial in the regulation of microtubule dynamics. Based on the type of PTMs, specific MAPs are recruited to the C-ter tail of alpha tubulin. De-tyrosination is one such PTM, critical for maintaining microtubule stability.[132] MTs maintain a delicate balance between their de-tyrosinated and tyrosinated forms, as well as their interactions with microtubule-associated proteins (MAPs). Any alterations in the de-tyrosination of MTs signifies myocardial dysfunction, which can be accompanied by mechanical and pathological stress such as disrupted redox homeostasis and calcium handling.[123]

In this study, we report a novel, heterozygous mutation in which glycine is replaced with serine at position 219 of the TTL enzyme. The TTL enzyme interacts with the de-tyrosinated α/β-tubulin dimer to form a complex, and the interaction between the two is dependent on a specific conformation of the dimer.[115,133] This conformation is lost when α/β-tubulin dimers are incorporated into microtubules, which prevents TTL from tyrosination of microtubules.[134,135]

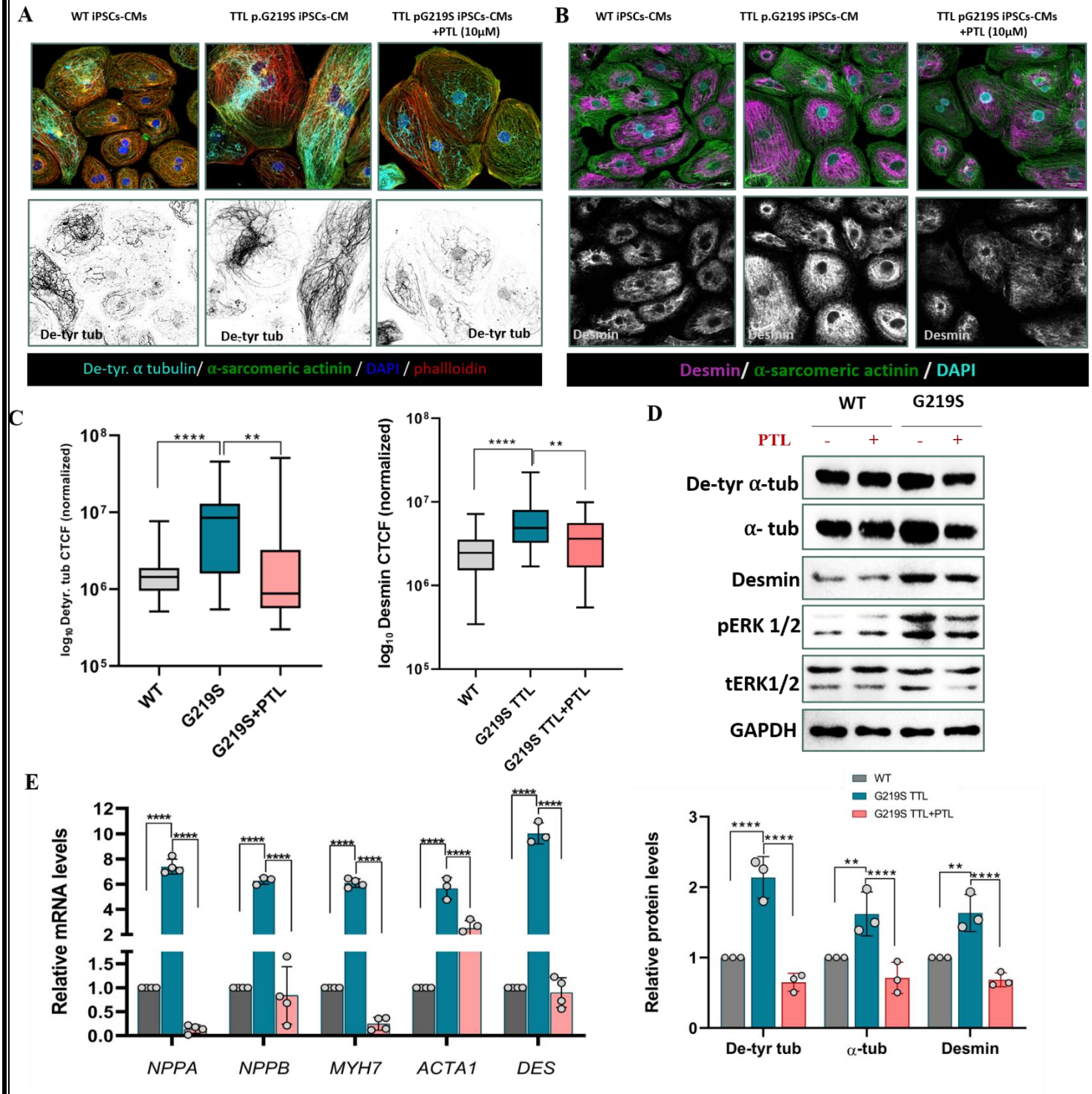

Figure 5.10: Parthenolide (PTL)treatment blocks hypertrophy in TTL p.G129S iPSC-CMs.

Representative **(A)** Immunofluorescence images of de-tyrosinated a-tubulin (in cyan), a-sarcomeric actinin (in green), phalloidin (in red), and Hoechst (in blue) were captured in wild-type (WT), untreated mutant TTL iPSCs-CMs, and treated mutant TTL iPSCs-CMs with PTL (10M). The WT, regardless of treatment or no treatment, showed no

significant differences. The WT serves merely as a comparative control. The lower panel displays the grey-scale representation of the de-tyrosinated a-tubulin in the same image. **(B)** Immunofluorescence images of desmin (magenta), a-sarcomeric actinin (green), and Hoechst (cyan) in WT, untreated mutant TTL iPSCs-CMs and treated TTL iPSCs-CMs with PTL (10μM). Lower panel is the grey scale for desmin of the same image. **(C)** Levels of de-tyrosinated a-tubulin and desmin have been quantified based on intensity and corrected total cell fluorescence have been calculated. **(D)** Immunoblots from the lysates from WT and TTL p.G219S iPSCs-CMs with and without with 10μM PTL treatment, with quantifications below. **(E)** qRT-PCR analysis of hypertrophic gene (fetal gene markers) in WT, TTL p.G219S untreated and TTL p.G219S treated with PTL. Values are shown as means±SEM with each experiment performed in triplicate (n=3). Significance was evaluated by One-way ANOVA (n=50-60 cells per group)), **P < 0.01 and ****P < 0.0001.

Our MD simulation of the α/β-tubulin dimer and the mutant TTL protein revealed alterations in the conformation of the mutant protein near its catalytic region. This alteration may reduce its ability to attach to the α/β-tubulin heterodimer compared to the wild-type protein. Our in vitro tyrosination assay confirmed this in silico finding, showing delayed activity of the TTL p.G219S mutant, which resulted in increased de-tyrosinated alpha tubulin. To gain a deeper understanding of the patient's cellular environment, we utilized patient-specific induced pluripotent stem cells (iPSCs) to create a disease model. We generated iPSCs from the patient's peripheral blood mononuclear cells (PBMCs) and differentiated them into cardiomyocytes to simulate the actual patient's condition. Our results showed an increase in cell surface area, as expected in HCM, along with the upregulation of fetal gene re-expression and activated RAS-MAPK signaling, as indicated by higher levels of p-ERK 1/2.[95] We also observed two distinct cell states across time, one with increased sarcomeric organization, which represents a hypertrophic response and the other with decreased sarcomeric disorganization, which represents a state of heart failure stage.[136] Our findings suggest that TTL p.G219S patient are at risk of heart failure.

We also observed increased de-tyrosinated tubulin form in patient specific cardiomyocyte confirming the delayed activity of TTL p.G219S variant. De-tyrosinated microtubules in cardiomyocytes offer mechanical resistance, hindering the movement of contracting cardiomyocytes and resulting in reduced cell biomechanics, contractility and mechano-transduction.[123] A prominent characteristic upon increased stability of microtubules which happens when de-tyrosinated form are more in cardiomyocyte is the heightened manifestation of cytoskeletal proteins, specifically intermediate filaments like desmin.[123] It is hypothesized that, like other forms of cardiac remodeling, these alterations may initially serve an adaptive purpose, perhaps safeguarding a heart under significant mechanical strain.[137]

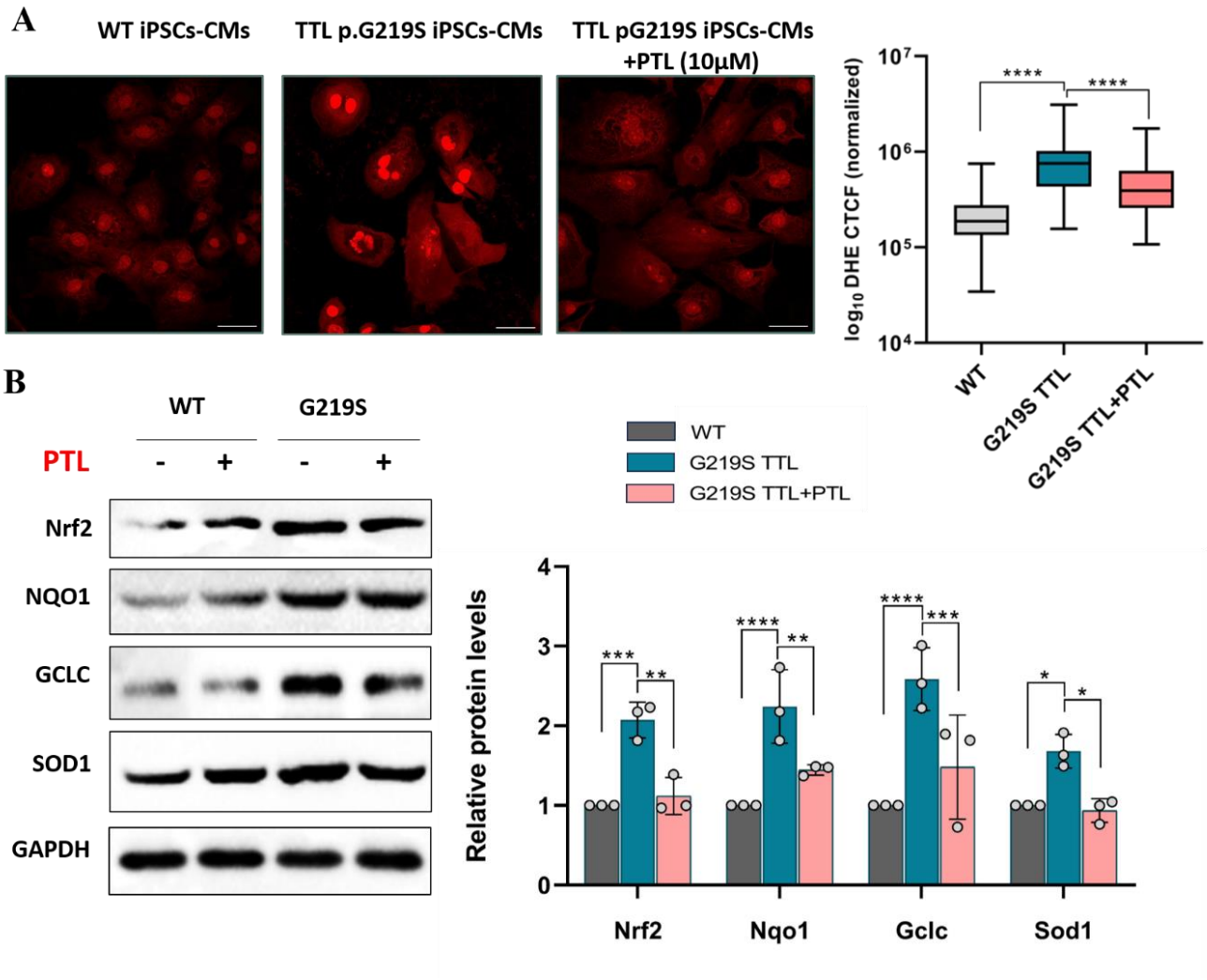

Figure 5.11: PTL treatment rescues oxidative stress and anti-oxidant response element (ARE) expression in TTL p.G219S iPSC-CMs.

(A) Representative immunofluorescence of reactive oxygen species (ROS) by dihyrdoethidium (DHE) in WT and TTL p.G219S iPSC-CMs with and without PTL treatment (10μM) (live cell staining). The WT, regardless of treatment or no treatment, showed no significant differences. The WT serves merely as a comparative control. **(B)** Representative immunoblots results probed for Nrf2 and antioxidant response element genes (NQO1, SOD1 and GCLC) upon treatment with PTL (10μM) in mutant TTL iPSC-CMs. Levels of ROS have been quantified based on intensity and corrected total cell fluorescence have been calculated as shown on right side. For DHE staining, n=80-90 cells per group were taken for analysis. Values are shown as means±SEM with each experiment performed in triplicate (n=3). Significance was evaluated by One-way ANOVA *P < 0.05, **P < 0.01, ***P < 0.001, and ****P < 0. 0001.

However, as they advance, these changes might become maladaptive by further increasing the microtubule stability impairing sarcomeric contraction and relaxation.[137] In our study we have found that desmin levels are significantly high in mutant versus wild type which is reversed upon

treatment with PTL suggesting the increased levels of desmin are due to increased stability of microtubules in mutant because of de-tyrosinated tubulin form.[123] We also found that this increase in de-tyrosinated tubulin form is not a common phenomenon in other genetically predisposed HCM cases like SHOC2 p.S2G and MyBPC3$^{\Delta 25bp}$.

A growing body of evidence suggests that oxidative stress is implicated in cardiac dysfunctions associated with microtubules. Specifically, the role of reactive oxygen species (ROS) regulatory components, such as NADPH oxidases (e.g., NOX2 and NOX4) and its downstream pathways (NRF2/AKT axis) in the progression of cardiac hypertrophy is well-documented.[129] In our study, we observed a significant increase in ROS regulatory components (NOX4 and NRF2/AKT) in mutant cardiomyocytes compared to wild-type cells. This is also confirmed by DHE staining, suggesting that increased oxidative stress plays a role in the TTL p.G219S iPSC-CMs.

The interplay between increased reactive oxygen species ROS and calcium signaling in the heart is a complex yet crucial aspect of cardiac physiopathology.[128] ROS led oxidation adjusts the sensitivity of the RyR2s, leading to an elevated rate of Ca2+ sparks and an improvement in Ca2+ signaling. ROS can directly influence the activity of calcium-handling proteins such as ryanodine receptors (RyRs) and sarcoplasmic reticulum calcium ATPase (SERCA), thereby impacting calcium release and reuptake kinetics within the cardiac myocyte.[138] Additionally, ROS can induce post-translational modifications of key calcium-handling proteins,[139] altering their function and contributing to aberrant calcium handling observed in conditions such as heart failure and ischemia-reperfusion injury. In line with this we have observed dysregulation of calcium handling protein.

In our study, we utilized Parthenolide (PTL) to investigate the influence of TTL p.G219S induced pathogenesis. PTL acts as an inhibitor that prevents tubulin de-tyrosination and de-tyrosination cycle by inhibiting tubulin carboxy peptidases (TCP).[121] These enzymes are responsible for removing tyrosine residues from the C-ter tail of alpha tubulin. After administering Parthenolide (PTL), we observed a reduction in hypertrophy response by decreasing the levels of de-tyrosinated alpha tubulin in TTL p.G219S, as compared to the WT iPSC-CMs. This might be attributed to the delayed activity of the TTL variant. Furthermore, PTL treatment eliminated the levels of ROS and oxidative stress-induced antioxidant response pathway. These results imply that disruption of the

redox balance is the primary pathway that leads to the hypertrophic response caused by the TTL p.G219S variant.

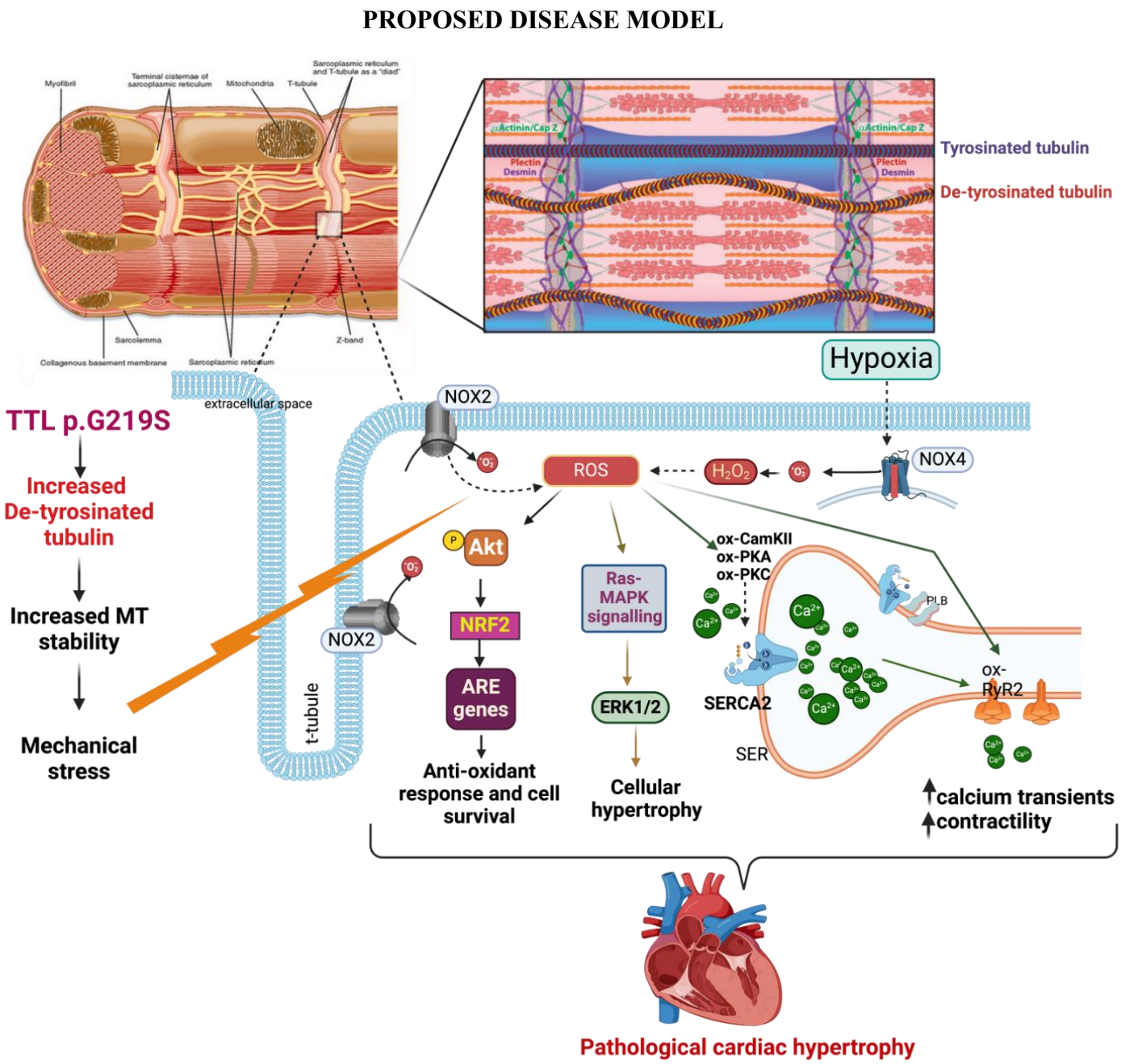

Figure 5.12: Proposed disease pathogenesis model for TTL p.G219S induced HCM via redox perturbation.

Our current study has made an important discovery in the HCM field by identifying a novel gene TTL and its variant, which has been proven to play a critical role in the context of the HCM. Overall, our findings provide a mechanistic framework for the TTL variant, where a decrease in its activity leads to an accumulation of de-tyrosinated alpha tubulin in cardiomyocytes, causing redox imbalance and contractile dysfunction. In conclusion, our data suggest that the TTL variant is a novel gene associated with HCM and can contribute to disease pathogenesis by disrupting redox homeostasis. Furthermore, small molecule inhibitors targeting the TCPs may be beneficial for individuals with TTL mutations.

CHAPTER: 6

SUMMARY

Hypertrophic cardiomyopathy (HCM) is a hereditary heart condition in which the heart muscle experiences an increase in size without any additional causes. This condition is characterized by a preserved or increased ejection fraction, which refers to the percentage of blood that is pumped out of the heart with each beat. The primary cause of HCM is mutations in genes that encode for sarcomeric proteins. However, there is limited understanding of the genes impacting the signaling proteins have on the development of HCM.

This study aims to address a research gap by discovering novel gene loci pertaining to signaling proteins using next-generation sequencing (NGS) and examining their functional implications through a multi-model approach. By integrating data from multiple models and conducting functional studies, it seeks to provide a deeper understanding of signaling gene traits. The ultimate goal is to develop personalized therapies or medicines based on an individual's unique genetic make-up.

Our method led to the discovery of two previously unidentified HCM genes and their variants, RPS6KB1 and TTL. This finding is of great clinical relevance, as RPS6KB1 has been acknowledged by the global HCM expert committee of the Clinical Genome Resource (ClinGen) as a new gene to be tested for this condition.

The RPS6KB1 gene encodes the ribosomal protein S6 kinase beta 1, which we have found to have pathological novel variants, primarily in the N-terminal region, that is critical for maintaining the protein in an auto-inhibitory state. The variants fail to maintain this auto inhibitory state. Thus, RPS6KB1 variants tends to function in a gain-of-function manner, stimulating the protein synthesis pathway by activating ribosomal S6 protein (rpS6) and eukaryotic initiation factor 4F complex (eIF4F) components, as well as the ERK1/2 pathways. In contrast, the TTL gene codes for tubulin tyrosine ligase, and its variant results in a loss-of-function, that leads to delayed activity and the accumulation of de-tyrosinated tubulin in cardiac cells, disrupting redox homeostasis. Therefore, different genes can exert influences on multiple pathways culminating to HCM.

Understanding these complex interactions is crucial as it can have significant implications for the design of targeted therapeutic interventions and the delivery of personalized care to affected individuals. By elucidating the intricate genetic underpinnings of HCM and their relationship to various biological pathways helps in tailored medicine leading to improved outcomes and patient-specific management strategies.

CHAPTER 7

BIBLIOGRAPHY

1. Braunwald E. Cardiomyopathies: An Overview. *Circ Res*. 2017;121(7):711-721. doi:10.1161/CIRCRESAHA.117.311812

2. McKenna WJ, Maron BJ, Thiene G. Classification, Epidemiology, and Global Burden of Cardiomyopathies. *Circ Res*. 2017;121(7):722-730. doi:10.1161/CIRCRESAHA.117.309711

3. McKenna WJ, Maron BJ, Thiene G. Classification, Epidemiology, and Global Burden of Cardiomyopathies. *Circ Res*. 2017;121(7):722-730. doi:10.1161/CIRCRESAHA.117.309711

4. Rakowski H, Carasso S. Quantifying Diastolic Function in Hypertrophic Cardiomyopathy. *Circulation*. 2007;116(23):2662-2665. doi:10.1161/CIRCULATIONAHA.107.742395

5. Muchtar E, Blauwet LA, Gertz MA. Restrictive Cardiomyopathy: Genetics, Pathogenesis, Clinical Manifestations, Diagnosis, and Therapy. *Circ Res*. 2017;121(7):819-837. doi:10.1161/CIRCRESAHA.117.310982

6. McNally E, MacLeod H, Dellefave-Castillo L. Arrhythmogenic Right Ventricular Cardiomyopathy Overview. In: Adam MP, Feldman J, Mirzaa GM, et al., eds. *GeneReviews*®. University of Washington, Seattle; 1993. Accessed February 1, 2024. http://www.ncbi.nlm.nih.gov/books/NBK1131/

7. Vaduganathan M, Mensah GA, Turco JV, Fuster V, Roth GA. The Global Burden of Cardiovascular Diseases and Risk. *J Am Coll Cardiol*. 2022;80(25):2361-2371. doi:10.1016/j.jacc.2022.11.005

8. Maron BJ, Towbin JA, Thiene G, et al. Contemporary definitions and classification of the cardiomyopathies: an American Heart Association Scientific Statement from the Council on Clinical Cardiology, Heart Failure and Transplantation Committee; Quality of Care and Outcomes Research and Functional Genomics and Translational Biology Interdisciplinary Working Groups; and Council on Epidemiology and Prevention. *Circulation*. 2006;113(14):1807-1816. doi:10.1161/CIRCULATIONAHA.106.174287

9. Marian AJ, Braunwald E. Hypertrophic Cardiomyopathy. *Circ Res*. 2017;121(7):749-770. doi:10.1161/CIRCRESAHA.117.311059

10. Marian A j. Molecular Genetic Basis of Hypertrophic Cardiomyopathy. *Circ Res*. 2021;128(10):1533-1553. doi:10.1161/CIRCRESAHA.121.318346

11. Arad M, Benson DW, Perez-Atayde AR, et al. Constitutively active AMP kinase mutations cause glycogen storage disease mimicking hypertrophic cardiomyopathy. *J Clin Invest*. 2002;109(3):357-362. doi:10.1172/JCI14571

12. Maron BJ, Roberts WC, Arad M, et al. CLINICAL OUTCOME AND PHENOTYPIC EXPRESSION IN LAMP2 CARDIOMYOPATHY. *JAMA J Am Med Assoc*. 2009;301(12):1253-1259. doi:10.1001/jama.2009.371

13. Arad M, Maron BJ, Gorham JM, et al. Glycogen storage diseases presenting as hypertrophic cardiomyopathy. *N Engl J Med*. 2005;352(4):362-372. doi:10.1056/NEJMoa033349

14. Nishimura RA, Holmes DR. Hypertrophic Obstructive Cardiomyopathy. *N Engl J Med*. 2004;350(13):1320-1327. doi:10.1056/NEJMcp030779

15. Braunwald E, Lambrew CT, Rockoff SD, Ross J, Morrow AG. IDIOPATHIC HYPERTROPHIC SUBAORTIC STENOSIS. I. A DESCRIPTION OF THE DISEASE BASED UPON AN ANALYSIS OF 64 PATIENTS. *Circulation*. 1964;30:SUPPL 4:3-119. doi:10.1161/01.cir.29.5s4.iv-3

16. Pelliccia F, Pasceri V, Limongelli G, et al. Long-term outcome of nonobstructive versus obstructive hypertrophic cardiomyopathy: A systematic review and meta-analysis. *Int J Cardiol*. 2017;243:379-384. doi:10.1016/j.ijcard.2017.06.071

17. Maron MS, Olivotto I, Betocchi S, et al. Effect of Left Ventricular Outflow Tract Obstruction on Clinical Outcome in Hypertrophic Cardiomyopathy. *N Engl J Med*. 2003;348(4):295-303. doi:10.1056/NEJMoa021332

18. Gersh BJ, Maron BJ, Bonow RO, et al. 2011 ACCF/AHA guideline for the diagnosis and treatment of hypertrophic cardiomyopathy: executive summary: a report of the American College of Cardiology Foundation/American Heart Association Task Force on Practice Guidelines. *Circulation*. 2011;124(24):2761-2796. doi:10.1161/CIR.0b013e318223e230

19. Authors/Task Force members, Elliott PM, Anastasakis A, et al. 2014 ESC Guidelines on diagnosis and management of hypertrophic cardiomyopathy: the Task Force for the Diagnosis and Management of Hypertrophic Cardiomyopathy of the European Society of Cardiology (ESC). *Eur Heart J*. 2014;35(39):2733-2779. doi:10.1093/eurheartj/ehu284

20. Lu D, Pozios I, Haileselassie B, et al. Clinical Outcomes in Patients With Nonobstructive, Labile, and Obstructive Hypertrophic Cardiomyopathy. *J Am Heart Assoc*. 7(5):e006657. doi:10.1161/JAHA.117.006657

21. Afonso LC, Bernal J, Bax JJ, Abraham TP. Echocardiography in Hypertrophic Cardiomyopathy: The Role of Conventional and Emerging Technologies. *JACC Cardiovasc Imaging*. 2008;1(6):787-800. doi:10.1016/j.jcmg.2008.09.002

22. Ohsato K, Shimizu M, Sugihara N, Konishi K, Takeda R. Histopathological factors related to diastolic function in myocardial hypertrophy. *Jpn Circ J*. 1992;56(4):325-333. doi:10.1253/jcj.56.325

23. Little WC. Diastolic Dysfunction Beyond Distensibility: Adverse Effects of Ventricular Dilatation. *Circulation*. 2005;112(19):2888-2890. doi:10.1161/CIRCULATIONAHA.105.578161

24. Zile MR, Brutsaert DL. New Concepts in Diastolic Dysfunction and Diastolic Heart Failure: Part I. *Circulation*. 2002;105(11):1387-1393. doi:10.1161/hc1102.105289

25. Lo Q, Thomas L. Echocardiographic evaluation of diastolic heart failure. *Australas J Ultrasound Med*. 2010;13(1):14-26. doi:10.1002/j.2205-0140.2010.tb00214.x

26. Patel P, Dhillon A, Popovic ZB, et al. Left Ventricular Outflow Tract Obstruction in Hypertrophic Cardiomyopathy Patients Without Severe Septal Hypertrophy. *Circ Cardiovasc Imaging*. 2015;8(7):e003132. doi:10.1161/CIRCIMAGING.115.003132

27. Aboulhosn J, Child JS. Left Ventricular Outflow Obstruction. *Circulation*. 2006;114(22):2412-2422. doi:10.1161/CIRCULATIONAHA.105.592089

28. Austin BA, Kwon DH, Smedira NG, Thamilarasan M, Lever HM, Desai MY. Abnormally Thickened Papillary Muscle Resulting in Dynamic Left Ventricular Outflow Tract Obstruction: An Unusual Presentation of Hypertrophic Cardiomyopathy. *J Am Soc Echocardiogr*. 2009;22(1):105.e5-105.e6. doi:10.1016/j.echo.2008.10.022

29. Maron BJ, Wolfson JK, Epstein SE, Roberts WC. Intramural ("small vessel") coronary artery disease in hypertrophic cardiomyopathy. *J Am Coll Cardiol*. 1986;8(3):545-557. doi:10.1016/s0735-1097(86)80181-4

30. Olivotto I, Cecchi F, Casey SA, Dolara A, Traverse JH, Maron BJ. Impact of atrial fibrillation on the clinical course of hypertrophic cardiomyopathy. *Circulation*. 2001;104(21):2517-2524. doi:10.1161/hc4601.097997

31. Siontis KC, Geske JB, Ong K, Nishimura RA, Ommen SR, Gersh BJ. Atrial fibrillation in hypertrophic cardiomyopathy: prevalence, clinical correlations, and mortality in a large high-risk population. *J Am Heart Assoc*. 2014;3(3):e001002. doi:10.1161/JAHA.114.001002

32. Guttmann OP, Rahman MS, O'Mahony C, Anastasakis A, Elliott PM. Atrial fibrillation and thromboembolism in patients with hypertrophic cardiomyopathy: systematic review. *Heart Br Card Soc*. 2014;100(6):465-472. doi:10.1136/heartjnl-2013-304276

33. Omar AMS, Bansal M, Sengupta PP. Advances in Echocardiographic Imaging in Heart Failure With Reduced and Preserved Ejection Fraction. *Circ Res*. 2016;119(2):357-374. doi:10.1161/CIRCRESAHA.116.309128

34. Jarcho JA, McKenna W, Pare JA, et al. Mapping a gene for familial hypertrophic cardiomyopathy to chromosome 14q1. *N Engl J Med*. 1989;321(20):1372-1378. doi:10.1056/NEJM198911163212005

35. Geisterfer-Lowrance AAT, Kass S, Tanigawa G, et al. A molecular basis for familial hypertrophic cardiomyopathy: A β cardiac myosin heavy chain gene missense mutation. *Cell*. 1990;62(5):999-1006. doi:10.1016/0092-8674(90)90274-I

36. Zhu M, Zhao S. Candidate Gene Identification Approach: Progress and Challenges. *Int J Biol Sci*. 2007;3(7):420-427.

37. Carrier L, Bonne G, Bahrend E, et al. Organization and Sequence of Human Cardiac Myosin Binding Protein C Gene (MYBPC3) and Identification of Mutations Predicted to Produce Truncated Proteins in Familial Hypertrophic Cardiomyopathy. *Circ Res*. 1997;80(3):427-434. doi:10.1161/01.res.0000435859.24609.b3

38. Watkins H, McKenna WJ, Thierfelder L, et al. Mutations in the Genes for Cardiac Troponin T and α-Tropomyosin in Hypertrophic Cardiomyopathy. *N Engl J Med*. 1995;332(16):1058-1065. doi:10.1056/NEJM199504203321603

39. Kimura A, Harada H, Park JE, et al. Mutations in the cardiac troponin I gene associated with hypertrophic cardiomyopathy. *Nat Genet*. 1997;16(4):379-382. doi:10.1038/ng0897-379

40. Zhong Y, Xu F, Wu J, Schubert J, Li MM. Application of Next Generation Sequencing in Laboratory Medicine. *Ann Lab Med*. 2021;41(1):25-43. doi:10.3343/alm.2021.41.1.25

41. Agarwal R, Wakimoto H, Paulo JA, et al. Pathogenesis of Cardiomyopathy Caused by Variants in ALPK3, an Essential Pseudokinase in the Cardiomyocyte Nucleus and Sarcomere. *Circulation*. 2022;146(22):1674-1693. doi:10.1161/CIRCULATIONAHA.122.059688

42. Dhandapany PS, Razzaque MA, Muthusami U, et al. RAF1 mutations in childhood-onset dilated cardiomyopathy. *Nat Genet*. 2014;46(6):635-639. doi:10.1038/ng.2963

43. Jaffré F, Miller CL, Schänzer A, et al. Inducible Pluripotent Stem Cell-Derived Cardiomyocytes Reveal Aberrant Extracellular Regulated Kinase 5 and Mitogen-Activated Protein Kinase Kinase 1/2 Signaling Concomitantly Promote Hypertrophic Cardiomyopathy in RAF1-Associated Noonan Syndrome. *Circulation*. 2019;140(3):207-224. doi:10.1161/CIRCULATIONAHA.118.037227

44. Dhandapany PS, Kang S, Kashyap DK, et al. Adiponectin receptor 1 variants contribute to hypertrophic cardiomyopathy that can be reversed by rapamycin. *Sci Adv*. 2021;7(2):eabb3991. doi:10.1126/sciadv.abb3991

45. Jain PK, Jayappa S, Sairam T, et al. Ribosomal protein S6 kinase beta-1 gene variants cause hypertrophic cardiomyopathy. *J Med Genet*. 2022;59(10):984-992. doi:10.1136/jmedgenet-2021-107866

46. Preston CG, Wright MW, Madhavrao R, et al. ClinGen Variant Curation Interface: a variant classification platform for the application of evidence criteria from ACMG/AMP guidelines. *Genome Med*. 2022;14(1):6. doi:10.1186/s13073-021-01004-8

47. Bonne G, Carrier L, Bercovici J, et al. Cardiac myosin binding protein-C gene splice acceptor site mutation is associated with familial hypertrophic cardiomyopathy. *Nat Genet*. 1995;11(4):438-440. doi:10.1038/ng1295-438

48. Mogensen J, Klausen IC, Pedersen AK, et al. Alpha-cardiac actin is a novel disease gene in familial hypertrophic cardiomyopathy. *J Clin Invest*. 1999;103(10):R39-43. doi:10.1172/JCI6460

49. Poetter K, Jiang H, Hassanzadeh S, et al. Mutations in either the essential or regulatory light chains of myosin are associated with a rare myopathy in human heart and skeletal muscle. *Nat Genet*. 1996;13(1):63-69. doi:10.1038/ng0596-63

50. Geier C, Gehmlich K, Ehler E, et al. Beyond the sarcomere: CSRP3 mutations cause hypertrophic cardiomyopathy. *Hum Mol Genet*. 2008;17(18):2753-2765. doi:10.1093/hmg/ddn160

51. Friedrich FW, Wilding BR, Reischmann S, et al. Evidence for FHL1 as a novel disease gene for isolated hypertrophic cardiomyopathy. *Hum Mol Genet*. 2012;21(14):3237-3254. doi:10.1093/hmg/dds157

52. Christodoulou DC, Wakimoto H, Onoue K, et al. 5'RNA-Seq identifies Fhl1 as a genetic modifier in cardiomyopathy. *J Clin Invest*. 2014;124(3):1364-1370. doi:10.1172/JCI70108

53. Osio A, Tan L, Chen SN, et al. Myozenin 2 Is a Novel Gene for Human Hypertrophic Cardiomyopathy. *Circ Res*. 2007;100(6):766-768. doi:10.1161/01.RES.0000263008.66799.aa

54. Chiu C, Tebo M, Ingles J, et al. Genetic screening of calcium regulation genes in familial hypertrophic cardiomyopathy. *J Mol Cell Cardiol*. 2007;43(3):337-343. doi:10.1016/j.yjmcc.2007.06.009

55. Hayashi T, Arimura T, Itoh-Satoh M, et al. Tcap gene mutations in hypertrophic cardiomyopathy and dilated cardiomyopathy. *J Am Coll Cardiol*. 2004;44(11):2192-2201. doi:10.1016/j.jacc.2004.08.058

56. Chen SN, Czernuszewicz G, Tan Y, et al. Human molecular genetic and functional studies identify TRIM63, encoding Muscle RING Finger Protein 1, as a novel gene for human hypertrophic cardiomyopathy. *Circ Res*. 2012;111(7):907-919. doi:10.1161/CIRCRESAHA.112.270207

57. Satoh M, Takahashi M, Sakamoto T, Hiroe M, Marumo F, Kimura A. Structural Analysis of the Titin Gene in Hypertrophic Cardiomyopathy: Identification of a Novel Disease Gene. *Biochem Biophys Res Commun*. 1999;262(2):411-417. doi:10.1006/bbrc.1999.1221

58. Chiu C, Bagnall RD, Ingles J, et al. Mutations in alpha-actinin-2 cause hypertrophic cardiomyopathy: a genome-wide analysis. *J Am Coll Cardiol*. 2010;55(11):1127-1135. doi:10.1016/j.jacc.2009.11.016

59. Arimura T, Bos JM, Sato A, et al. Cardiac Ankyrin Repeat Protein Gene (ANKRD1) Mutations in Hypertrophic Cardiomyopathy. *J Am Coll Cardiol*. 2009;54(4):334-342. doi:10.1016/j.jacc.2008.12.082

60. Hayashi T, Arimura T, Ueda K, et al. Identification and functional analysis of a caveolin-3 mutation associated with familial hypertrophic cardiomyopathy. *Biochem Biophys Res Commun*. 2004;313(1):178-184. doi:10.1016/j.bbrc.2003.11.101

61. Matsushita Y, Furukawa T, Kasanuki H, et al. Mutation of junctophilin type 2 associated with hypertrophic cardiomyopathy. *J Hum Genet*. 2007;52(6):543-548. doi:10.1007/s10038-007-0149-y

62. Fratev F, Mihaylova E, Pajeva I. Combination of genetic screening and molecular dynamics as a useful tool for identification of disease-related mutations: ZASP PDZ domain G54S mutation case. *J Chem Inf Model*. 2014;54(5):1524-1536. doi:10.1021/ci5001136

63. Carniel E, Taylor MRG, Sinagra G, et al. Alpha-myosin heavy chain: a sarcomeric gene associated with dilated and hypertrophic phenotypes of cardiomyopathy. *Circulation*. 2005;112(1):54-59. doi:10.1161/CIRCULATIONAHA.104.507699

64. Davis JS, Hassanzadeh S, Winitsky S, et al. The overall pattern of cardiac contraction depends on a spatial gradient of myosin regulatory light chain phosphorylation. *Cell*. 2001;107(5):631-641. doi:10.1016/s0092-8674(01)00586-4

65. Wang H, Li Z, Wang J, et al. Mutations in *NEXN*, a Z-Disc Gene, Are Associated with Hypertrophic Cardiomyopathy. *Am J Hum Genet*. 2010;87(5):687-693. doi:10.1016/j.ajhg.2010.10.002

66. Landstrom AP, Parvatiyar MS, Pinto JR, et al. Molecular and functional characterization of novel hypertrophic cardiomyopathy susceptibility mutations in TNNC1-encoded troponin C. *J Mol Cell Cardiol*. 2008;45(2):281-288. doi:10.1016/j.yjmcc.2008.05.003

67. Vasile VC, Ommen SR, Edwards WD, Ackerman MJ. A missense mutation in a ubiquitously expressed protein, vinculin, confers susceptibility to hypertrophic cardiomyopathy. *Biochem Biophys Res Commun*. 2006;345(3):998-1003. doi:10.1016/j.bbrc.2006.04.151

68. Almomani R, Verhagen JMA, Herkert JC, et al. Biallelic Truncating Mutations in ALPK3 Cause Severe Pediatric Cardiomyopathy. *J Am Coll Cardiol*. 2016;67(5):515-525. doi:10.1016/j.jacc.2015.10.093

69. Valdés-Mas R, Gutiérrez-Fernández A, Gómez J, et al. Mutations in filamin C cause a new form of familial hypertrophic cardiomyopathy. *Nat Commun*. 2014;5:5326. doi:10.1038/ncomms6326

70. Wu G, Ruan J, Liu J, et al. Variant Spectrum of Formin Homology 2 Domain-Containing 3 Gene in Chinese Patients With Hypertrophic Cardiomyopathy. *J Am Heart Assoc*. 2021;10(5):e018236. doi:10.1161/JAHA.120.018236

71. Bello J, Pellegrini MV. Mavacamten. In: *StatPearls*. StatPearls Publishing; 2024. Accessed March 22, 2024. http://www.ncbi.nlm.nih.gov/books/NBK582152/

72. Dhandapany PS, Kang S, Kashyap DK, et al. Adiponectin receptor 1 variants contribute to hypertrophic cardiomyopathy that can be reversed by rapamycin. *Sci Adv*. 2021;7(2):eabb3991. doi:10.1126/sciadv.abb3991

73. Dhandapany PS, Sadayappan S, Xue Y, et al. A common MYBPC3 (cardiac myosin binding protein C) variant associated with cardiomyopathies in South Asia. *Nat Genet*. 2009;41(2):187-191. doi:10.1038/ng.309

74. Jain A, Bhoyar RC, Pandhare K, et al. IndiGenomes: a comprehensive resource of genetic variants from over 1000 Indian genomes. *Nucleic Acids Res*. 2021;49(D1):D1225-D1232. doi:10.1093/nar/gkaa923

75. Wall JD, Stawiski EW, Ratan A, et al. The GenomeAsia 100K Project enables genetic discoveries across Asia. *Nature*. 2019;576(7785):106-111. doi:10.1038/s41586-019-1793-z

76. Tang H, Thomas PD. PANTHER-PSEP: predicting disease-causing genetic variants using position-specific evolutionary preservation. *Bioinformatics*. 2016;32(14):2230-2232. doi:10.1093/bioinformatics/btw222

77. Wiel L, Baakman C, Gilissen D, Veltman JA, Vriend G, Gilissen C. MetaDome: Pathogenicity analysis of genetic variants through aggregation of homologous human protein domains. *Hum Mutat*. 2019;40(8):1030-1038. doi:10.1002/humu.23798

78. Rentzsch P, Witten D, Cooper GM, Shendure J, Kircher M. CADD: predicting the deleteriousness of variants throughout the human genome. *Nucleic Acids Res*. 2019;47(D1):D886-D894. doi:10.1093/nar/gky1016

79. Jagadeesh KA, Wenger AM, Berger MJ, et al. M-CAP eliminates a majority of variants of uncertain significance in clinical exomes at high sensitivity. *Nat Genet*. 2016;48(12):1581-1586. doi:10.1038/ng.3703

80. Uhlén M, Fagerberg L, Hallström BM, et al. Proteomics. Tissue-based map of the human proteome. *Science*. 2015;347(6220):1260419. doi:10.1126/science.1260419

81. Cui Y, Zheng Y, Liu X, et al. Single-Cell Transcriptome Analysis Maps the Developmental Track of the Human Heart. *Cell Rep*. 2019;26(7):1934-1950.e5. doi:10.1016/j.celrep.2019.01.079

82. Thomson KL, Ormondroyd E, Harper AR, et al. Analysis of 51 proposed hypertrophic cardiomyopathy genes from genome sequencing data in sarcomere negative cases has negligible diagnostic yield. *Genet Med Off J Am Coll Med Genet*. 2019;21(7):1576-1584. doi:10.1038/s41436-018-0375-z

83. Szklarczyk D, Gable AL, Nastou KC, et al. The STRING database in 2021: customizable protein-protein networks, and functional characterization of user-uploaded gene/measurement sets. *Nucleic Acids Res*. 2021;49(D1):D605-D612. doi:10.1093/nar/gkaa1074

84. Szustakowski JD, Balasubramanian S, Kvikstad E, et al. Advancing human genetics research and drug discovery through exome sequencing of the UK Biobank. *Nat Genet*. 2021;53(7):942-948. doi:10.1038/s41588-021-00885-0

85. Musunuru K, Hershberger RE, Day SM, et al. Genetic Testing for Inherited Cardiovascular Diseases: A Scientific Statement From the American Heart Association. *Circ Genomic Precis Med*. 2020;13(4):e000067. doi:10.1161/HCG.0000000000000067

86. Yotti R, Seidman CE, Seidman JG. Advances in the Genetic Basis and Pathogenesis of Sarcomere Cardiomyopathies. *Annu Rev Genomics Hum Genet*. 2019;20:129-153. doi:10.1146/annurev-genom-083118-015306

87. Sciarretta S, Forte M, Frati G, Sadoshima J. New Insights Into the Role of mTOR Signaling in the Cardiovascular System. *Circ Res*. 2018;122(3):489-505. doi:10.1161/CIRCRESAHA.117.311147

88. Jain A, Bhoyar RC, Pandhare K, et al. IndiGenomes: a comprehensive resource of genetic variants from over 1000 Indian genomes. *Nucleic Acids Res*. 2021;49(D1):D1225-D1232. doi:10.1093/nar/gkaa923

89. Magnuson B, Ekim B, Fingar DC. Regulation and function of ribosomal protein S6 kinase (S6K) within mTOR signalling networks. *Biochem J*. 2012;441(1):1-21. doi:10.1042/BJ20110892

90. McMullen JR, Shioi T, Zhang L, et al. Deletion of ribosomal S6 kinases does not attenuate pathological, physiological, or insulin-like growth factor 1 receptor-phosphoinositide 3-kinase-induced cardiac hypertrophy. *Mol Cell Biol*. 2004;24(14):6231-6240. doi:10.1128/MCB.24.14.6231-6240.2004

91. Hizli AA, Chi Y, Swanger J, et al. Phosphorylation of eukaryotic elongation factor 2 (eEF2) by cyclin A-cyclin-dependent kinase 2 regulates its inhibition by eEF2 kinase. *Mol Cell Biol*. 2013;33(3):596-604. doi:10.1128/MCB.01270-12

92. Batool A, Majeed ST, Aashaq S, Majeed R, Bhat NN, Andrabi KI. Eukaryotic initiation factor 4E is a novel effector of mTORC1 signaling pathway in cross talk with Mnk1. *Mol Cell Biochem*. 2020;465(1-2):13-26. doi:10.1007/s11010-019-03663-z

93. de la Parra C, Ernlund A, Alard A, Ruggles K, Ueberheide B, Schneider RJ. A widespread alternate form of cap-dependent mRNA translation initiation. *Nat Commun*. 2018;9(1):3068. doi:10.1038/s41467-018-05539-0

94. Rios-Fuller TJ, Mahe M, Walters B, et al. Translation Regulation by eIF2α Phosphorylation and mTORC1 Signaling Pathways in Non-Communicable Diseases (NCDs). *Int J Mol Sci*. 2020;21(15):5301. doi:10.3390/ijms21155301

95. Gallo S, Vitacolonna A, Bonzano A, Comoglio P, Crepaldi T. ERK: A Key Player in the Pathophysiology of Cardiac Hypertrophy. *Int J Mol Sci*. 2019;20(9):2164. doi:10.3390/ijms20092164

96. Walsh R, Thomson KL, Ware JS, et al. Reassessment of Mendelian gene pathogenicity using 7,855 cardiomyopathy cases and 60,706 reference samples. *Genet Med Off J Am Coll Med Genet*. 2017;19(2):192-203. doi:10.1038/gim.2016.90

97. Peterson RT, Schreiber SL. Translation control: connecting mitogens and the ribosome. *Curr Biol CB*. 1998;8(7):R248-250. doi:10.1016/s0960-9822(98)70152-6

98. Montagne J, Stewart MJ, Stocker H, Hafen E, Kozma SC, Thomas G. Drosophila S6 kinase: a regulator of cell size. *Science*. 1999;285(5436):2126-2129. doi:10.1126/science.285.5436.2126

99. Pende M, Um SH, Mieulet V, et al. S6K1(-/-)/S6K2(-/-) mice exhibit perinatal lethality and rapamycin-sensitive 5'-terminal oligopyrimidine mRNA translation and reveal a mitogen-activated protein kinase-dependent S6 kinase pathway. *Mol Cell Biol*. 2004;24(8):3112-3124. doi:10.1128/MCB.24.8.3112-3124.2004

100. Richardson CJ, Bröenstrup M, Fingar DC, et al. SKAR is a specific target of S6 kinase 1 in cell growth control. *Curr Biol CB*. 2004;14(17):1540-1549. doi:10.1016/j.cub.2004.08.061

101. Lane HA, Fernandez A, Lamb NJ, Thomas G. p70s6k function is essential for G1 progression. *Nature*. 1993;363(6425):170-172. doi:10.1038/363170a0

102. Viñals F, Chambard JC, Pouysségur J. p70 S6 kinase-mediated protein synthesis is a critical step for vascular endothelial cell proliferation. *J Biol Chem*. 1999;274(38):26776-26782. doi:10.1074/jbc.274.38.26776

103. Blommaart EF, Luiken JJ, Blommaart PJ, van Woerkom GM, Meijer AJ. Phosphorylation of ribosomal protein S6 is inhibitory for autophagy in isolated rat hepatocytes. *J Biol Chem*. 1995;270(5):2320-2326. doi:10.1074/jbc.270.5.2320

104. Hoeffer CA, Klann E. mTOR signaling: at the crossroads of plasticity, memory and disease. *Trends Neurosci*. 2010;33(2):67-75. doi:10.1016/j.tins.2009.11.003

105. Harrington LS, Findlay GM, Gray A, et al. The TSC1-2 tumor suppressor controls insulin-PI3K signaling via regulation of IRS proteins. *J Cell Biol*. 2004;166(2):213-223. doi:10.1083/jcb.200403069

106. Wu X, Xie W, Xie W, Wei W, Guo J. Beyond controlling cell size: functional analyses of S6K in tumorigenesis. *Cell Death Dis*. 2022;13(7):1-19. doi:10.1038/s41419-022-05081-4

107. Goul C, Peruzzo R, Zoncu R. The molecular basis of nutrient sensing and signalling by mTORC1 in metabolism regulation and disease. *Nat Rev Mol Cell Biol*. 2023;24(12):857-875. doi:10.1038/s41580-023-00641-8

108. Moschella PC, Rao VU, McDermott PJ, Kuppuswamy D. Regulation of mTOR and S6K1 activation by the nPKC isoforms, PKCepsilon and PKCdelta, in adult cardiac muscle cells. *J Mol Cell Cardiol*. 2007;43(6):754-766. doi:10.1016/j.yjmcc.2007.09.015

109. Nieuwenhuis J, Brummelkamp TR. The Tubulin Detyrosination Cycle: Function and Enzymes. *Trends Cell Biol*. 2019;29(1):80-92. doi:10.1016/j.tcb.2018.08.003

110. Janke C, Chloë Bulinski J. Post-translational regulation of the microtubule cytoskeleton: mechanisms and functions. *Nat Rev Mol Cell Biol*. 2011;12(12):773-786. doi:10.1038/nrm3227

111. Caporizzo MA, Chen CY, Prosser BL. Cardiac microtubules in health and heart disease. *Exp Biol Med*. 2019;244(15):1255-1272. doi:10.1177/1535370219868960

112. Caporizzo MA, Prosser BL. The microtubule cytoskeleton in cardiac mechanics and heart failure. *Nat Rev Cardiol*. 2022;19(6):364-378. doi:10.1038/s41569-022-00692-y

113. Abraham MJ, Murtola T, Schulz R, et al. GROMACS: High performance molecular simulations through multi-level parallelism from laptops to supercomputers. *SoftwareX*. 2015;1-2:19-25. doi:10.1016/j.softx.2015.06.001

114. Yang Z, Lasker K, Schneidman-Duhovny D, et al. UCSF Chimera, MODELLER, and IMP: an integrated modeling system. *J Struct Biol*. 2012;179(3):269-278. doi:10.1016/j.jsb.2011.09.006

115. Szyk A, Deaconescu AM, Piszczek G, Roll-Mecak A. Tubulin tyrosine ligase structure reveals adaptation of an ancient fold to bind and modify tubulin. *Nat Struct Mol Biol*. 2011;18(11):1250-1258. doi:10.1038/nsmb.2148

116. Lobanov MYu, Bogatyreva NS, Galzitskaya OV. Radius of gyration as an indicator of protein structure compactness. *Mol Biol*. 2008;42(4):623-628. doi:10.1134/S0026893308040195

117. Burridge PW, Matsa E, Shukla P, et al. Chemically defined generation of human cardiomyocytes. *Nat Methods*. 2014;11(8):855-860. doi:10.1038/nmeth.2999

118. Parker KK, Tan J, Chen CS, Tung L. Myofibrillar architecture in engineered cardiac myocytes. *Circ Res*. 2008;103(4):340-342. doi:10.1161/CIRCRESAHA.108.182469

119. Eisner DA, Caldwell JL, Kistamás K, Trafford AW. Calcium and Excitation-Contraction Coupling in the Heart. *Circ Res*. 2017;121(2):181-195. doi:10.1161/CIRCRESAHA.117.310230

120. Giorgi C, Marchi S, Pinton P. The machineries, regulation and cellular functions of mitochondrial calcium. *Nat Rev Mol Cell Biol*. 2018;19(11):713-730. doi:10.1038/s41580-018-0052-8

121. MacLennan DH, Kranias EG. Phospholamban: a crucial regulator of cardiac contractility. *Nat Rev Mol Cell Biol*. 2003;4(7):566-577. doi:10.1038/nrm1151

122. Kranias EG, Hajjar RJ. Modulation of Cardiac Contractility by the Phopholamban/SERCA2a Regulatome. *Circ Res*. 2012;110(12):1646-1660. doi:10.1161/CIRCRESAHA.111.259754

123. Kerr JP, Robison P, Shi G, et al. Detyrosinated microtubules modulate mechanotransduction in heart and skeletal muscle. *Nat Commun*. 2015;6(1):8526. doi:10.1038/ncomms9526

124. Salomon AK, Phyo SA, Okami N, et al. Desmin intermediate filaments and tubulin detyrosination stabilize growing microtubules in the cardiomyocyte. *Basic Res Cardiol*. 2022;117(1):53. doi:10.1007/s00395-022-00962-3

125. Cordeddu V, Di Schiavi E, Pennacchio LA, et al. Mutation of SHOC2 promotes aberrant protein N-myristoylation and causes Noonan-like syndrome with loose anagen hair. *Nat Genet*. 2009;41(9):1022-1026. doi:10.1038/ng.425

126. Luo M, Anderson ME. Mechanisms of Altered Ca2+ Handling in Heart Failure. *Circ Res*. 2013;113(6):690-708. doi:10.1161/CIRCRESAHA.113.301651

127. Reis J, Gorgulla C, Massari M, et al. Targeting ROS production through inhibition of NADPH oxidases. *Nat Chem Biol*. 2023;19(12):1540-1550. doi:10.1038/s41589-023-01457-5

128. Görlach A, Bertram K, Hudecova S, Krizanova O. Calcium and ROS: A mutual interplay. *Redox Biol*. 2015;6:260-271. doi:10.1016/j.redox.2015.08.010

129. Chen QM, Maltagliati AJ. Nrf2 at the heart of oxidative stress and cardiac protection. *Physiol Genomics*. 2018;50(2):77-97. doi:10.1152/physiolgenomics.00041.2017

130. Margulies KB, Prosser BL. Tubulin Detyrosination. *Circ Heart Fail*. 2021;14(1):e008006. doi:10.1161/CIRCHEARTFAILURE.120.008006

131. Janke C, Magiera MM. The tubulin code and its role in controlling microtubule properties and functions. *Nat Rev Mol Cell Biol*. 2020;21(6):307-326. doi:10.1038/s41580-020-0214-3

132. Westermann S, Weber K. Post-translational modifications regulate microtubule function. *Nat Rev Mol Cell Biol*. 2003;4(12):938-948. doi:10.1038/nrm1260

133. Prota AE, Magiera MM, Kuijpers M, et al. Structural basis of tubulin tyrosination by tubulin tyrosine ligase. *J Cell Biol*. 2013;200(3):259-270. doi:10.1083/jcb.201211017

134. Wehland J, Weber K. Tubulin-tyrosine ligase has a binding site on beta-tubulin: a two-domain structure of the enzyme. *J Cell Biol*. 1987;104(4):1059-1067. doi:10.1083/jcb.104.4.1059

135. Beltramo DM, Arce CA, Barra HS. Tubulin, but not microtubules, is the substrate for tubulin:tyrosine ligase in mature avian erythrocytes. *J Biol Chem*. 1987;262(32):15673-15677.

136. Ayers MP, Kramer CM. Imaging Myofibrillar Disarray and Microvascular Dysfunction in Hypertrophic Cardiomyopathy: Novel Imaging Biomarkers for a New Era in Therapeutics. *Circulation*. 2023;148(10):819-821. doi:10.1161/CIRCULATIONAHA.123.065789

137. Chen CY, Caporizzo MA, Bedi K, et al. Suppression of detyrosinated microtubules improves cardiomyocyte function in human heart failure. *Nat Med*. 2018;24(8):1225-1233. doi:10.1038/s41591-018-0046-2

138. Zima AV, Mazurek SR. Functional Impact of Ryanodine Receptor Oxidation on Intracellular Calcium Regulation in the Heart. *Rev Physiol Biochem Pharmacol*. 2016;171:39-62. doi:10.1007/112_2016_2

139. Sies H, Jones DP. Reactive oxygen species (ROS) as pleiotropic physiological signalling agents. *Nat Rev Mol Cell Biol*. 2020;21(7):363-383. doi:10.1038/s41580-020-0230-3

PRATUL THESIS 2024

ORIGINALITY REPORT

7%
SIMILARITY INDEX

PRIMARY SOURCES

1	circ.ahajournals.org Internet	93 words — < 1%
2	www.ncbi.nlm.nih.gov Internet	71 words — < 1%
3	www.mdpi.com Internet	70 words — < 1%
4	Susobhan Mahanty, Darpan Raghav, Krishnan Rathinasamy. "Vanadocene dichloride induces apoptosis in HeLa cells through depolymerization of microtubules and inhibition of Eg5", JBIC Journal of Biological Inorganic Chemistry, 2021 Crossref	61 words — < 1%
5	www.frontiersin.org Internet	57 words — < 1%
6	www.biorxiv.org Internet	51 words — < 1%
7	Shubham Kesarwani, Prakash Lama, Anchal Chandra, P. Purushotam Reddy et al. "Genetically encoded live-cell sensor for tyrosinated microtubules", Journal of Cell Biology, 2020 Crossref	35 words — < 1%

8	pdfs.semanticscholar.org Internet	33 words — < 1%
9	circresaha.smart01.highwire.org Internet	32 words — < 1%
10	pubmed.ncbi.nlm.nih.gov Internet	32 words — < 1%
11	www.researchgate.net Internet	32 words — < 1%
12	usermanual.wiki Internet	26 words — < 1%
13	Karl B. Kern. "Antithrombotic therapies for cardiac arrest: Have we missed the mark?*", Critical Care Medicine, 03/2008 Crossref	23 words — < 1%
14	repository.hanyang.ac.kr Internet	23 words — < 1%
15	www.medchemexpress.cn Internet	23 words — < 1%
16	rupress.org Internet	22 words — < 1%
17	Alessio Biagioni, Ileana Skalamera, Sara Peri, Nicola Schiavone, Fabio Cianchi, Elisa Giommoni, Lucia Magnelli, Laura Papucci. "Update on gastric cancer treatments and gene therapies", Cancer and Metastasis Reviews, 2019 Crossref	20 words — < 1%
18	authors.library.caltech.edu	

Internet

18 words — < 1%

19 pure.rug.nl
Internet

18 words — < 1%

20 Mohammad Shariq, Vinaya Sahasrabuddhe, Sreevatsan Krishna, Swathi Radha et al. " Adult neural stem cells have latent inflammatory potential that is kept suppressed by to facilitate adult neurogenesis ", Science Advances, 2021
Crossref

17 words — < 1%

21 link.springer.com
Internet

17 words — < 1%

22 www.foxsports.com
Internet

17 words — < 1%

23 Lisandra Herrera Belén, Carlota de Oliveira Rangel-Yagui, Jorge F. Beltrán Lissabet, Brian Effer et al. "From Synthesis to Characterization of Site-Selective PEGylated Proteins", Frontiers in Pharmacology, 2019
Crossref

16 words — < 1%

24 Thaker, Akhil. "Functional Characterization of Genes Involved in Pathogenicity of the Rice Blast Fungus Magnaporthe oryzae", Maharaja Sayajirao University of Baroda (India), 2023
ProQuest

16 words — < 1%

25 cbl-gorilla.cs.technion.ac.il
Internet

16 words — < 1%

26 worldwidescience.org
Internet

16 words — < 1%

27	www.scribd.com Internet	16 words — < 1%
28	5dok.org Internet	15 words — < 1%
29	Eveljn Scarian, Matteo Bordoni, Valentina Fantini, Emanuela Jacchetti et al. "Patients' Stem Cells Differentiation in a 3D Environment as a Promising Experimental Tool for the Study of Amyotrophic Lateral Sclerosis", International Journal of Molecular Sciences, 2022 Crossref	15 words — < 1%
30	d.docksci.com Internet	15 words — < 1%
31	journals.biologists.com Internet	15 words — < 1%
32	n.neurology.org Internet	15 words — < 1%
33	cob.silverchair-cdn.com Internet	14 words — < 1%
34	espace.etsmtl.ca Internet	14 words — < 1%
35	Acchia N. J. Albury, Nicholas Swindle, Darl R. Swartz, Svetlana B. Tikunova. "Effect of Hypertrophic Cardiomyopathy-Linked Troponin C Mutations on the Response of Reconstituted Thin Filaments to Calcium upon Troponin I Phosphorylation", Biochemistry, 2012 Crossref	13 words — < 1%
36	P. Robison, M. A. Caporizzo, H. Ahmadzadeh, A. I. Bogush, C. Y. Chen, K. B. Margulies, V. B. Shenoy,	13 words — < 1%

B. L. Prosser. "Detyrosinated microtubules buckle and bear load in contracting cardiomyocytes", Science, 2016
Crossref

37	W. Friedrich, Felix, and Lucie Carrier. "Genetics of Hypertrophic and Dilated Cardiomyopathy", Current Pharmaceutical Biotechnology, 2012. Crossref	13 words — < 1%
38	Yang, L., J. Zhang, M. Kamelgarn, C. Niu, J. Gal, W. Gong, and H. Zhu. "Subcellular localization and RNAs determine FUS architecture in different cellular compartments", Human Molecular Genetics, 2015. Crossref	13 words — < 1%
39	core.ac.uk Internet	13 words — < 1%
40	research.vu.nl Internet	13 words — < 1%
41	ri.conicet.gov.ar Internet	13 words — < 1%
42	seejca.eu Internet	13 words — < 1%
43	www.theinsightpartners.com Internet	13 words — < 1%
44	www.thieme-connect.com Internet	13 words — < 1%
45	Piret Raudsepp, Dagmar Adeline Brüggemann. "Spatiotemporal studies of lipid oxidation by optical microscopy", Elsevier BV, 2021 Crossref	12 words — < 1%

46	Shirley Pei Shan Chia, Jeremy Kah Sheng Pang, Boon-Seng Soh. "Current RNA strategies in treating cardiovascular diseases", Molecular Therapy, 2024 Crossref	12 words — < 1%
47	aacr.silverchair-cdn.com Internet	12 words — < 1%
48	cardiab.biomedcentral.com Internet	12 words — < 1%
49	n3.datasn.io Internet	12 words — < 1%
50	onlinelibrary.wiley.com Internet	12 words — < 1%
51	pubs.rsc.org Internet	12 words — < 1%
52	www.aerjournal.com Internet	12 words — < 1%
53	www.science.gov Internet	12 words — < 1%
54	0-www-ncbi-nlm-nih-gov.brum.beds.ac.uk Internet	11 words — < 1%
55	B. Rivas-Santiago, R. Hernandez-Pando, C. Carranza, E. Juarez, J. L. Contreras, D. Aguilar-Leon, M. Torres, E. Sada. "Expression of Cathelicidin LL-37 during Mycobacterium tuberculosis Infection in Human Alveolar Macrophages, Monocytes, Neutrophils, and Epithelial Cells", Infection and Immunity, 2007 Crossref	11 words — < 1%

56	Garrett C. VanHecke, Maheeshi Yapa Abeywardana, Young-Hoon Ahn. "Proteomic Identification of Protein Glutathionylation in Cardiomyocytes", Journal of Proteome Research, 2019 Crossref	11 words — < 1%
57	Luis E., Eduardo Moreyr. "Chapter 23 Hypertrophic Cardiomyopathy in Infants and Children", IntechOpen, 2012 Crossref	11 words — < 1%
58	Zhong-Hao Zhang, Chen Chen, Shi-Zheng Jia, Xian-Chun Cao et al. "Selenium Restores Synaptic Deficits by Modulating NMDA Receptors and Selenoprotein K in an Alzheimer's Disease Model", Antioxidants & Redox Signaling, 2021 Crossref	11 words — < 1%
59	bioinfo.ihb.ac.cn Internet	11 words — < 1%
60	d-nb.info Internet	11 words — < 1%
61	dergipark.org.tr Internet	11 words — < 1%
62	researchonline.federation.edu.au Internet	11 words — < 1%
63	researchspace.ukzn.ac.za Internet	11 words — < 1%
64	www.humanimmunologyportal.com Internet	11 words — < 1%
65	www.intechopen.com	

Internet

11 words — < 1%

66 www.researchsquare.com
Internet

11 words — < 1%

67 www.spandidos-publications.com
Internet

11 words — < 1%

68 "De Nederlandse gezondheidszorg", Springer Nature, 2014
Crossref

10 words — < 1%

69 "Genetic Causes of Cardiac Disease", Springer Science and Business Media LLC, 2019
Crossref

10 words — < 1%

70 Caitlin M Logan, A Sue Menko. "Microtubules: Evolving roles and critical cellular interactions", Experimental Biology and Medicine, 2019
Crossref

10 words — < 1%

71 Chia-Jung Li, Chien-Sheng Chen, Giou-Teng Yiang, Andy Po-Yi Tsai, Wan-Ting Liao, Meng-Yu Wu. "Advanced Evolution of Pathogenesis Concepts in Cardiomyopathies", Journal of Clinical Medicine, 2019
Crossref

10 words — < 1%

72 Fabrice Jaffré, Clint L. Miller, Anne Schänzer, Todd Evans, Amy E. Roberts, Andreas Hahn, Maria I. Kontaridis. " Inducible Pluripotent Stem Cell–Derived Cardiomyocytes Reveal Aberrant Extracellular Regulated Kinase 5 and Mitogen-Activated Protein Kinase Kinase 1/2 Signaling Concomitantly Promote Hypertrophic Cardiomyopathy in -Associated Noonan Syndrome ", Circulation, 2019
Crossref

10 words — < 1%

73 Farzin Sohraby, Mostafa Javaheri Moghadam, Masoud Aliyar, Hassan Aryapour. "A boosted unbiased molecular dynamics method for predicting ligands binding mechanisms: Probing the binding pathway of dasatinib to Src-kinase", Cold Spring Harbor Laboratory, 2020
Crossref Posted Content
10 words — < 1%

74 Higgins, Erin Marie. "Elucidation of MRAS-Mediated Noonan Syndrome", College of Medicine - Mayo Clinic, 2021
ProQuest
10 words — < 1%

75 Jose Rubio Alvarez, Laura Reija Lopez, Juan Sierra Quiroga, Jose M Martinez Comendador et al. "Internal mammary artery dilatation in a patient with aortic coarctation, aortic stenosis, and coronary disease. Case report", Journal of Cardiothoracic Surgery, 2011
Crossref
10 words — < 1%

76 Kannarkat, G.T.. "Microtubules are more stable and more highly acetylated in ethanol-treated hepatic cells", Journal of Hepatology, 200605
Crossref
10 words — < 1%

77 Liina Kuuluvainen, Karri Kaivola, Saana Mönkäre, Hannu Laaksovirta et al. "Oligogenic basis of sporadic ALS", Neurology Genetics, 2019
Crossref
10 words — < 1%

78 Pollen, Alexander Aaron. "Searching for Genomic Events Contributing to Brain Expansion in the Human Lineage.", Stanford University, 2020
ProQuest
10 words — < 1%

79 Shemy Carasso, Hua Yang, Anna Woo, Michal Jamorski, E. Douglas Wigle, Harry Rakowski. "Diastolic Myocardial Mechanics in Hypertrophic
10 words — < 1%

Cardiomyopathy", Journal of the American Society of Echocardiography, 2010
Crossref

80 Tithi Roy, Sergette Banang-Mbeumi, Samuel T. Boateng, Emmanuelle M. Ruiz et al. "Dual targeting of mTOR/IL-17A and autophagy by fisetin alleviates psoriasis-like skin inflammation", Frontiers in Immunology, 2023 — 10 words — < 1%
Crossref

81 Trevor J. Mathias, Julia A. Ju, Rachel M. Lee, Keyata N. Thompson et al. "Tubulin Carboxypeptidase Activity Promotes Focal Gelatin Degradation in Breast Tumor Cells and Induces Apoptosis in Breast Epithelial Cells That Is Overcome by Oncogenic Signaling", Cancers, 2022 — 10 words — < 1%
Crossref

82 coek.info — 10 words — < 1%
Internet

83 ddfv.ufv.es — 10 words — < 1%
Internet

84 edoc.site — 10 words — < 1%
Internet

85 ejournals.epublishing.ekt.gr — 10 words — < 1%
Internet

86 hive.rochesterregional.org — 10 words — < 1%
Internet

87 hpscreg.eu — 10 words — < 1%
Internet

88 jultika.oulu.fi
Internet

10 words — < 1%

89	mts.intechopen.com Internet	10 words — < 1%
90	olida.ibsquare.be Internet	10 words — < 1%
91	open.uct.ac.za Internet	10 words — < 1%
92	regmedsrv1.wustl.edu Internet	10 words — < 1%
93	www.atsjournals.org Internet	10 words — < 1%
94	www.koreascience.or.kr Internet	10 words — < 1%
95	www.zora.uzh.ch Internet	10 words — < 1%

EXCLUDE QUOTES	ON	EXCLUDE SOURCES	OFF
EXCLUDE BIBLIOGRAPHY	ON	EXCLUDE MATCHES	< 10 WORDS